FREE VIBRATIONS OF FREELY SUPPORTED OVAL CYLINDRICAL SHELLS

By

LARRY DALE CULBERSON

Bachelor of Science
Bradley University
Peoria, Illinois
June, 1966

Master of Science
Oklahoma State University
Stillwater, Oklahoma
May, 1968

Submitted to the Faculty of the Graduate College
of the Oklahoma State University
in partial fulfillment of the requirements
for the Degree of
DOCTOR OF PHILOSOPHY
July, 1970

FREE VIBRATIONS OF FREELY SUPPORTED

OVAL CYLINDRICAL SHELLS

Thesis Approved:

Donald E. Boyd
Thesis Adviser

R L James

Kenneth

D. Dunbar
Dean of the Graduate College

ACKNOWLEDGEMENTS

The author wishes to express his sincere appreciation and indebtedness to the following individuals and organizations:

To Dr. Donald E. Boyd, who served as the author's major adviser and committee chairman, for his instruction, advice, and personal guidance during the author's graduate study;

To Doctors R. K. Munshi, R. L. Janes, and A. E. Salama, for serving on the author's committee;

To the National Aeronautics and Space Administration, for providing the traineeship which helped to make this graduate study financially possible;

To the School of Civil Engineering for its financial support;

To Dr. Walter W. Hu, Bradley University, who encouraged the author to attend graduate school;

To Mr. C. P. Rao and R. C. Ikard, for their assistance in the work on the computer, and to fellow graduate students in the School of Civil Engineering for their friendship;

To Mr. Eldon Hardy and Mrs. Carl Estes, for their assistance in the preparation of the final manuscript.

And finally, to the author's wife, Carole, for her undying love, support, and encouragement during the four years of graduate study.

Larry D. Culberson

July, 1970
Stillwater, Oklahoma

TABLE OF CONTENTS

LIST OF TABLES

LIST OF FIGURES

Figure Page

NOMENCLATURE

2a, 2b	Minor and major axes of shell, respectively
A_{mn}, B_{mn}, C_{mn}	Displacement constants
e_x, e_s, e_{xs}	Axial, circumferential, and shear strain components, respectively
E	Young's modulus
h	Shell thickness
k	Number of terms in circumferential direction for convergence
L	= 1, for Love's equations = 0, for Donnell's equations
L_s, L_x	Circumferential and longitudinal length of the shell, respectively
m, n	Indices on displacement summation
r	Radius of curvature
r_o	Mean radius of curvature, $L_s/2\pi$
t	Time
u, v, w	Orthogonal Displacements
x, s, z	Spatial Coordinates
[X]	Frequency matrix
α	$\frac{1 + \mu}{2}$
β	L_s/L_x
γ	$\frac{1 - \mu}{2}$
δ^i_j	Kronecker delta
ϵ	Eccentricity parameter ($\lvert\epsilon\rvert \leq 1$)

η	Nondimensional x-coordinate, x/L_x
λ	Circular frequency of a noncircular cylindrical shell
μ	Poisson's ratio
ξ	Nondimensional s-coordinate, s/L_s
ρ	Mass Density
ω	Nondimensional frequency of a noncircular cylindrical shell, $\left[\omega^2 = \frac{(1 - \mu^2)\ \rho\ L_s^2 \lambda^2}{E\pi^2}\right]$
$\bar{\omega}$	$\omega/2$

CHAPTER I

INTRODUCTION

1.1 Discussion

The purpose of this study is to investigate the free vibrations of freely supported noncircular (oval) cylindrical shells having the radius of curvature expressed as a function of the circumferential coordinate.

In the past years, cylindrical shells having circular cross-sections have been studied very thoroughly. But many times an engineer may be called upon to design noncircular cylindrical shells. Cylindrical shells having noncircular cross-sections have been used in many industrial applications; for example, in submarine and aircraft structures. In addition, shells designed to be circular often deviate measurably from perfect circularity once they are fabricated.

This study is important because the out-of-roundness may adversely affect the natural frequencies and mode shapes. Also, investigations of the free-vibration characteristics of the oval shell are necessary if the forced vibrations of oval cylindrical shells are to be studied.

1.2 Background

For the discussions to follow, reference should be to the geometry and nomenclature of Figure 1. The quantities appearing in Figure 1 are defined as follows: s, x, and z are the orthogonal coordinates;

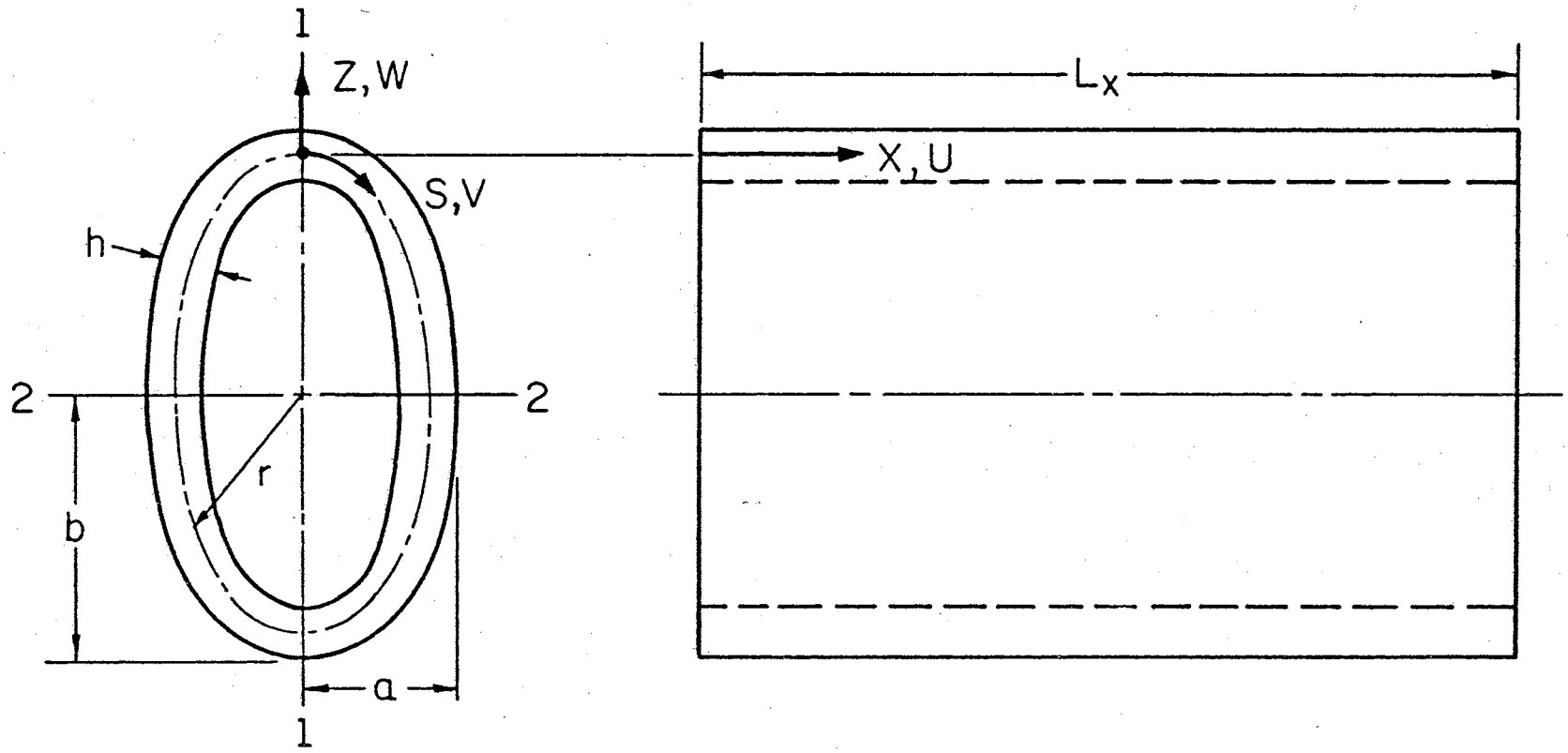

Figure 1. Geometry of the Oval Shell

v, u, and w are the corresponding displacement components; r is the variable radius of curvature; h is the shell thickness; L_x is the length of the shell in the x-direction; L_s (not shown) is the circumferential arc length of the cylindrical shell measured along the middle surface in the s-direction; and 2b and 2a are the lengths of the major and minor axes of the oval cylindrical shell, respectively.

Many frequency studies have been performed on circular cylindrical shells. Rayleigh (1) derived an expression for the natural frequencies of simply supported circular cylinders. He assumed the middle surface would bend but not stretch. In 1948, Arnold and Warburton (2) considered both bending and stretching of the shell and clarified the consequences of Rayleigh's inextensional assumption. Using an energy approach, they calculated natural frequencies and verified the lower frequencies experimentally. Since the time of their studies, many papers have been published for circular cylinders with various end conditions (3-14). These papers deal with both parametric studies and experiments.

Armenakas (15) studied the accuracy of two frequently employed shell theories of dynamic analysis, i.e., the Flügge (16) bending theory and a Donnell-type theory (not to be mistaken as the Donnell (17) theory). In this study he also showed which displacement components predominate for the three frequencies obtained for each mode shape.

Marguerre (18) was probably the first to attempt to solve noncircular cylindrical shell problems. He expressed the variable curvature as an infinite Fourier series when studying the stability of simply supported noncircular cylinders. He expressed the curvature as follows:

$$\frac{1}{r} = \frac{1}{r_o}\left[1 + \sum_{k=2,4}^{\infty} b_k \cos\frac{k\pi s}{L_s}\right] \tag{1.1}$$

where, in addition to notation introduced earlier,

r_o = mean radius of curvature, and

b_k = eccentricity constants dependent on k.

Malkina (19), when studying the free vibrations of noncircular cylindrical shells, assumed the following radius of curvature:

$$\frac{1}{r} = \frac{1}{r_o}\left[1 + \epsilon \sum_{k=1}^{\infty} b_k \cos\frac{2k\pi s}{s_o}\right] \tag{1.2}$$

where, in addition to notation introduced earlier,

ϵ = eccentricity constant, and

s_o = half the arc length of the cross-section.

Herrmann and Mirsky (20) investigated the longitudinal, torsional, and flexural vibrations of cylindrical shells having elliptic cross-sections. It was necessary to restrict the magnitude of the eccentricity in determining the longitudinal modes, and an energy procedure was used to obtain the axi-symmetric flexural modes. No solution for the remaining flexural modes or the transverse modes was presented.

Sewall (21) currently is investigating the natural frequencies and mode shapes of ellipses both theoretically (with the Rayleigh-Ritz method) and experimentally.

Kempner (22), when solving the static problem, assumed a simplified version of Marguerre's expression, Equation (1.1), for the curvature. This curvature expression, which represents a doubly symmetric oval, approximates an ellipse which has the same major to

minor axis ratio as the oval. This expression is given as

$$\frac{1}{r} = \frac{1}{r_o}\left[1 + \epsilon \cos \frac{4\pi s}{L_s}\right] \tag{1.3}$$

where, in addition to notation introduced earlier,

r_o = radius of a circle whose circumference L_s is equal to that of the oval, i.e., $L_s = 2\pi r_o$, and

ϵ = eccentricity constant, $|\epsilon| \leq 1$.

Although this expression is limited to a maximum major-minor axis ratio of 2.06, it includes cross-sections that are of practical importance. This ratio is limited because of the bounds on the eccentricity ϵ. The oval is not allowed to have any reverse or negative curvature at any of its points. When the value of the eccentricity parameter ϵ is negative, this is equivalent to a 90^o rigid body transformation of the noncircular shell. Referring to Figure 1, when $\epsilon > 1$, then $b > a$, but when $\epsilon < 1$, then $b < a$. The full geometry of the oval is presented in (23).

Klosner (24, 25, 26), assuming the curvature expression given by Kempner, Equation (1.3), studied the free and forced vibrations of an infinitely long oval cylindrical shell. He used the Love equations of motion and assumed a power series in the eccentricity parameter ϵ for the natural frequencies. This enabled him to uncouple the three coupled partial differential equations of motion. The expression for the nondimensional frequency of a noncircular cylindrical shell was given as

$$\bar{P}_{il}^2 = P_{il}^2 + C_{1il}\epsilon + C_{2il}\epsilon^2 + \ldots \tag{1.4}$$

where

P_{il} = nondimensional frequency of a circular cylindrical shell of

radius r_o

$$\left[P_{il}^2 = (r_o^2 \rho)(1 - \nu^2)p_{il}^2/E\right] ,$$

C_{pil} = coefficient of ϵ^p - term of the nondimensional perturbed frequency of the il^{th} mode,

p_{il} = natural frequency of a circular cylindrical shell of radius r_o,

E = Young's modulus,

ρ = mass density of shell,

ν = Poisson's ratio, and

l = nondimensionalized length of the longitudinal half-wave.

There are some limitations and errors in this perturbation technique which will be discussed in Chapter IV.

1.3 Approach

The equations used herein are those derived by Klosner (25) (the Love equations) and those derived by Kempner (22, 27) (the Donnell equations, modified to include the translational inertia terms). In this research, the displacements (u, v, w) were expanded in a double Fourier series similar to those used by Arnold and Warburton (2), but were modified to include the anti-symmetric mode shapes. These displacements satisfy the freely supported boundary conditions on the two ends. The curvature expression used was that given by Kempner, Equation (1.3).

When the displacement and curvature expressions were substituted into the field equations, a set of recurrence formulas relating the coefficients of the displacement series was obtained. From these formulas, the natural frequencies were found. Once the natural

frequencies were found, the corresponding mode shapes were calculated.

A comparative study was made with known circular and noncircular cases and then a parametric study was made to determine the affects of eccentricity on the natural frequencies and mode shapes of oval cylindrical shells. Also a comparative study was made of the results obtained by the Love and Donnell equations.

CHAPTER II

FORMULATION OF THE SOLUTION

2.1 Shell Vibration Equations

The relations given in this part are for a homogeneous, isotropic, elastic, thin-walled, cylindrical shell. The cross-section is identified by a convex-outward, closed, plane curve resulting from the intersection of the middle surface and a plane normal to the axis of the cylinder. The sides of the shell are assumed to be at distances $z = \pm h/2$ from the middle surface, where z is measured along the normal to this surface and h is the thickness of the shell. The thickness is considered small in comparison with the longitudinal length L_x and the radius of curvature r of the middle surface.

The relations are based upon the usual Kirchhoff-Love assumptions of classical shell theory. The strain-displacement relationships used for Love's and Donnell's equations correspond to those given by Reissner (28) and Kempner (22, 27).

The differential equations of equilibrium, Equations (2.1) and (2.2), follow from the application of Hamilton's principle (29). For a freely vibrating cylindrical shell, these equations are (with Love's assumptions)

$$u_{xx} + \frac{(1-\mu)}{2} u_{ss} + \frac{(1+\mu)}{2} v_{xs} + \frac{\mu}{r} w_x - \frac{(1-\mu^2)\rho}{E} u_{tt} = 0$$

$$\frac{(1-\mu)}{2} v_{xx} + v_{ss} + \frac{(1+\mu)}{2} u_{xs} + \left(\frac{w}{r}\right)_s + \frac{h^2}{12}\left[\frac{(1-\mu)}{2}\frac{v_{xx}}{r^2} - \frac{w_{xxs}}{r} - \frac{w_{sss}}{r} + \frac{1}{r}\left(\frac{v}{r}\right)_{ss}\right]$$

$$- \frac{(1-\mu^2)}{E} \rho v_{tt} = 0 \qquad (2.1)$$

$$\frac{1}{r}\left[\frac{w}{r} + v_s + \mu u_x\right] + \frac{h^2}{12}\nabla^4 w - \frac{h^2}{12}\left[\left(\frac{v_{xx}}{r}\right)_s - \left(\frac{v}{r}\right)_{sss}\right] + \frac{(1-\mu^2)}{E} \rho w_{tt} = 0$$

and (with Donnell's assumptions)

$$u_{xx} + \frac{(1-\mu)}{2} u_{ss} + \frac{(1+\mu)}{2} v_{xs} + \frac{\mu}{r} w_x - \frac{(1-\mu^2)}{E} \rho u_{tt} = 0$$

$$\frac{(1-\mu)}{2} v_{xx} + v_{ss} + \frac{(1+\mu)}{2} u_{xs} + \left(\frac{w}{r}\right)_s - \frac{(1-\mu^2)}{E} \rho v_{tt} = 0$$

$$\frac{1}{r}\left[\frac{w}{r} + v_s + \mu u_x\right] + \frac{h^2}{12}\nabla^4 w + \frac{(1-\mu^2)}{E} \rho w_{tt} = 0 \quad . \qquad (2.2)$$

The geometry of the shell is shown in Figure 1. In the preceding equations the subscripts indicate differentiation and

x, s, z, t = longitudinal, circumferential, and radial coordinates, and time, respectively;

u, v, w = displacements in the x, s, and z directions, respectively;

r = variable radius of curvature;

μ = Poisson's ratio;

ρ = mass density;

E = Young's modulus; and

h = thickness (constant).

A summary of the derivation of these equations is given in Appendix A.

For simplicity, because the Love and Donnell equations vary only by a few additional terms, only the Love equations will be used in the discussion of the formulation. For this parametric study, Equations (2.1) can be rewritten in nondimensionalized form using the following dimensionless quantities:

$$\eta = \frac{x}{L_x}$$

$$\xi = \frac{s}{L_s}$$

$$\alpha = \frac{1 + \mu}{2}$$

$$\gamma = \frac{1 - \mu}{2} \quad . \tag{2.3}$$

Equations (2.1) thus rewritten are as follows:

$$\frac{1}{L_x^2} u_{\eta\eta} + \frac{\gamma}{L_s^2} u_{\xi\xi} + \frac{\alpha}{L_s L_x} v_{\eta\xi} + \frac{\mu}{rL_x} w_{\eta} - \frac{(1-\mu^2)}{E} \rho u_{tt} = 0 \tag{2.4a}$$

$$\frac{v_{\xi\xi}}{L_s^2} + \frac{\gamma}{L_x^2} v_{\eta\eta} + \frac{\alpha}{L_s L_x} u_{\eta\xi} + \frac{1}{L_s}\left(\frac{w}{r}\right)_{\xi} + \frac{h^2}{12}\left[\frac{\gamma}{L_x^2 r^2} v_{\eta\eta} - \frac{1}{rL_x^2 L_s} w_{\eta\eta\xi} - \frac{1}{rL_s^3} w_{\xi\xi\xi} + \frac{1}{rL_s^2}\left(\frac{v}{r}\right)_{\xi\xi}\right]$$

$$- \frac{(1-\mu^2)}{E} \rho v_{tt} = 0 \tag{2.4b}$$

$$\frac{1}{r}\left[\frac{w}{r} + \frac{v_{\xi}}{L_s} + \frac{\mu}{L_x} u_{\eta}\right] + \frac{h^2}{12} \bar{\nabla}^4 w - \frac{h^2}{12}\left[\frac{1}{L_x^2 L_s}\left(\frac{v_{\eta\eta}}{r}\right)_{\xi} - \frac{1}{L_s^3}\left(\frac{v}{r}\right)_{\xi\xi\xi}\right]$$

$$+ \frac{(1-\mu^2)}{E} \rho w_{tt} = 0 \tag{2.4c}$$

where

$$\bar{\nabla}^4 w = \frac{w_{\eta\eta\eta\eta}}{L_x^4} + \frac{2}{L_x^2 L_s^2} w_{\eta\eta\xi\xi} + \frac{w_{\xi\xi\xi\xi}}{L_s^4} \quad .$$

The curvature expression for a doubly-symmetric oval given by Kempner, Equation (1.3), can be expressed as

$$\frac{L_s}{r} = 2\pi[1 + \epsilon \cos(4\pi\xi)] \tag{2.5}$$

in nondimensionalized terms.

For this particular problem, displacements are assumed which satisfy the freely supported boundary conditions along the two edges $\eta = 0, 1$. These conditions are

$$\begin{aligned} u_\eta &= 0 \\ v &= 0 \\ w &= 0 \\ w_{\eta\eta} &= 0 \quad . \end{aligned} \tag{2.6}$$

Utilizing these boundary conditions, the symmetric displacements u, v, and w (nondimensionalized) may be expressed by the following double Fourier series:

$$\begin{aligned} u(\eta,\xi,t) &= \sum_{m=1}^{\infty} \sum_{n=0,2}^{\infty} A_{mn} \cos m\pi\eta \cos n\pi\xi \cos \lambda t \\ v(\eta,\xi,t) &= \sum_{m=1}^{\infty} \sum_{n=0,2}^{\infty} B_{mn} \sin m\pi\eta \sin n\pi\xi \cos \lambda t \\ w(\eta,\xi,t) &= \sum_{m=1}^{\infty} \sum_{n=0,2}^{\infty} C_{mn} \sin m\pi\eta \cos n\pi\xi \cos \lambda t \end{aligned} \tag{2.7}$$

where

A_{mn}, B_{mn}, C_{mn} = unknown constant coefficients dependent upon m and n, and

λ = circular frequency.

For anti-symmetric displacements the sine and cosine functions in the ξ-direction are replaced by the cosine and sine functions, respectively.

2.2 Recurrence Formulas (Symmetric Displacements)

When the assumed displacements, Equation (2.7), and the radius of curvature, Equation (2.5), are substituted into Love's equations, Equation (2.4), three coupled equations result. Making this substitution and simplifying, the three recurrence formulas for each m and n can be written as follows:

$$[\beta^2 m^2 + \gamma(2n-2)^2 - \omega^2]A_{mn} + [-\alpha\beta m(2n-2)]B_{mn}$$
$$+ [-\beta\mu m\,\epsilon\,(1+\delta_3^n)]C_{mn-2} + [-\beta\mu m(2+\epsilon\delta_2^n)]C_{mn}$$
$$+ [-\beta\mu m\,\epsilon\,]C_{mn+2} = 0 \qquad (2.8)$$

$$A_{mn}[-\alpha\beta m(2n-2)] + B_{mn-4}\,L\left[\frac{h^2\pi^2}{12L_s^2}\,\epsilon^2(1-\delta_5^n)\left\langle m^2\beta^2\gamma + (2n-6)^2\right\rangle\right]$$
$$+ B_{mn-2}\,L\left[\frac{h^2\pi^2}{3L_s^2}\left\{(2n-2)^2\,\frac{\epsilon}{2}\,(1-\delta_3^n) + \frac{\epsilon}{2}\,(2n-6)^2\,(1-\frac{\epsilon}{2}\,\delta_4^n)\right.\right.$$
$$\left.\left. + m^2\beta^2\gamma\left\langle\epsilon(1-\delta_3^n) - \frac{\epsilon^2}{4}\,\delta_4^n\right\rangle\right\}\right] + B_{mn}\Big[(2n-2)^2 + \gamma\beta^2 m^2$$
$$+ L\,\frac{h^2\pi^2}{3L_s^2}\left\langle(2n-2)^2\,(1-\epsilon\delta_2^n) + \frac{\epsilon^2}{4}\,(2n+2)^2\,(1-\delta_1^n)\right.$$
$$\left. + \frac{\epsilon^2}{4}\,(2n-6)^2 + \gamma m^2\beta^2(1+\frac{\epsilon^2}{2} - \epsilon\,\delta_2^n - \frac{\epsilon^2}{4}\,\delta_3^n)\right\rangle - \omega^2\Big] +$$

$$+ B_{mn+2} L \left[\frac{h^2\pi^2}{3L_s^2} \left\langle (2n-2)^2 \frac{\epsilon}{2} (1 - \frac{\epsilon}{2} \delta_2^n) + (2n+2)^2 \frac{\epsilon}{2} \right.\right.$$

$$\left.\left. + m^2\beta^2\gamma \ (\epsilon - \frac{\epsilon^2}{4} \delta_2^n) \right\rangle\right] + B_{mn+4} L \left[\frac{h^2\pi^2}{12L_s^2} \epsilon^2 \left\langle m^2\beta^2\gamma + (2n+2)^2 \right\rangle\right]$$

$$+ C_{mn-2} \left[(2n-2) \ \epsilon \ (1 + \delta_3^n) + L \frac{h^2\pi^2}{12L_s^2} \epsilon \ (2n-6) \left\langle \beta^2 m^2 + (2n-6)^2 \right\rangle\right]$$

$$+ C_{mn} \left[(2n-2)(2 + \epsilon\delta_2^n) + L \frac{h^2\pi^2}{6L_s^2} (2n-2) \ (1 - \frac{\epsilon}{2} \delta_2^n) \left\langle \beta^2 m^2 \right.\right.$$

$$\left.\left. + (2n-2)^2 \right\rangle\right] + C_{mn+2} \left[(2n-2) \ \epsilon + L \frac{h^2\pi^2}{12L_s^2} \epsilon \ (2n+2) \left\langle \beta^2 m^2 \right.\right.$$

$$\left.\left. + (2n+2)^2 \right\rangle\right] = 0 \qquad (2.9)$$

$$A_{mn-2} \left[-\mu m\beta\epsilon \ (1 + \delta_3^n)\right] + A_{mn} \left[-\mu m\beta(2 + \epsilon\delta_2^n)\right] + A_{mn+2} \left[-\mu m\beta\epsilon\right]$$

$$+ B_{mn-2} \left[\epsilon(2n-6)(1 + \delta_3^n) + L \frac{h^2\pi^2}{12L_s^2} (1 - \delta_3^n) \epsilon \ (2n-2) \left\langle \beta^2 m^2 \right.\right.$$

$$\left.\left. - (2n-2)^2 \right\rangle\right] + B_{mn} \left[(2n-2)(2 + \epsilon\delta_2^n) + L \frac{h^2\pi^2}{6L_s^2} (2n-2) \cdot \right.$$

$$\left. (1 - \frac{\epsilon}{2} \delta_2^n) \left\langle m^2\beta^2 - (2n-2)^2 \right\rangle\right] + B_{mn+2} \left[\epsilon(2n+2) \right.$$

$$\left. + L \frac{h^2\pi^2}{12L_s^2} \epsilon(2n-2) \left\langle m^2\beta^2 - (2n-2)^2 \right\rangle\right] + C_{mn+4} \left[\epsilon^2(1 + \delta_5^n)\right]$$

$$+ C_{mn-2} \left[\epsilon(4 + 4\delta_3^n + \epsilon \ \delta_4^n)\right] + C_{mn} \left[(4 + 2\epsilon^2 + \epsilon^2\delta_3^n + 4\epsilon \ \delta_2^n) \right.$$

$$\left. + \frac{h^2\pi^2}{12L_s^2} \left\langle \beta^2 m^2 + (2n-2)^2 \right\rangle^2 - \omega^2\right] + C_{mn+2} \left[\epsilon(4 + \epsilon \ \delta_2^n)\right] +$$

$$+ C_{mn+4}\left[\epsilon^2\right] = 0 \tag{2.10}$$

where

$$\beta = \frac{L_s}{L_x}$$

$$\omega^2 = \frac{(1-\mu^2)\rho L_s{}^2\lambda^2}{E\pi^2}$$

$$\delta^i_j = \left.\begin{matrix} 1 \\ 0 \end{matrix}\right\} \begin{matrix} i = j \\ i \neq j \end{matrix}$$

$$L = \left.\begin{matrix} 1 \\ 0 \end{matrix}\right\} \begin{matrix} \text{Love's equations} \\ \text{Donnell's equations} \end{matrix}$$

$$\left.\begin{matrix} A_{m-n} = 0 \\ B_{m-n} = 0 \\ C_{m-n} = 0 \end{matrix}\right\} \quad n \geq 0$$

$$m = 1, 2, 3, \ldots$$

$$n = 1, 2, 3, \ldots$$

For a derivation of these recurrence formulas see Appendix A.

These three equations, Equations (2.8), (2.9), and (2.10), cannot be solved explicitly for A_{mn}, B_{mn}, and C_{mn}. Noncircularity has coupled these equations together in the ξ-direction. In order to solve these equations, an infinite number of the equations must be taken. Because this is not possible, the number of equations must then be truncated at some point. The point selected is that which will insure convergence for the desired accuracy. Because of the large number of equations

involved, the use of a computer is essential. The next chapter will explain the calculation of the natural frequencies and mode shapes.

CHAPTER III

COMPUTER SOLUTION

3.1 General

The computer program developed is sufficiently general to determine the symmetric and anti-symmetric modes of vibration and the corresponding frequencies for a freely supported cylindrical shell by means of either Love's or Donnell's equations, Equations (2.1) or (2.2). The parameters in the program are the eccentricity (ECC), defining the radius of curvature, the L_s/L_x ratio (BET), the h/L_s ratio (HOLS), and Poisson's ratio (PR) for the shell. The program also includes the boundary conditions (infinitely long cylindrical shell) employed by Klosner (25). The calculations were made on the Oklahoma State University IBM Model 360/50 Computer. A listing of the program is given in Appendix B.

3.2 Natural Frequencies

If the number of n's in the recurrence formulas, Equations (2.8), (2.9), and (2.10), is taken to be k, then 3k simultaneous equations are obtained for each value of m. These equations can be written in matrix form as follows:

$$\begin{bmatrix} \text{Recurrence Formula} & 2.8 \\ \\ \hline \\ \text{Recurrence Formula} & 2.9 \\ \\ \hline \\ \text{Recurrence Formula} & 2.10 \\ \\ \end{bmatrix} \begin{bmatrix} A_{m1} \\ \vdots \\ A_{mk} \\ \hline B_{m1} \\ \vdots \\ B_{mk} \\ \hline C_{m1} \\ \vdots \\ C_{mk} \end{bmatrix} = \begin{bmatrix} 0 \end{bmatrix} \qquad (3.1)$$

$$\begin{bmatrix} X \end{bmatrix} \begin{bmatrix} A \\ B \\ C \end{bmatrix} = \begin{bmatrix} 0 \end{bmatrix} .$$

Equation (3.1) requires that

$$|[X'] - \omega^2[I]| = 0 \qquad (3.2)$$

where

$[X']$ = $[X]$ without the ω^2 terms, and

$[I]$ = identity matrix.

The squares of the nondimensionalized frequencies are those values of ω^2 which satisfy Equation (3.2).

The subroutine called EIGENP (30), with double precision, was used to calculate the eigenvalues (ω^2) of Equation (3.2) and the resulting eigenvectors

$$\begin{bmatrix} A \\ B \\ C \end{bmatrix} .$$

3.3 Mode Shapes

Once the natural frequencies and corresponding vectors were obtained, the corresponding mode shapes were found. As is the case for all free vibration problems, only normalized displacements can be found. All displacements were calculated at the point of maximum displacement along the axis of the shell.

The number of points around the circumference, at which the displacements were calculated, varied with k. The number of points chosen was sufficient to insure that all points of sign changes in displacements would be given. Due to symmetry of the cross-section, displacements were calculated for only half the circumferential length. The number of points was taken to be $3k - 2$.

In order to determine which frequency corresponded with which value of n, the number of times that the displacement changed sign in half the circumferential length was counted, and this was then taken to be the value of n, or the number of full waves. As the eccentricity became higher, the value of n could be determined in this manner, but it became meaningless. The value of n was then determined by comparing the higher eccentricity mode shapes with the lower eccentricity mode shapes found in the described manner. This procedure worked quite well.

CHAPTER IV

NUMERICAL RESULTS

4.1 Introduction

It was decided to substantiate the method of solution described in the preceding chapters by comparing the results of this study with the results of others; first, by comparing with known solutions for circular shells, and second, with those of noncircular shells.

4.2 Comparison of Results with Circular Shells

The first case studied was used to verify the applicability of the solution for obtaining the natural frequencies of circular cylinders. Armenakas (15) compared the natural frequencies obtained by the Flügge equations with those obtained on the basis of the theory of elasticity. The results obtained are given in Table I (using Armenakas's nondimensionalized frequency Ω). These results are for the first longitudinal mode (m = 1) and for the two higher frequencies of the three frequencies obtained for each mode shape. The shells had the following parameters and properties defined:

$$\bar{\omega}^2 = \frac{(1-\mu^2)\rho L_s{}^2\lambda^2}{4E\pi^2}$$

$$\Omega^2 = \left(\frac{8}{1-\mu}\right)\left(\frac{h}{L_s}\right)^2 \bar{\omega}^2$$

TABLE I

COMPARISON OF NONDIMENSIONAL FREQUENCIES OBTAINED BY THE THEORY OF ELASTICITY FLÜGGE, LOVE, AND DONNELL

$\frac{h}{R}$	$\frac{h}{L}$	SECOND FREQUENCY n = 1 Elasticity	Flügge	Love	Donnell	n = 2 Elasticity	Flügge	Love	Donnell	n = 4 Elasticity	Flügge	Love	Donnell
.1	.1	.10689	.10714	.10702	.10693	.12226	.12268	.12247	.12234	.16485	.16556	.16506	.16495
	.3	.30177	.30224	.30193	.30178	.30698	.30761	.30725	.30704	.32680	.32792	.32737	.32699
	.5	.50103	.50244	.50129	.50105	.50411	.50573	.50452	.50420	.51623	.51868	.51719	.51657
.3	.1	.16484	.16709	.16542	.16519	.22784	.23328	.22831	.22805	.39825	.41471	.39879	.39866
	.3	.32109	.32964	.32527	.32267	.36754	.38209	.37478	.37103	.49570	.52804	.50637	.50301
	.5	.51065	.52861	.51692	.51280	.54009	.56986	.55561	.54754	.63760	.71154	.68022	.66849

$\frac{h}{R}$	$\frac{h}{L}$	THIRD FREQUENCY n = 1 Elasticity	Flügge	Love	Donnell	n = 2 Elasticity	Flügge	Love	Donnell	n = 4 Elasticity	Flügge	Love	Donnell
.1	.1	.17842	.17853	.17859	.17857	.20201	.20226	.20237	.20233	.27561	.27649	.27671	.27662
	.3	.50648	.51015	.51024	.51023	.51473	.51861	.51873	.51872	.54638	.55119	.55140	.55135
	.5	.82707	.84691	.84707	.84706	.83174	.85202	.85219	.85219	.85006	.87216	.87240	.87238
.3	.1	.26027	.26284	.26380	.26327	.38247	.39092	.39306	.39194	.65666	.68488	.68962	.68752
	.3	.53121	.53487	.53627	.53604	.59752	.60552	.60856	.60763	.79703	.82759	.83439	.83174
	.5	.84138	.86084	.86268	.86254	.87975	.90500	.90827	.90767	1.00885	1.06365	1.07184	1.06933

$$\frac{h}{L_s} = 0.015915494,\ 0.047746483$$

$$\frac{L_s}{L_x} = 6.2831853,\ 18.849556,\ 31.415927$$

$$\mu = 0.30$$

where

Ω = nondimensional frequency given by Armenakas.

The values of h/L_s and L_s/L_x correspond to the following values:

$$\frac{h}{R} = 0.10,\ 0.30$$

$$\frac{h}{L_x} = 0.10,\ 0.30,\ 0.50$$

where

R = radius of the cylinder.

As is evident from Table I, the frequencies obtained by both the Love and Donnell equations are close to those obtained on the basis of the theory of elasticity and Flügge's equations for a wide range of shell parameters. Therefore, frequencies obtained by both the Love and Donnell equations can be used with confidence in studying the free vibrations of circular cylinders.

Once the natural frequencies had been found, the mode shapes could be calculated. For this purpose, the shells used to verify the calculations of the mode shapes were the same shells studied by Arnold and Warburton (2). Comparisons of the ratios of the maximum displacements for the low frequency (n = 4, m = 1) are given in Table II.

The results obtained by the Love and Donnell equations are quite accurate in comparison with those given by Arnold and Warburton for this range of shell parameters. Their frequency equation was based on

TABLE II

COMPARISON OF AMPLITUDE RATIOS

n = 4	m = 1		μ = 0.29		h/L_s = 0.008356			
L_s/L_x	.7734		3.094		5.414		7.734	
	A/C	B/C	A/C	B/C	A/C	B/C	A/C	B/C
Arnold and Warburton	.024	.252	.072	.257	.073	.246	.052	.218
Love	.024	.252	.072	.257	.073	.246	.052	.217
Donnell	.024	.252	.072	.256	.072	.245	.051	.216

strain relations given by Timoshenko. With these results, this would seem to indicate that both sets of equations can be used for determining the modal characteristics of circular cylindrical shells.

Klosner (26), in his study of infinitely long oval cylinders, derived a cubic equation for the natural frequencies of a circular cylinder of infinite length. Making the changes in the recurrence formulas to his boundary conditions was a simple task. Only a few sign changes had to be made in Equations (2.8), (2.9), and (2.10). Comparison of the low frequencies (m = 1) are given in Table III. This shell had the following properties:

$$\frac{L_s}{L_x} = 2\pi \qquad \frac{h}{L_s} = 0.0017356 \qquad \mu = 0.30 \ .$$

The greatest difference in these frequencies was found at n = 8. The percentage deviation was equal to 0.94%. This deviation was attributed to the difference in solving for the eigenvalues of a large matrix in comparison to solving a cubic equation for the natural frequencies. The results obtained by Klosner and the author are shown in Figure 2. For circular shells, the eigenvalue routine (EIGENP) gave accurate results for large matrices. Therefore this routine can be used with confidence in studying noncircular shells. For this shell the Love equations were used in the comparison. The Donnell equations gave almost identical frequencies as the Love equations, the greatest deviation being +0.16%.

The results of this study substantiated the applicability of the method of solution (and the related computer program) to the special case of the freely supported circular cylinder.

TABLE III

COMPARISON OF KLOSNER'S AND CULBERSON'S NONDIMENSIONAL FREQUENCIES ($\bar{\omega}$)

$L_s/L_x = 2\pi$ $\quad h/L_s = 1/(2\pi 91.7)$ $\quad \mu = 0.30$

	$\epsilon = 0.0$		$m = 0.10$		$\epsilon = 0.20$		$\epsilon = 0.30$		$\epsilon = 0.40$		$\epsilon = 0.50$	
n	Klosner	Culberson	Klosner	Culberson	Klosner	Culberson	Klosner	Culberson	Klosner	Culberson	Klosner	Culberson
0	0.94969	0.94969	0.95554	0.95855	0.97288	0.98249	1.00110	1.01631	1.03933	1.05571	1.08651	1.09797
1	0.84556	0.84556	0.84940	0.88729	0.86081	0.93179	0.87950	0.97776	0.90502	1.02428	0.93682	1.07067
2	0.65334	0.65337	0.65022	0.64567	0.64076	0.62551	0.62468	0.59902	0.60144	0.57204	0.57018	0.54898
3	0.48403	0.48417	0.48279	0.48323	0.47905	0.48143	0.47276	0.47993	0.46380	0.47964	0.45202	0.48080
4	0.36198	0.36237	0.36141	0.36177	0.35968	0.35974	0.35679	0.35577	0.35270	0.34839	0.34737	0.33789
5	0.28442	0.28524	0.28459	0.28538	0.28513	0.28542	0.28601	0.28468	0.28725	0.28289	0.28883	0.28024
6	0.24543	0.24685	0.24258	0.24414	0.23380	0.23775	0.21839	0.22927	0.19478	0.21895	0.15936	0.20638
7	0.23967	0.24167	0.23839	0.24005	0.23452	0.23542	0.22793	0.22828	0.21836	0.21909	0.20541	0.20817
8	0.26012	0.26255	0.26243	0.26413	0.26924	0.26706	0.28021	0.26954	0.29490	0.27079	0.31277	0.27003
9	0.29919	0.30188	0.29999	0.30213	0.30235	0.30298	0.30626	0.30461	0.31164	0.30692	0.31843	0.30965
10	0.35130	0.35413	0.35211	0.35421	0.35452	0.35444	0.35852	0.35469	0.36404	0.35553	0.37102	0.35630
11	0.41321	0.41612	0.41415	0.41616	0.41696	0.41626	0.42160	0.41643	0.42802	0.41666	0.43613	0.41696

$L_s/L_x = 2\pi$ $\quad h/L_s = 1/(2\pi 91.7)$ $\quad \mu = 0.30$

	$\epsilon = 0.60$		$\epsilon = 0.70$		$\epsilon = 0.80$		$\epsilon = 0.90$		$\epsilon = 1.0$	
n	Klosner	Culberson	Klosner	Culberson	Klosner	Culberson	Klosner	Culberson	Klosner	Culberson
0	1.14153	1.14145	1.20331	1.18515	1.27087	1.22842	1.34334	1.27084	1.41996	1.31209
1	0.97427	1.11641	1.01675	1.16111	1.06366	1.20445	1.11444	1.24618	1.16858	1.28607
2	0.52946	0.53429	0.47689	0.52308	0.40789	0.51971	0.31174	0.52090	0.14089	0.52535
3	0.43720	0.48357	0.41900	0.48789	0.39697	0.49360	0.37043	0.50048	0.33830	0.50836
4	0.34075	0.32551	0.33275	0.31493	0.32327	0.30859	0.31218	0.30572	0.29930	0.30485
5	0.29076	0.27707	0.29301	0.27368	0.29560	0.27033	0.29850	0.26723	0.30170	0.26453
6	0.10003	0.19058	---	0.17004	---	0.14362	---	0.11232	---	0.08093
7	0.18837	0.19581	0.16600	0.18233	0.13567	0.16813	0.08966	0.15366	---	0.13951
8	0.33331	0.26600	0.35606	0.25750	0.38062	0.25474	0.40667	0.23410	0.43394	0.22489
9	0.32654	0.31255	0.33587	0.31550	0.34632	0.31842	0.35780	0.32131	0.37020	0.32418
10	0.37937	0.35728	0.38901	0.35844	0.39985	0.35978	0.41178	0.36130	0.42472	0.36298
11	0.44584	0.41778	0.45705	0.41778	0.46965	0.41830	0.48354	0.41888	0.49861	0.41954

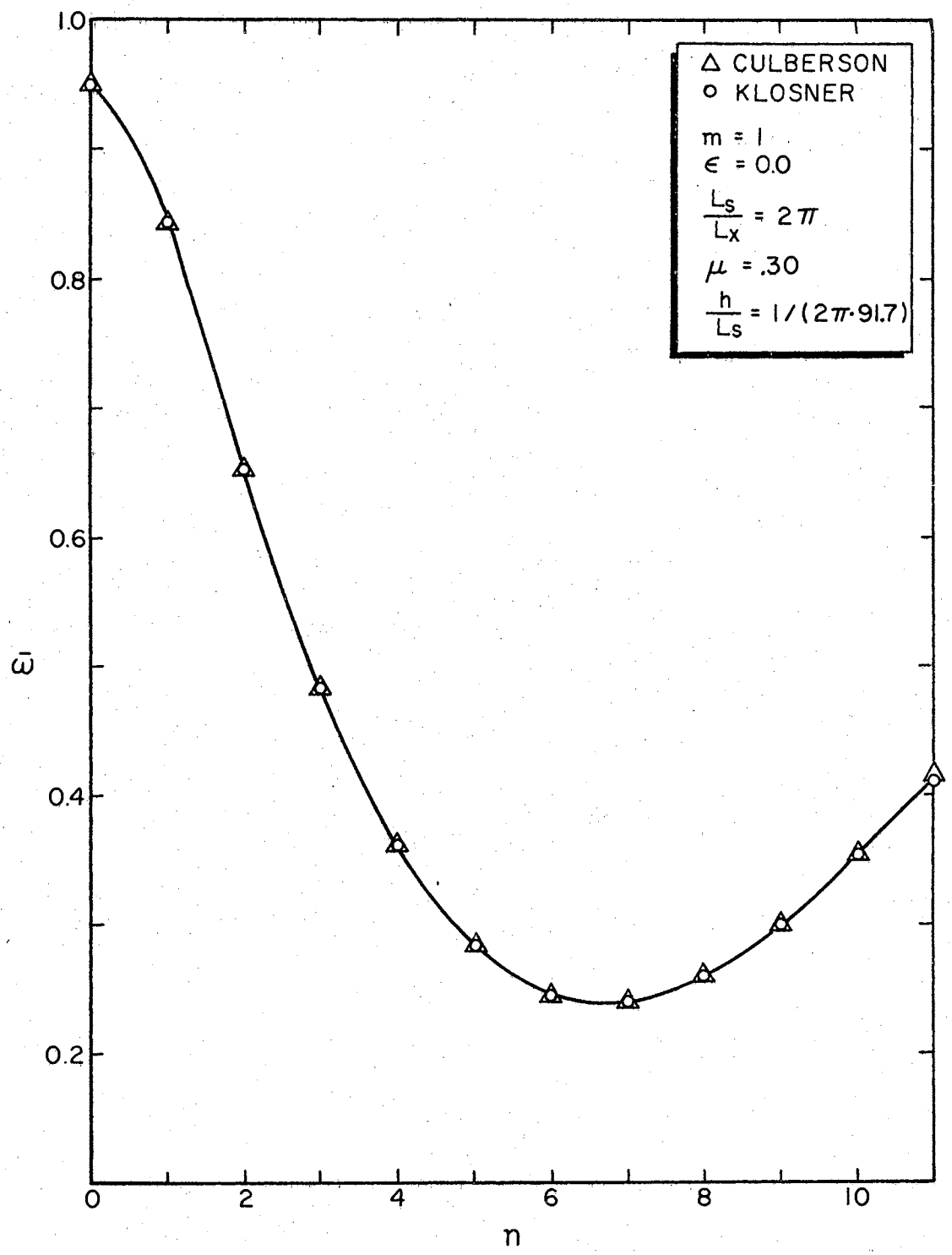

Figure 2. Nondimensional Circular Frequency ($\bar{w}$) Versus Mode Number n (Klosner and Culberson)

4.3 Comparison of Results with Noncircular Shells

Having established good results for known circular shells, non-circular (oval) shells were then studied. Another computer program was written based on the results given by Klosner (26). Results obtained from this program and the author's results (Love's equations) are given in Table III. These results are for the lowest frequency (m = 1) and the following parameters:

$$\frac{L_s}{L_x} = 2\pi \qquad \frac{h}{L_s} = 0.0017356 \qquad \mu = 0.30 \ .$$

For the accuracy desired, convergence was obtained with k = 21 (i.e., with 21 terms in the circumferential direction). As can be readily seen from Table III, there is quite a discrepancy in the results. As the eccentricity increases, there is more deviation. Figures 3 through 7 show the variation of the frequency ($\bar{\omega}$) versus the eccentricity parameter (ϵ). Figures 8 through 12 show the variation of the frequency versus the mode number n. All of these cases are for modes symmetric about the vertical axis (axis 1-1 in Figure 1) and for $\epsilon > 1$.

For n = 6 and 7, all the frequencies cannot be calculated by Klosner's perturbation technique because $\bar{\omega}^2$ becomes negative, meaning the natural frequency $\bar{\omega}$ is imaginary.

There are a few reasons which may be offered to explain these discrepancies. First, Klosner's equations (recurrence formulas) do not include the terms involving the Kronecker delta δ^i_j. The author's equations are identical with Klosner's equations except for those terms. Second, there may be the possibility of error in the derivation of the perturbation method. This was not checked by the author. Third, the

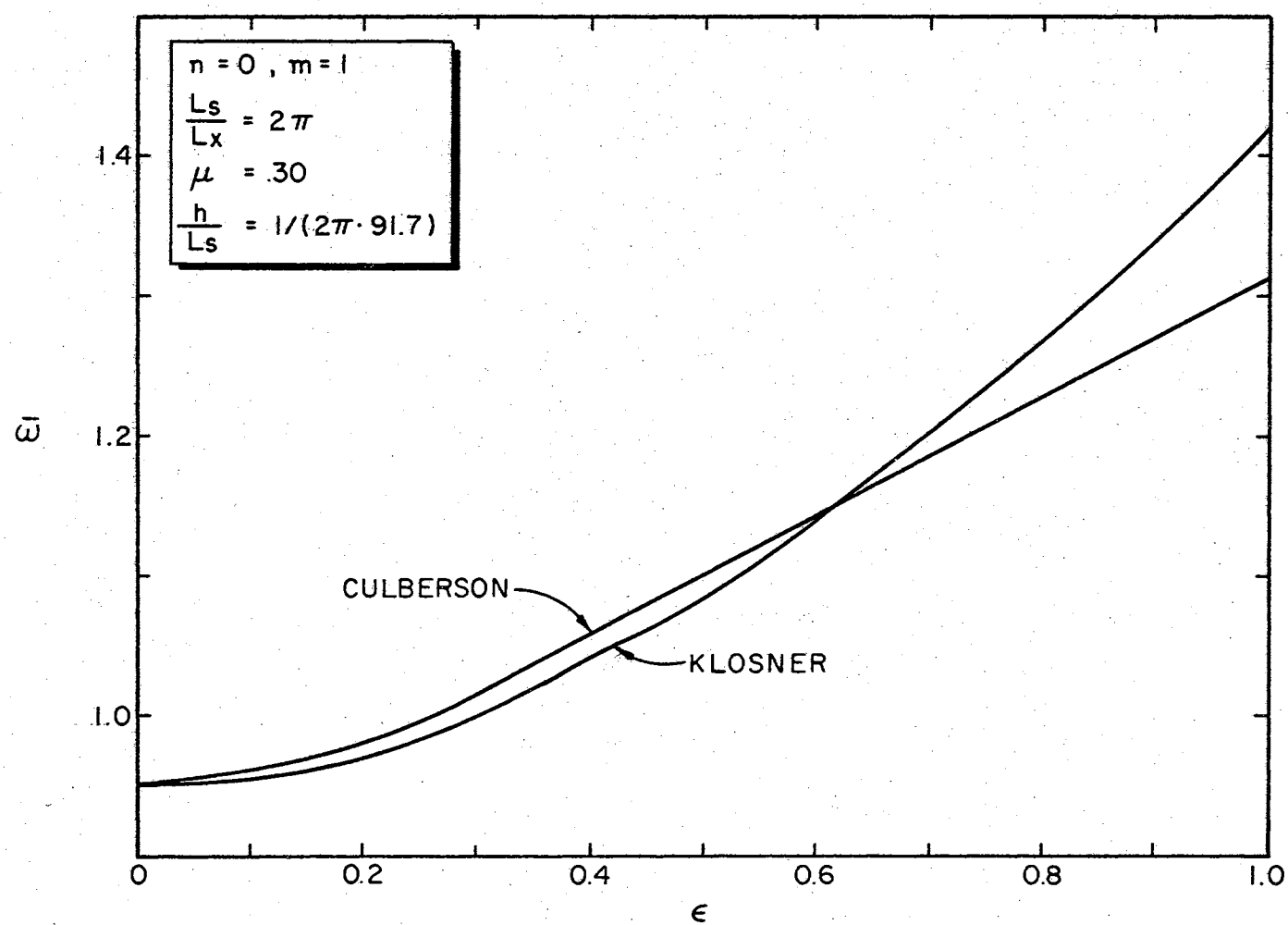

Figure 3. Nondimensional Frequency ($\bar{w}$) Versus Eccentricity (n = 0, m = 1, Klosner and Culberson)

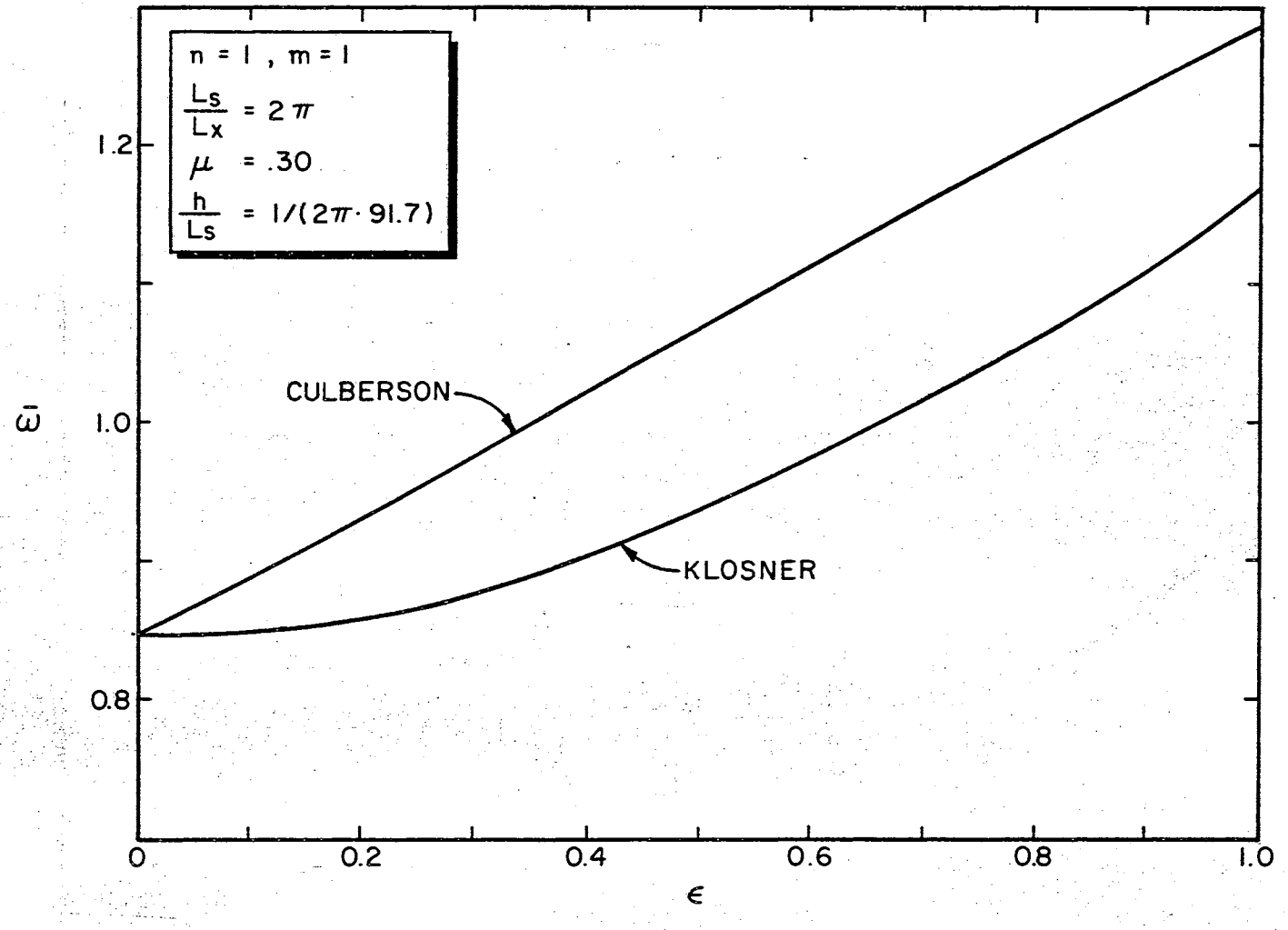

Figure 4. Nondimensional Frequency ($\bar{\omega}$) Versus Eccentricity (n = 1, m = 1, Klosner and Culberson)

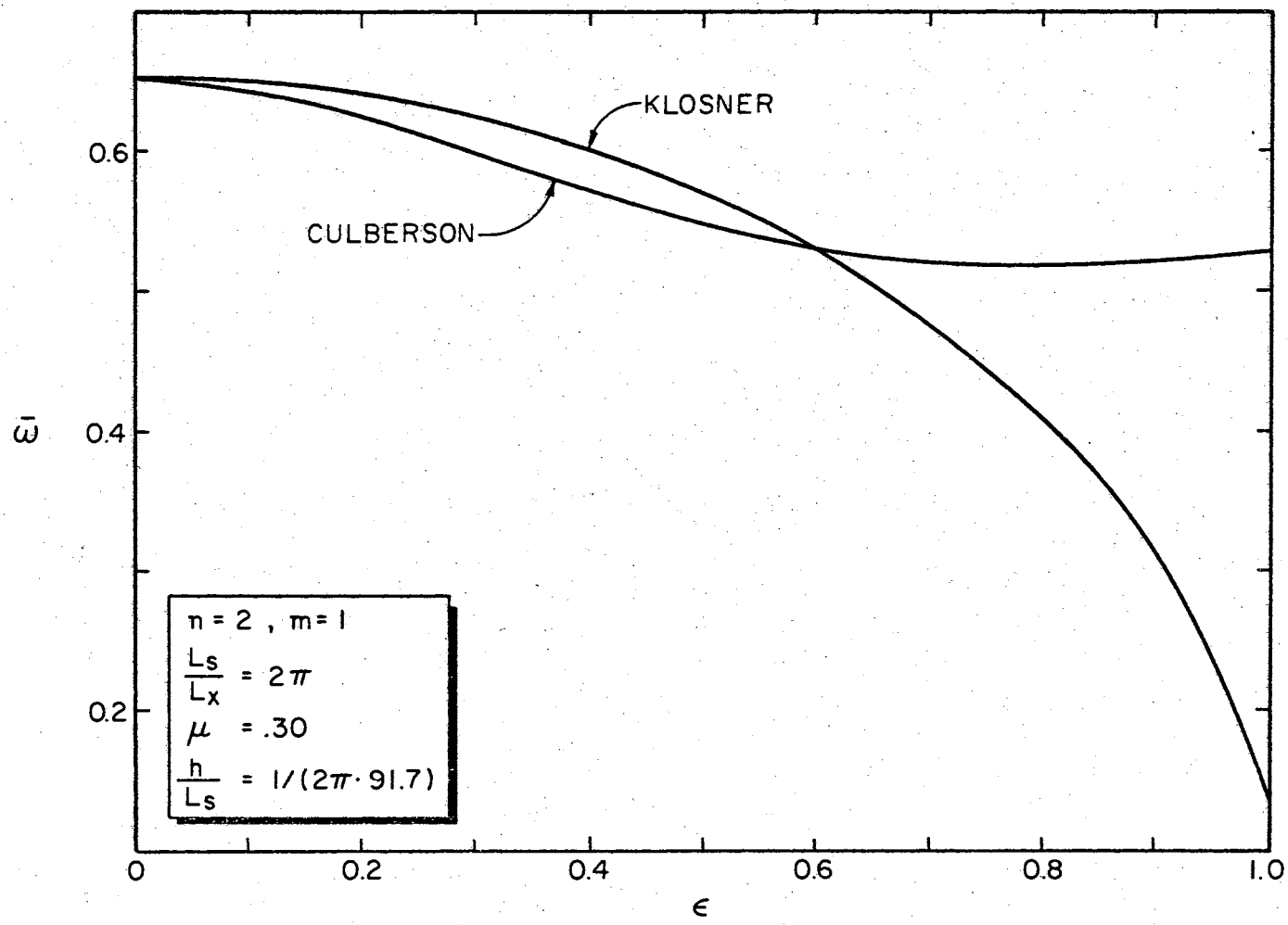

Figure 5. Nondimensional Frequency ($\bar{\omega}$) Versus Eccentricity (n = 2, m = 1, Klosner and Culberson)

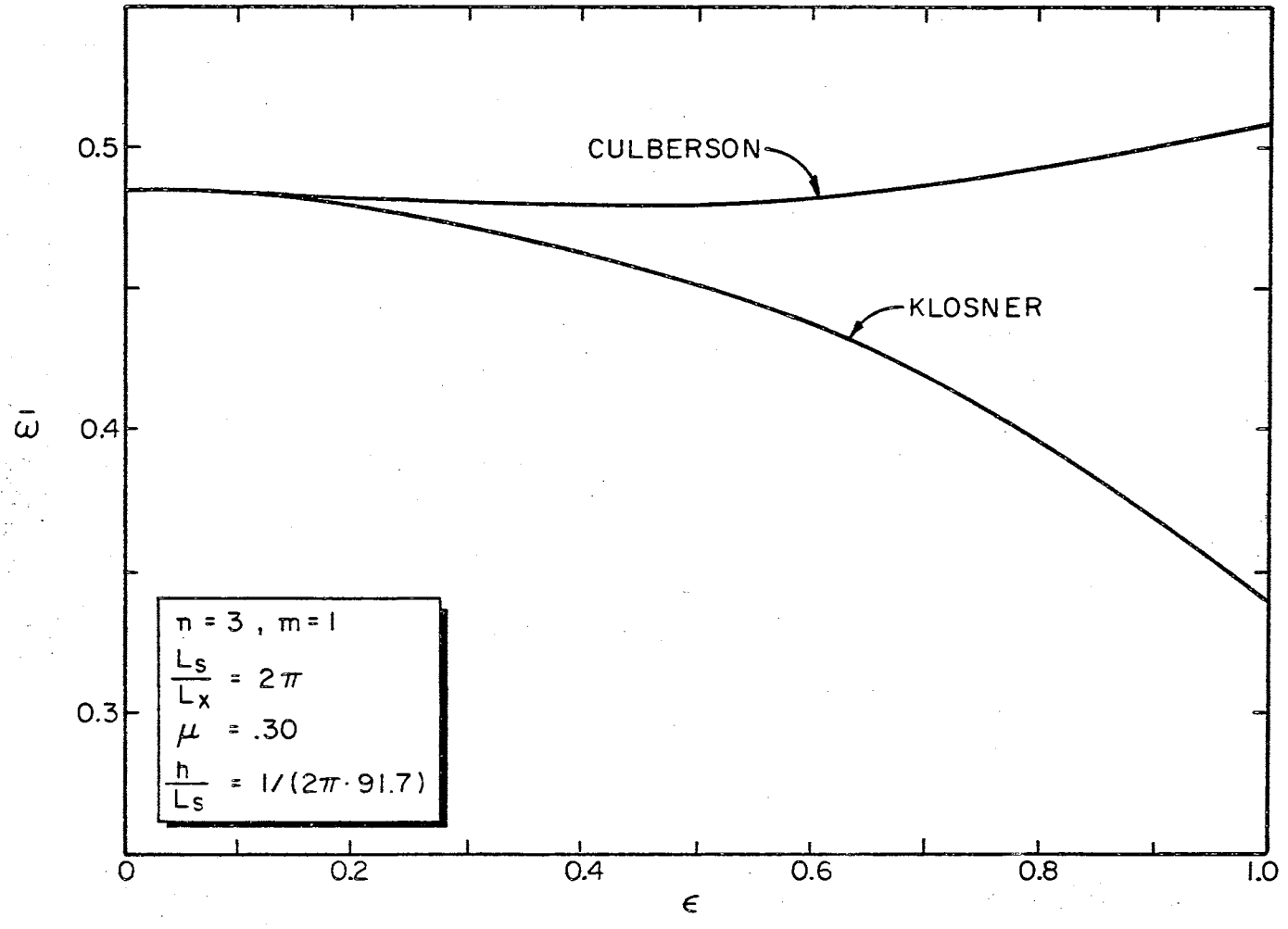

Figure 6. Nondimensional Frequency ($\bar{\omega}$) Versus Eccentricity (n = 3, m = 1, Klosner and Culberson)

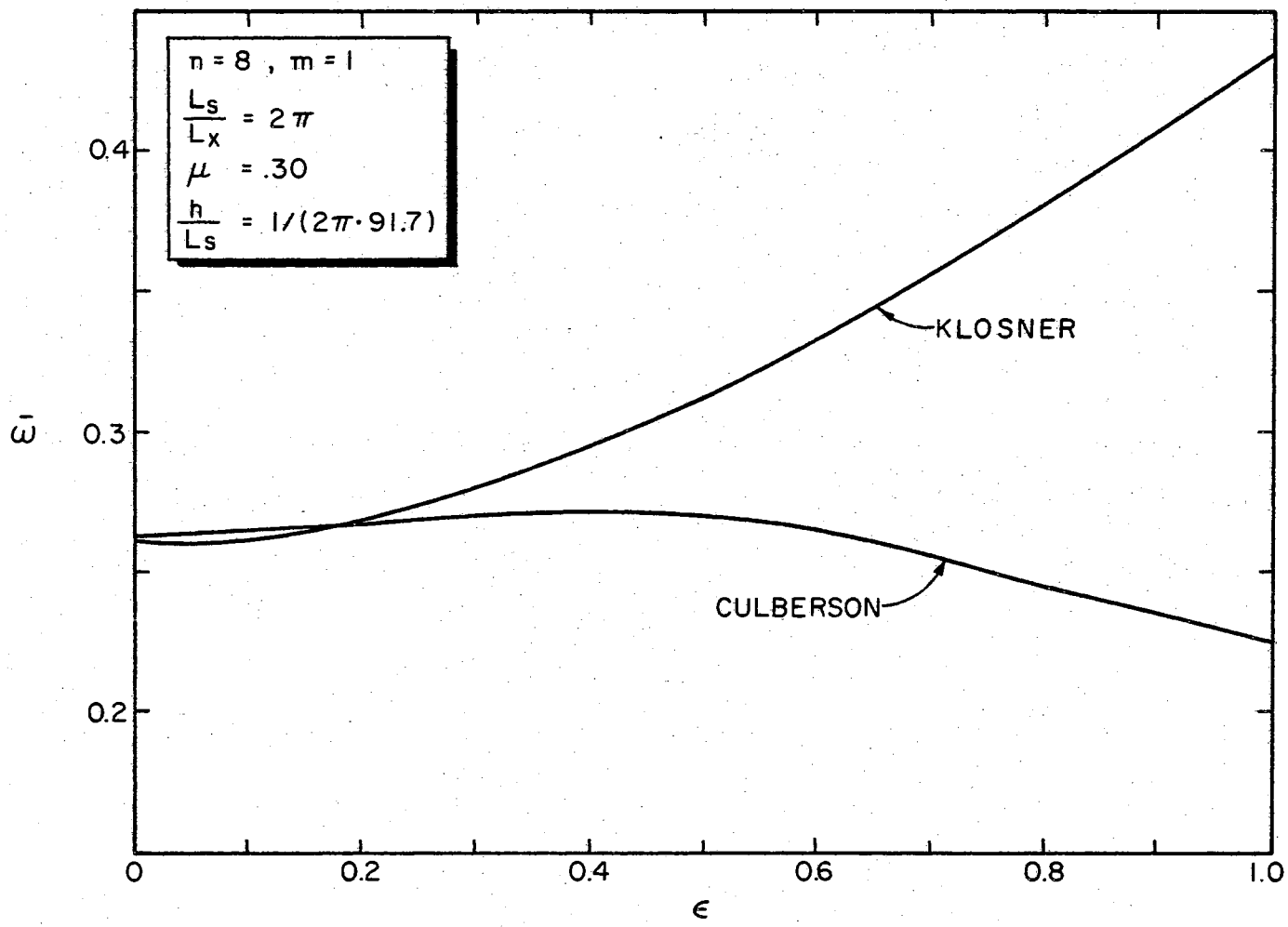

Figure 7. Nondimensional Frequency ($\bar{\omega}$) Versus Eccentricity (n = 8, m = 1, Klosner and Culberson)

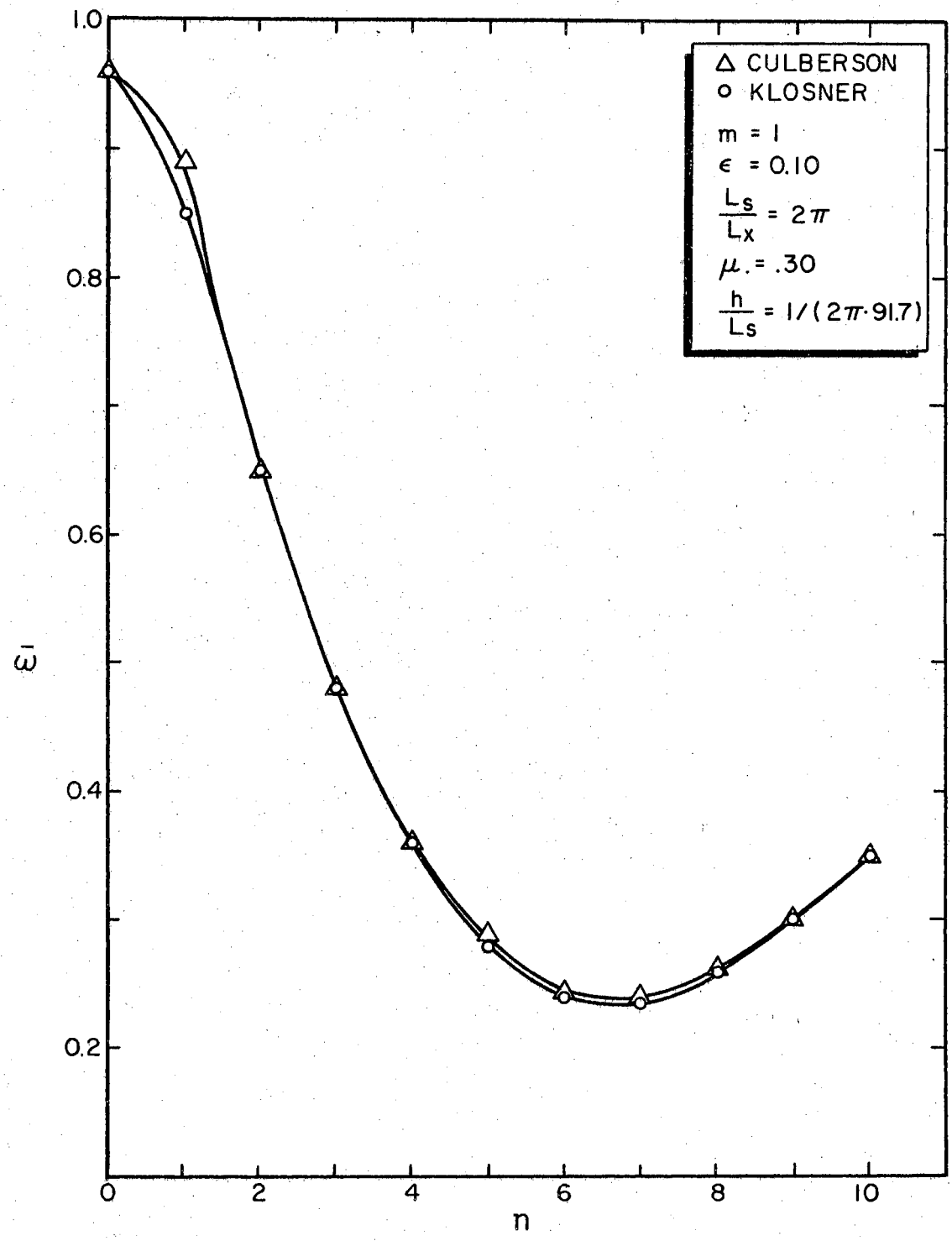

Figure 8. Nondimensional Frequency ($\bar{w}$) Versus Mode Number n (ϵ = 0.10, Klosner and Culberson)

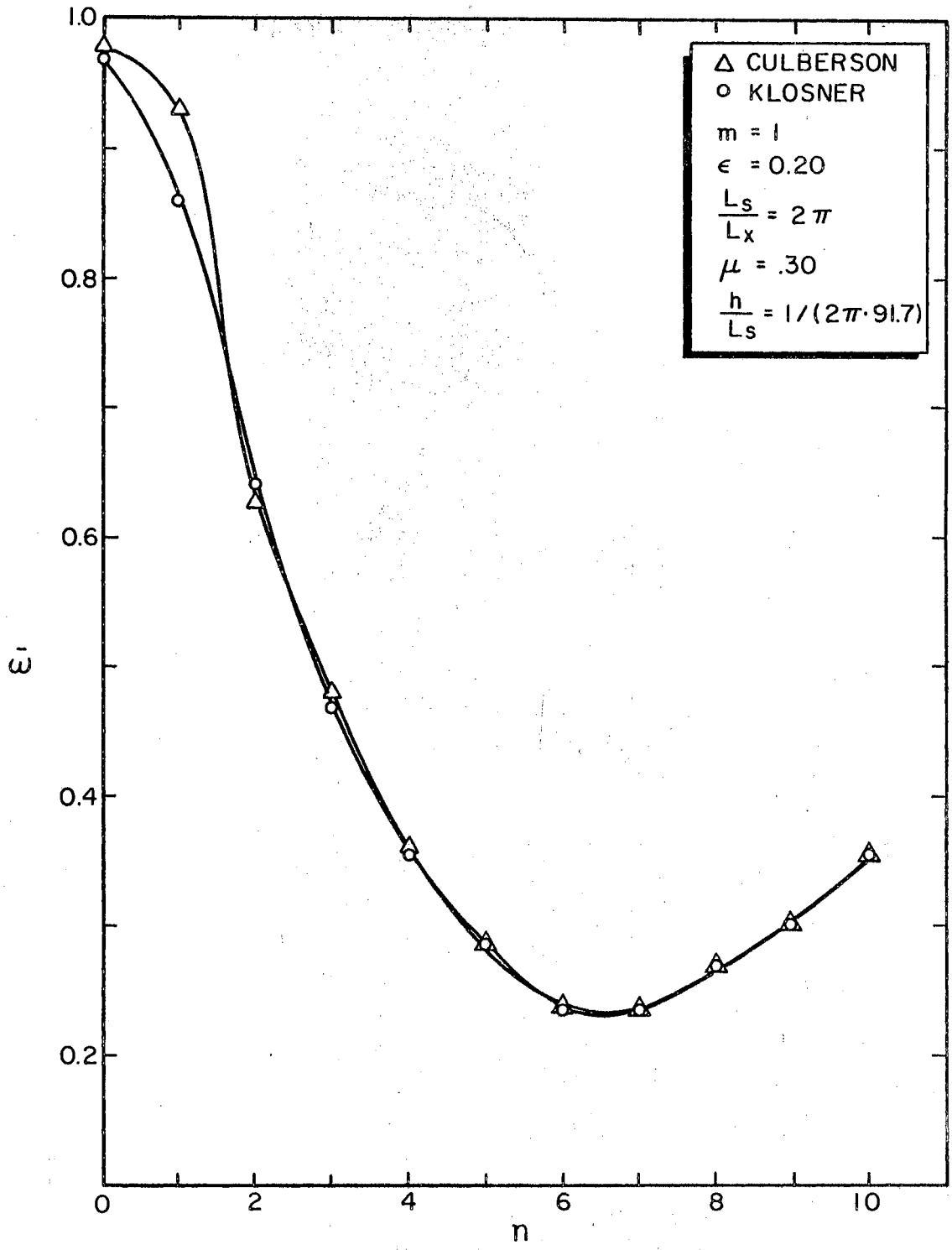

Figure 9. Nondimensional Frequency ($\bar{\omega}$) Versus Mode Number n (ϵ = 0.20, Klosner and Culberson)

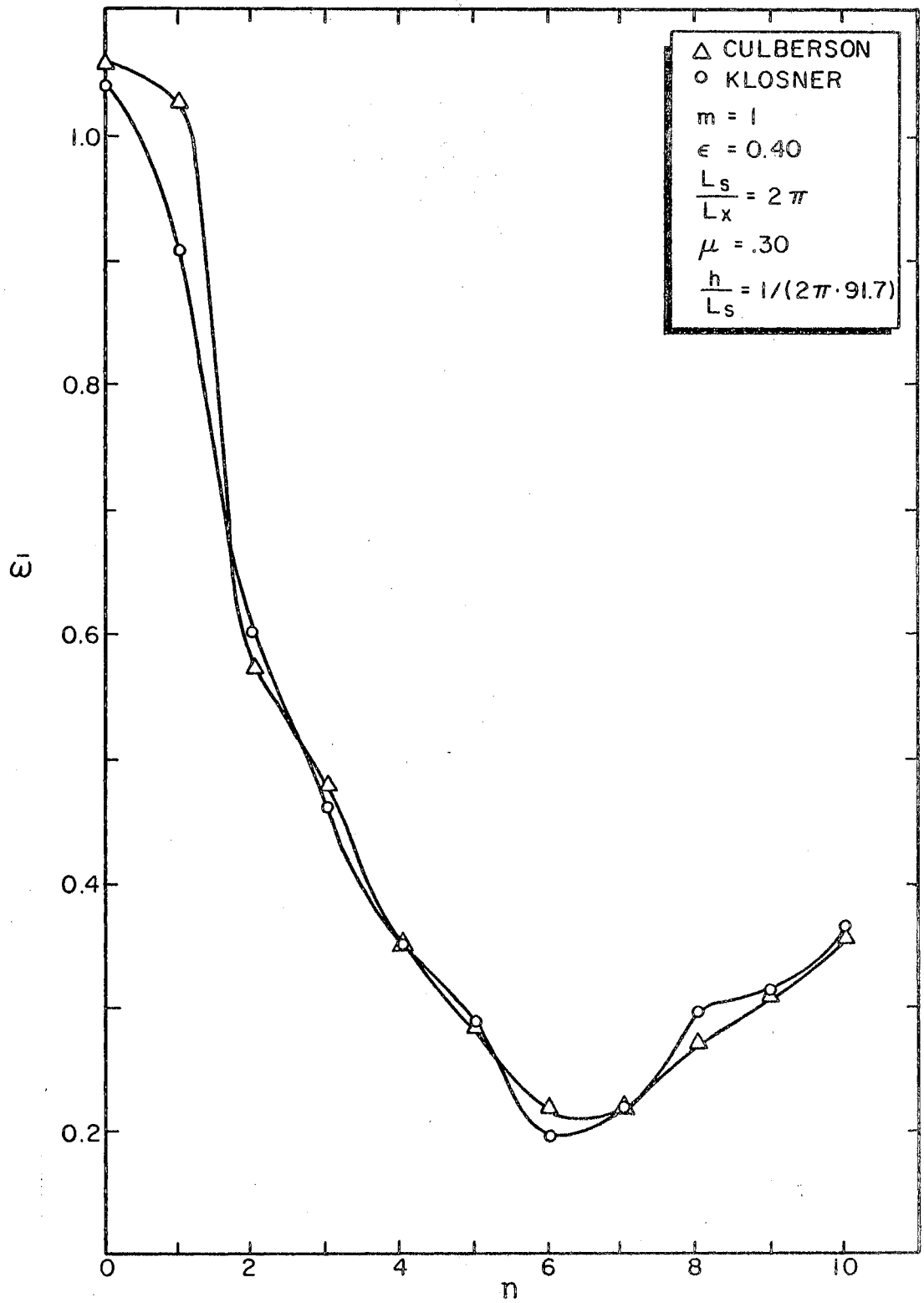

Figure 10. Nondimensional Frequency ($\bar{\omega}$) Versus Mode Number n (ϵ = 0.40, Klosner and Culberson)

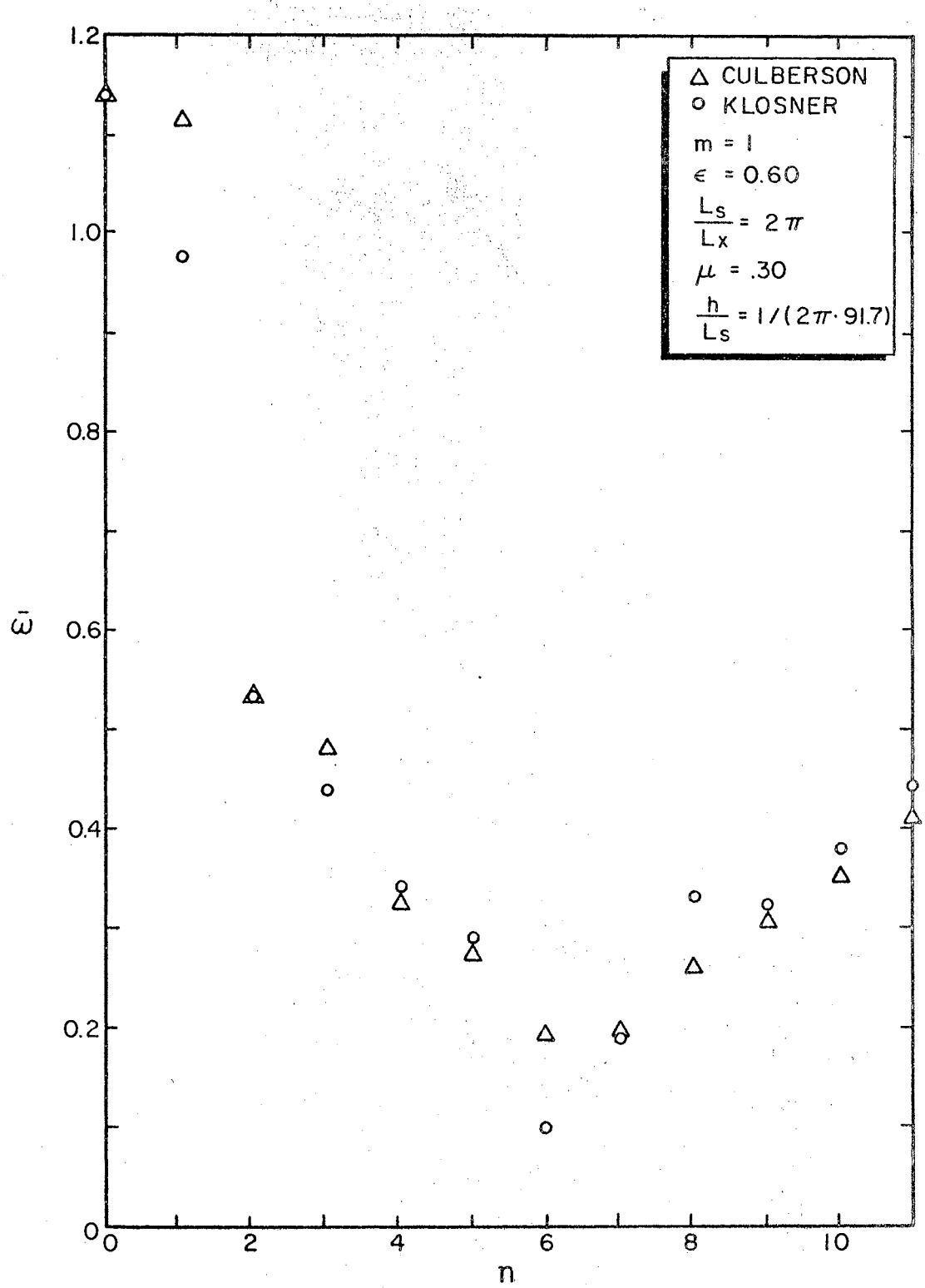

Figure 11. Nondimensional Frequency ($\bar{\omega}$) Versus Mode Number n (ϵ = 0.60, Klosner and Culberson)

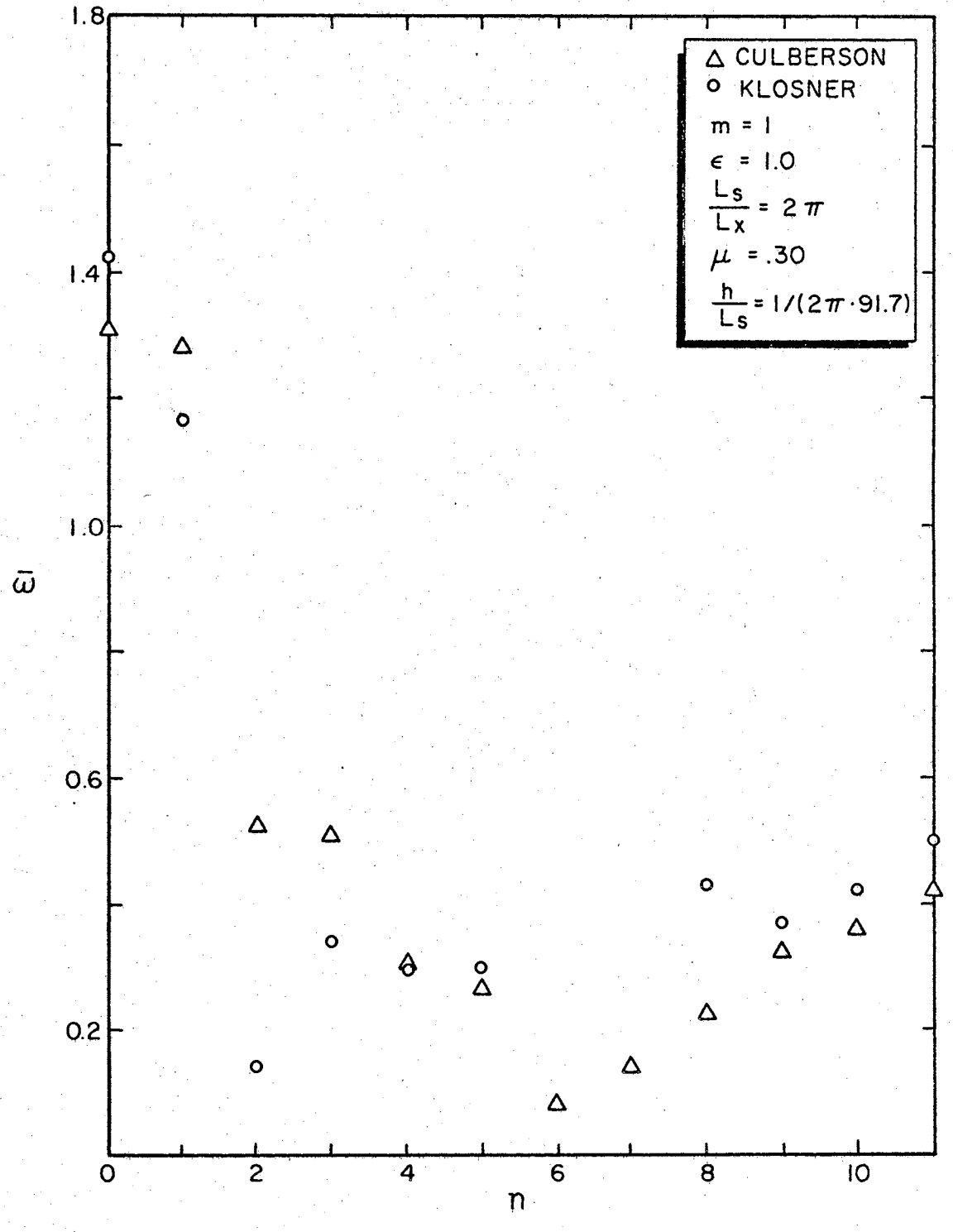

Figure 12. Nondimensional Frequency ($\bar{\omega}$) Versus Mode Number n (ϵ = 1.00, Klosner and Culberson)

assumed solution for the frequency should include the odd terms of the series.

Klosner states that the flexural modes are not affected by the sign of ϵ. Evidently, this is not true. The example case of $|\epsilon| = 0.50$ was studied to verify this conclusion. The odd numbered frequencies (i.e., n = 1, 3, 5, ...) changed, but the even numbered frequencies (i.e., n = 2, 4, 6, ...) remained the same. He also states that the anti-symmetric displacement expressions lead to the identical expressions for the constant (C_{2i1}) in the series (Equation (1.4)), and therefore the same frequency. Evidently, this is not true. The results are shown in Table IV.

These results show that for $+\epsilon$, n = 2, 4, 6, ..., and symmetric displacement expressions, the same frequencies are obtained for $-\epsilon$. For $+\epsilon$, n = 2, 4, 6, ..., and anti-symmetric displacement expressions, the same frequencies are obtained for $-\epsilon$. For $+\epsilon$, n = 1, 3, 5, ..., and symmetric displacement expressions, the same frequencies are obtained for $-\epsilon$ and anti-symmetric displacement expressions. For $+\epsilon$, n = 1, 3, 5, ..., and anti-symmetric displacement expressions, the same frequencies are obtained for $-\epsilon$ and symmetric displacement expressions. Displacements are symmetric and anti-symmetric with respect to the vertical axis in both cases of $+\epsilon$ and $-\epsilon$.

Because the frequencies of Klosner's were quite different, the corresponding mode shapes would also be different. Therefore the mode shapes were not compared. The mode shapes obtained by the exact method are very interesting. The mode shapes vary a great deal as the eccentricity increases. Figures 13 and 14 show the variation in two of the symmetric mode shapes as the eccentricity increases. These

TABLE IV

NONDIMENSIONAL FREQUENCIES ($\bar{\omega}$) FOR SYMMETRIC AND ANTI-SYMMETRIC CASES ($|\epsilon| = 0.50$).

	$L_s/L_x = 2\pi$		$h/L_s = 1/(2\pi \cdot 91.7)$		m = 1	
	$\epsilon = 0.50$		$\epsilon = -0.50$		$\epsilon = 0.50$	$\epsilon = -0.50$
n	Symmetric		Symmetric		Anti-Symmetric	Anti-Symmetric
0	1.09797		1.09797		1.01268	1.01268
1	1.07067		0.74000		0.74000	1.07067
2	0.54898		0.54898		0.69257	0.69257
3	0.48080		0.42624		0.42624	0.48080
4	0.33789		0.33789		0.35395	0.35395
5	0.28024		0.27569		0.27569	0.28024
6	0.20638		0.20638		0.20810	0.20810
7	0.20817		0.20655		0.20655	0.20817
8	0.27003		0.27003		0.27152	0.27152
9	0.30965		0.30899		0.30899	0.30965
10	0.35630		0.35630		0.35735	0.35735
11	0.41696		0.41696		0.41696	0.41696
12	0.48658		0.48658		0.48658	0.48658
13	0.56371		0.56371		0.56371	0.56371
14	0.64779		0.64779		0.64779	0.64779

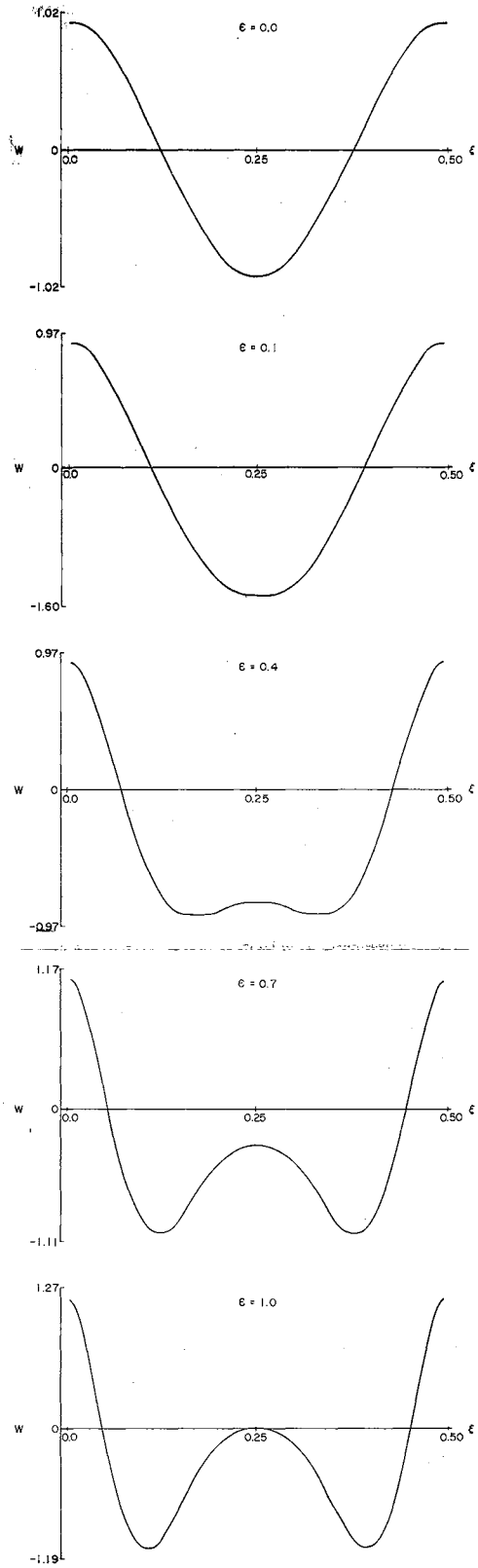

Figure 13. Mode Shapes (n = 2, m = 1, Klosner Comparison

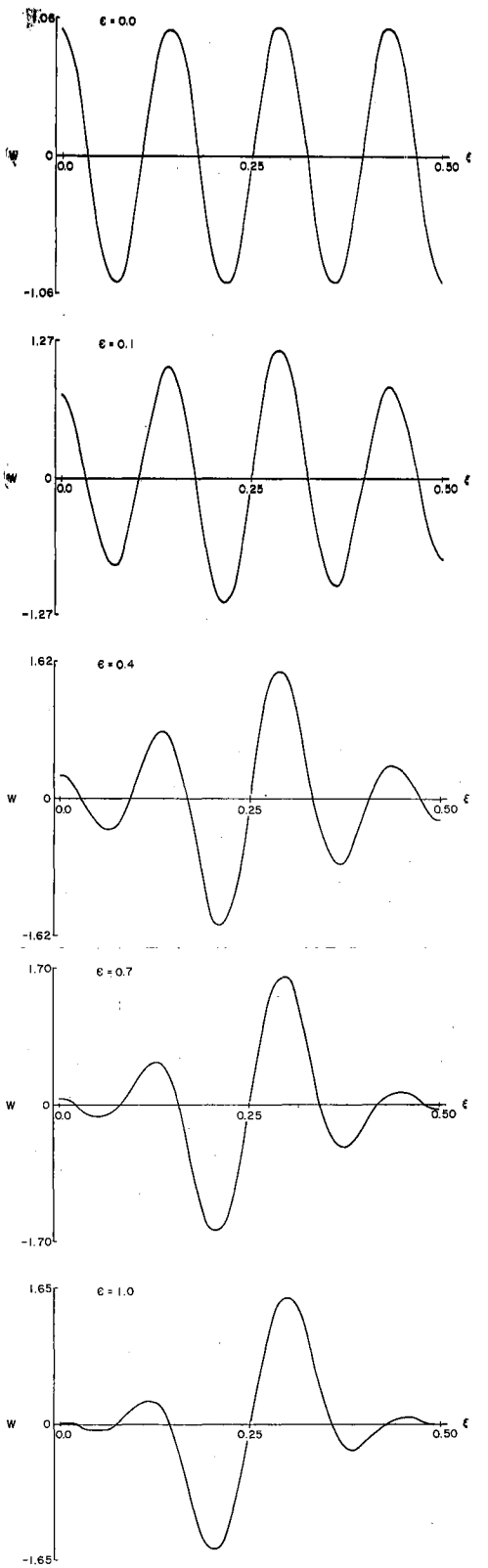

Figure 14. Mode Shapes (n = 7, m = 1, Klosner Comparison

mode shapes are only for the radial displacement.

Results obtained by the use of Donnell's equations are from 0 to 1% higher than those obtained by Love's equations. A comparison between Donnell's and Love's equations is studied more thoroughly in Section 4.5.

The author's method was further verified because of the differences encountered in Klosner's and the author's results. Because the oval approximates an ellipse, an elliptic cross-section was studied. Sewall (21), presently, is studying (both theoretically and experimentally) the natural frequencies of freely supported elliptical shells. He is studying the following cases:

$$L_s = 75.4"$$

$$L_x = 24.0"$$

$$h = 0.032"$$

$$E = 10^7 \text{ psi}$$

$$\mu = 0.30$$

$$\rho = 2.588\ 10^{-4} \text{ lbs-sec}^2/\text{in}^4 \text{ (6061 Al)}$$

Case I : $a = b = 12"$

Case II : $a = 12.95"$; $b = 11.01"$

Case III: $a = 14.39"$; $b = 9.35"$.

With the following transformations (23),

$$p = (b/a - 1)/(b/a + 1)$$

$$\epsilon = 3p - 36/35\ p^3 ,$$

Sewall's ellipses correspond to ovals with eccentricities of 0.0, -0.24236, and -0.62706, respectively. The results are shown in Table V. These frequencies are the natural frequencies $\lambda/2\pi$ in cycles

TABLE V

COMPARISON OF NATURAL FREQUENCIES (CPS) OBTAINED BY SEWALL AND BY CULBERSON

a = b = 12"

m	n	Sewall	Culberson
1	3	529.8	529.9
	7	162.2	163.5
	10	221.3	223.3
2	4	968.4	968.5
	10	325.7	327.1
	12	361.0	362.9

a = 12.95" b = 11.01"

		Symmetric		Anti-Symmetric	
m	n	Sewall	Culberson	Sewall	Culberson
1	3	524.1	522.0	524.2	526.3
	7	157.1	157.8	157.0	157.8
	10	221.9	223.9	221.9	223.9
2	4	956.5	954.8	956.7	957.9
	10	310.6	310.4	310.6	310.4
	12	359.4	363.2	359.4	363.2

a = 14.39" b = 9.35"

		Symmetric		Anti-Symmetric	
m	n	Sewall	Culberson	Sewall	Culberson
1	3	491.2	459.7	492.4	521.5
	7	138.5	129.6	138.5	131.3
	10	223.9	227.0	223.9	227.1
2	4	886.1	828.2	893.0	929.4
	10	268.1	245.7	268.1	246.7
		328.2	336.1		
	12	382.3	391.7	328.2	337.8
				382.3	393.3

per second. Love's equations have been used for the author's work. For the desired accuracy, convergence was attained with k = 25.

The question that may now arise is "Why for Case III, m = 2, are there two frequencies for n = 10 in the symmetric case, and two frequencies for n = 12 in the anti-symmetric case?". By the method of counting described in Chapter III, these are the results. This is the same method used by Sewall. But with the author's additional technique, the upper n = 10 frequency, symmetric case, is actually the frequency for n = 12 and the frequency at n = 12 is actually the frequency for n = 8. For the anti-symmetric case, the upper n = 12 frequency is actually the frequency for n = 8.

Comparing the results of the elliptical and oval shells for Case I, ϵ = 0.0, the results are seen to be very close; the greatest deviation being 0.9%. For Case II, ϵ = -0.24236, the frequencies obtained for the oval deviate from -0.4% to +0.8% from those of the ellipse. These results are considered accurate. For Case III, ϵ = -0.62806, the frequencies obtained for the oval deviate from -9.1% to +5.9%. This error would increase as the eccentricity increases because the oval deviates more from the ellipse as ϵ increases. But the results are still good, considering that Sewall used an ellipse and an approximate procedure, and the author used an oval and an exact procedure in solving for the natural frequencies. Because the author's results have been verified for both circular and noncircular shells, the noncircular (oval) shell will now be studied in more depth.

4.4 Freely Supported Oval Shells

A detailed study was made of oval shells having the same properties as those of Sewall's elliptical shells; that is, shells having the same longitudinal and circumferential lengths and thicknesses. This study was restricted to a thorough investigation of the symmetric modes for only positive values of the eccentricity parameter ϵ--the restriction made because of computer time. Love's equations were used in this detailed study. The eccentricity parameter (ϵ) was varied from 0.0 - 1.0; the longitudinal mode m from 1 - 4; and the circumferential mode n from 0 - 12,16. Values of n varied between 12 and 16 in order to include the lowest frequency and a few of the higher frequencies near this lowest value of $\bar{\omega}$. These are shown in Figures 19 through 22. It was desired to use higher values of m, but, due to computer space and time limitations, m = 4 was the largest feasible value. For the accuracy desired, adequate convergence for m = 1-3 was attained with k = 25; for m = 4, k = 27.

Tables VI through IX give the values of the nondimensional frequency $\bar{\omega}$ for the values of m = 1 - 4. Figures 15 through 18 show the frequency ($\bar{\omega}$) variation with the eccentricity ϵ and mode number m for a few selected values of n. As the value of m increases, the frequencies ($\bar{\omega}$) do not vary monotonically. Figures 17 and 18 show that the frequencies (for high values of eccentricity) decrease with the value of m and subsequently increase.

Figures 19 through 22 show the frequency ($\bar{\omega}$) variation with the mode number n and m for a few selected values of ϵ. As the value of eccentricity (ϵ) increases, the curves become more irregular. This irregularity can be partially attributed to the symmetric forms being

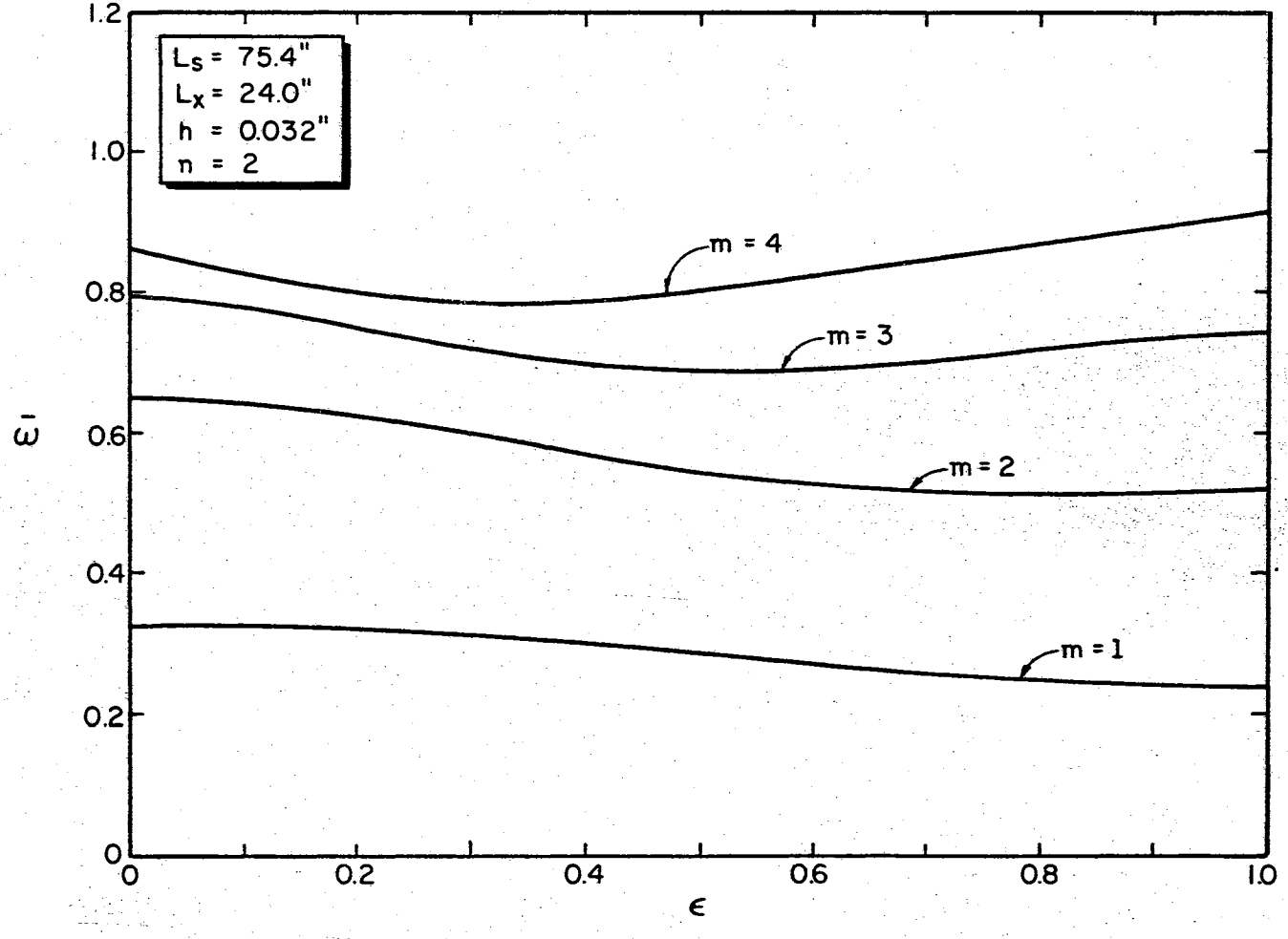

Figure 15. Nondimensional Frequency ($\bar{\omega}$) Versus Eccentricity (n = 2)

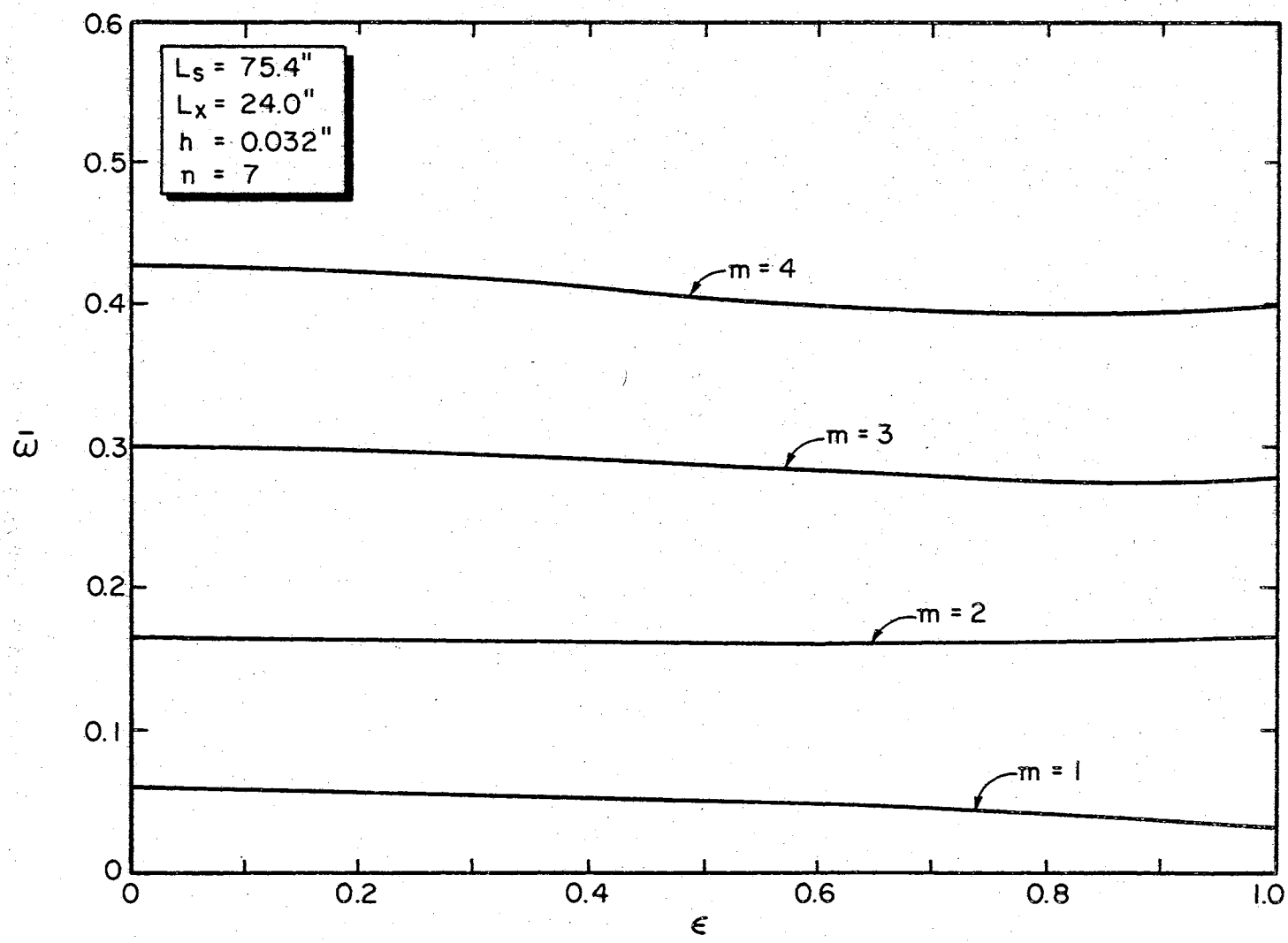

Figure 16. Nondimensional Frequency ($\bar{\omega}$) Versus Eccentricity (n = 7)

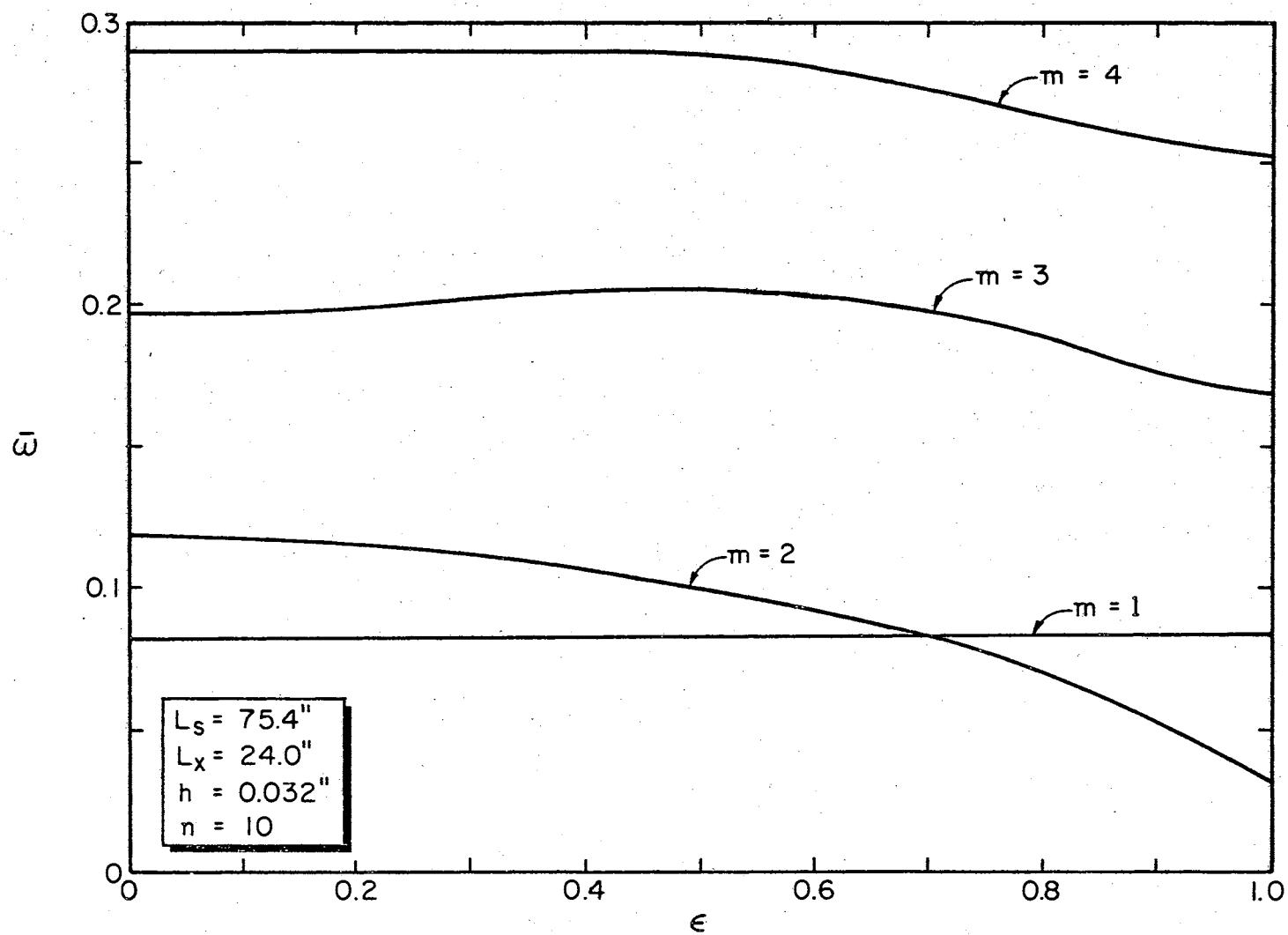

Figure 17. Nondimensional Frequency ($\bar{\omega}$) Versus Eccentricity (n = 10)

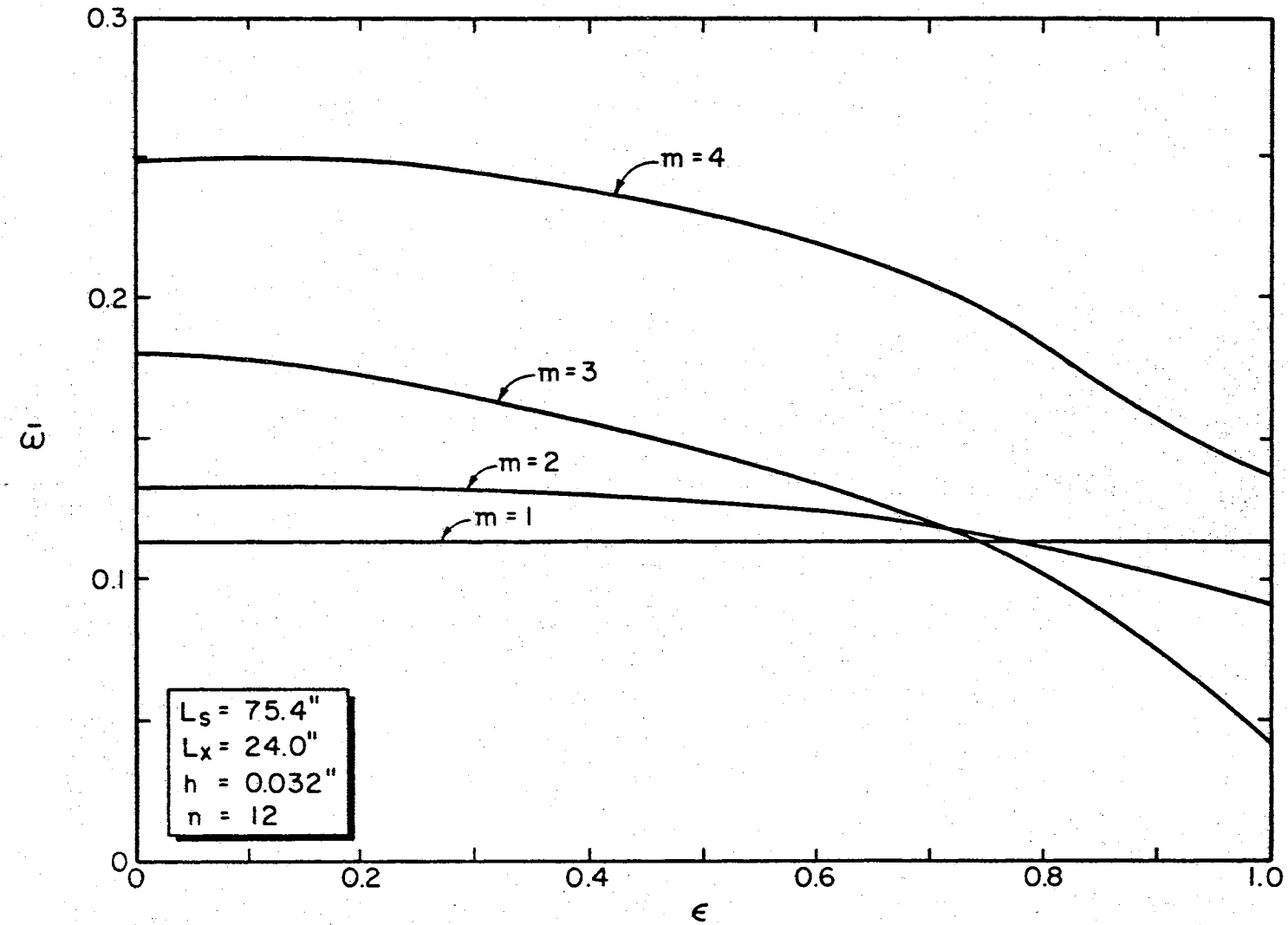

Figure 18. Nondimensional Frequency ($\bar{\omega}$) Versus Eccentricity (n = 12)

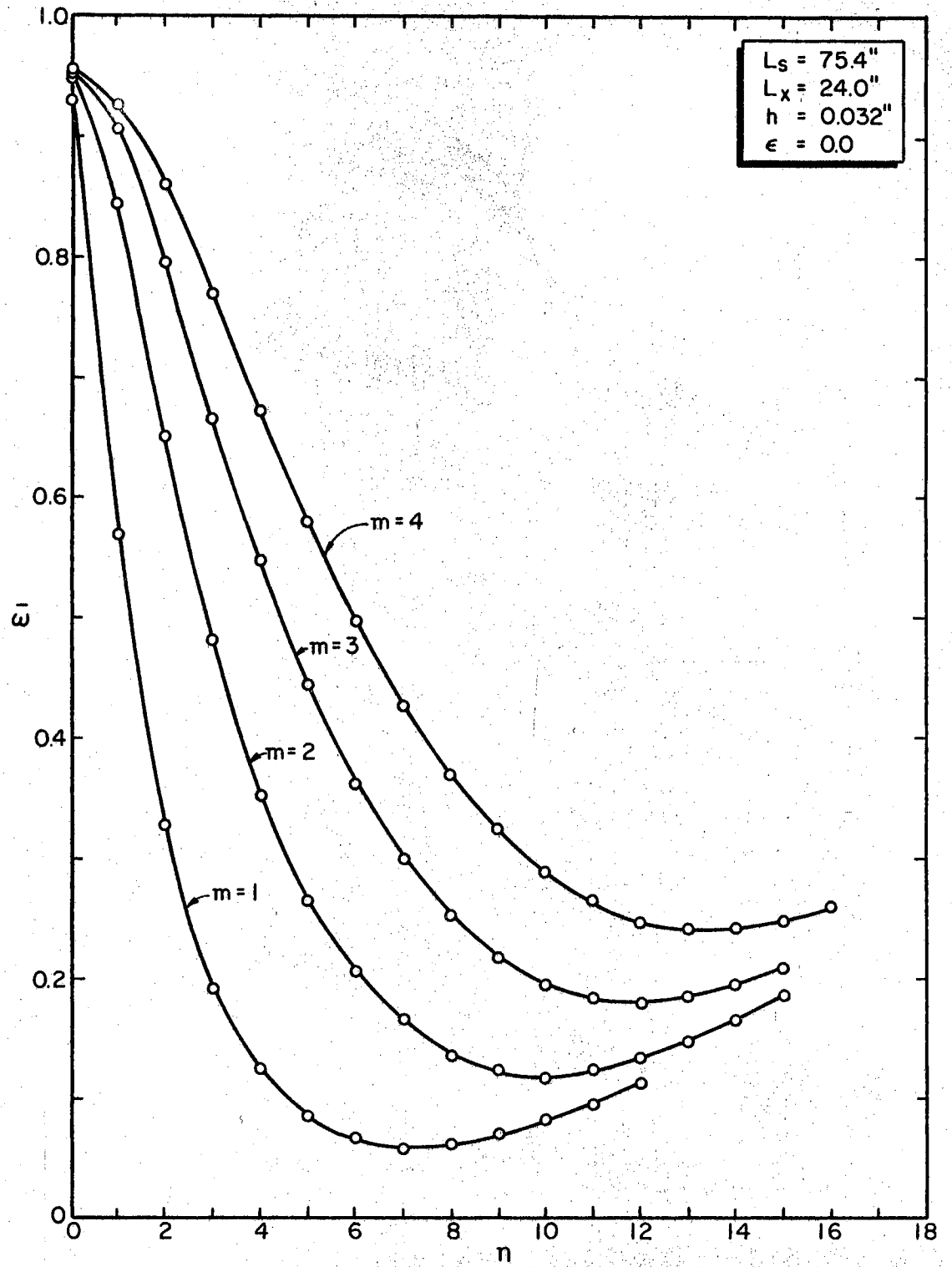

Figure 19. Symmetric Nondimensional Frequency ($\bar{\omega}$) Versus Mode Number n (ϵ = 0.00)

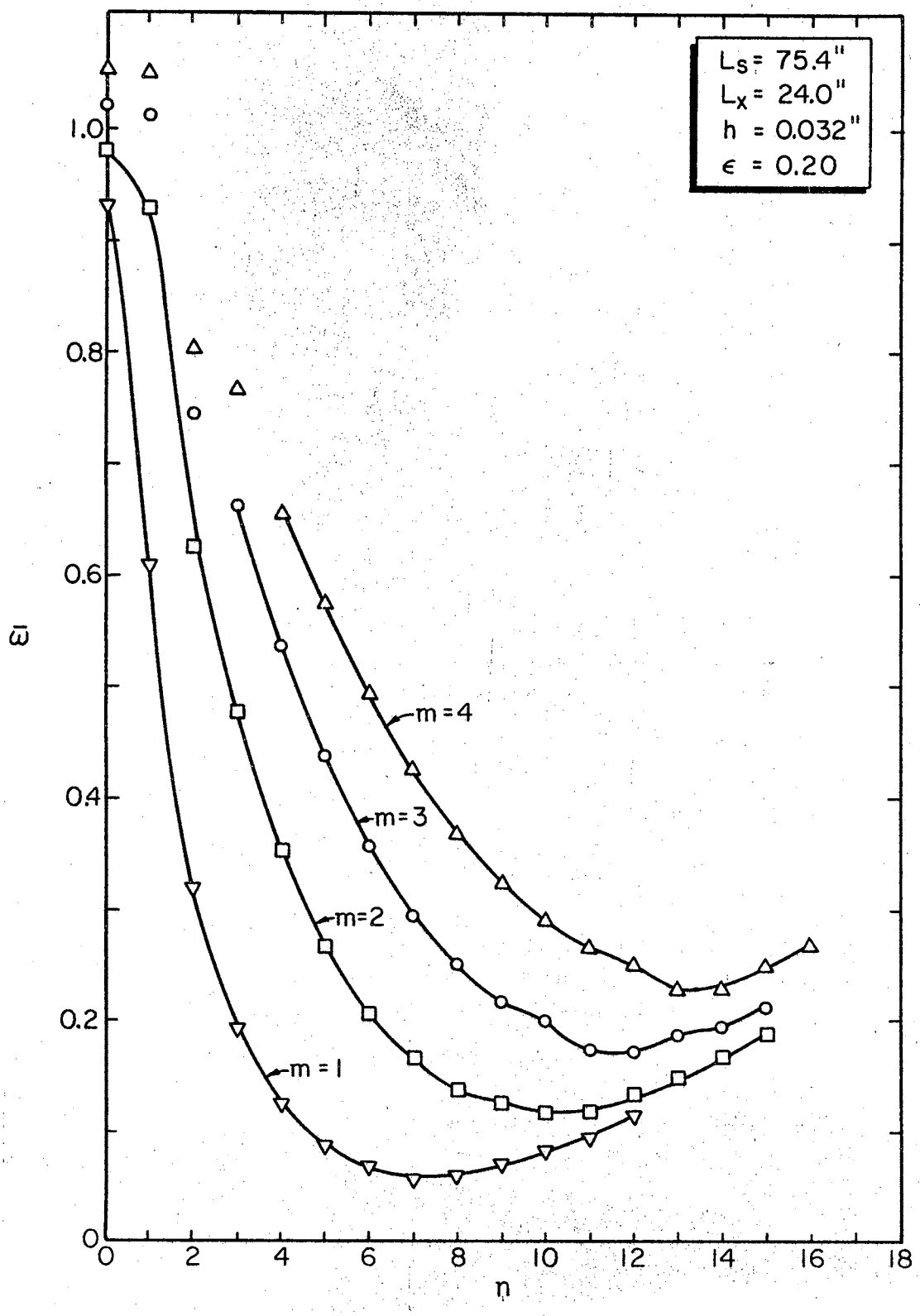

Figure 20. Symmetric Nondimensional Frequency ($\bar{\omega}$) Versus Mode Number n (ϵ = 0.20)

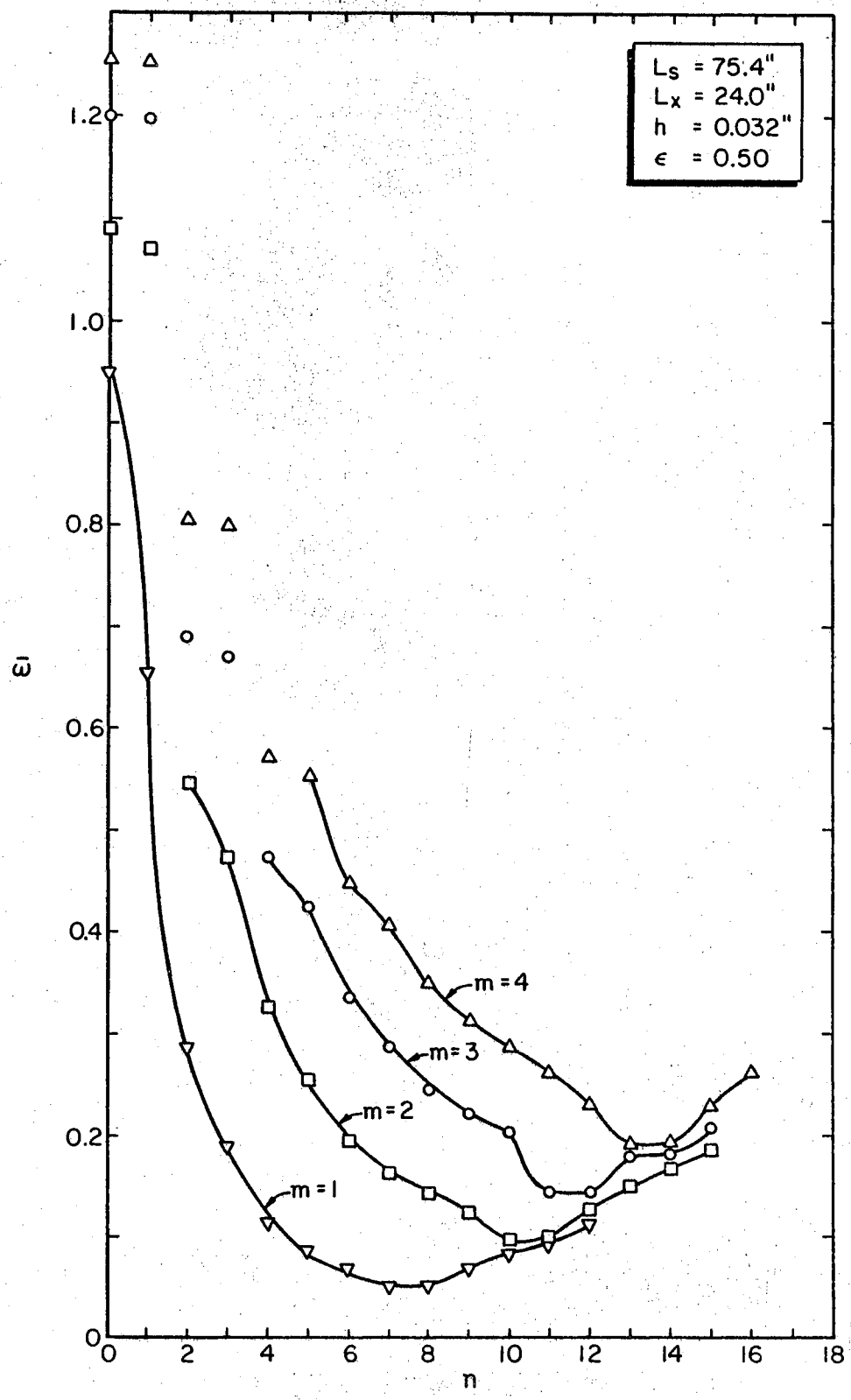

Figure 21. Symmetric Nondimensional Frequency ($\bar{\omega}$) Versus Mode Number n (ϵ = 0.50)

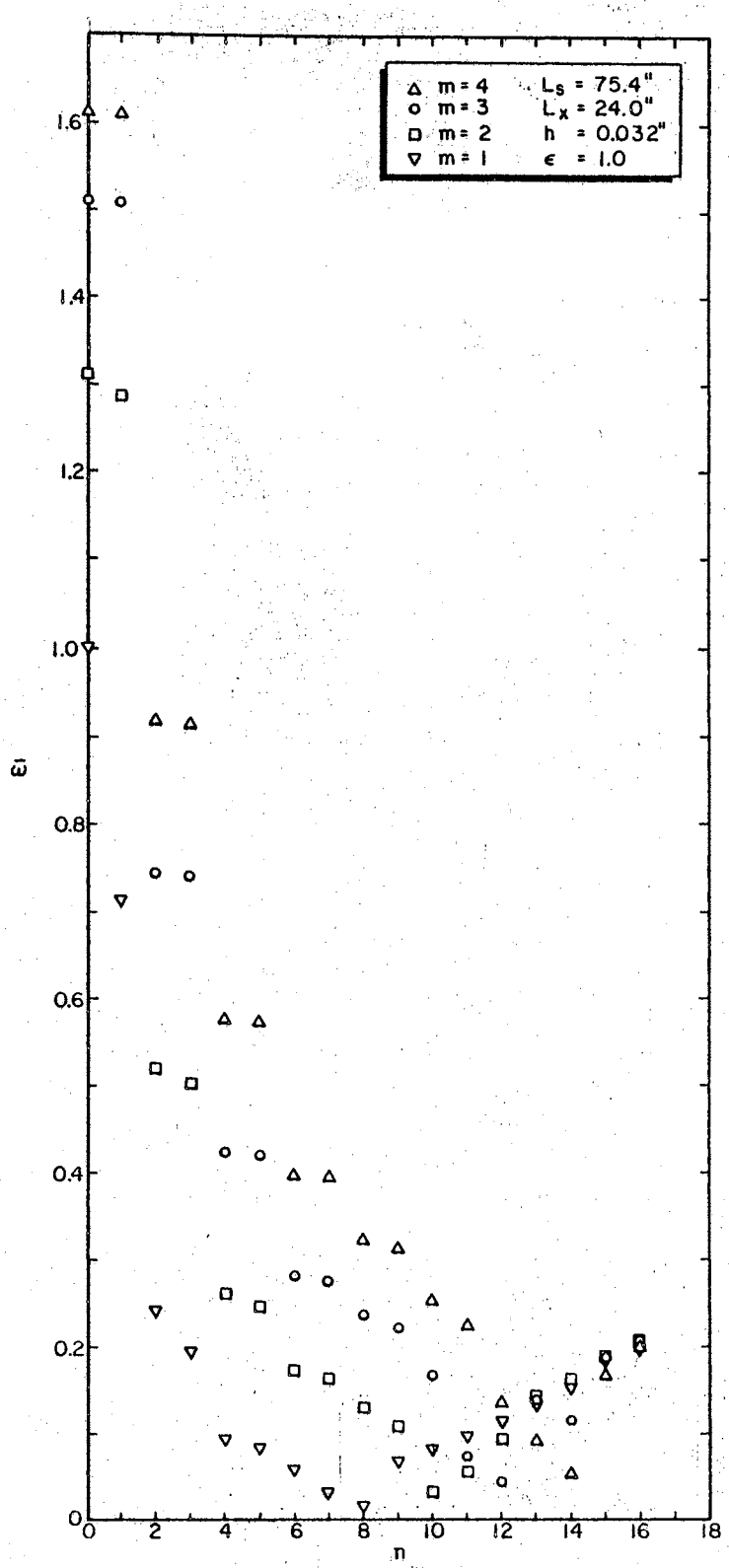

Figure 22. Symmetric Nondimensional Frequency ($\bar{\omega}$) Versus Mode Number n (ϵ = 1.00)

TABLE VI

SYMMETRIC NONDIMENSIONAL FREQUENCIES ($\bar{\omega}$) OF AN OVAL CYLINDRICAL SHELL (m = 1)

m = 1				L_s = 75.4"			L_x = 24.0"			h = 0.032"	
ϵ / n	0.0	0.1	0.2	0.3	0.4	0.5	0.6	0.7	0.8	0.9	1.0
0	0.92828	0.92913	0.93163	0.93570	0.94122	0.94806	0.95610	0.96522	0.97538	0.98654	0.99869
1	0.57277	0.59122	0.60902	0.62591	0.64175	0.65646	0.67001	0.68244	0.69378	0.70411	0.71349
2	0.32718	0.32532	0.31987	0.31128	0.30024	0.28770	0.27481	0.26284	0.25288	0.24571	0.24164
3	0.19391	0.19361	0.19292	0.19210	0.19137	0.19089	0.19078	0.19109	0.19187	0.19310	0.19477
4	0.12399	0.12380	0.12318	0.12202	0.12013	0.11728	0.11332	0.10836	0.10307	0.09868	0.09626
5	0.08638	0.08630	0.08608	0.08574	0.08533	0.08494	0.08466	0.08456	0.08467	0.08497	0.08544
6	0.06697	0.06725	0.06783	0.06836	0.06864	0.06855	0.06799	0.06681	0.06489	0.06243	0.06013
7	0.05984	0.05946	0.05839	0.05673	0.05458	0.05197	0.04893	0.04546	0.04162	0.03749	0.03321
8	0.06170	0.06114	0.05970	0.05770	0.05526	0.05234	0.04879	0.04428	0.03817	0.02972	0.01909
9	0.06970	0.06983	0.07015	0.07051	0.07076	0.07080	0.07060	0.07007	0.06937	0.06856	0.06776
10	0.08172	0.08175	0.08185	0.08203	0.08228	0.08260	0.08297	0.08333	0.08358	0.08362	0.08342
11	0.09651	0.09653	0.09657	0.09663	0.09672	0.09684	0.09699	0.09717	0.09739	0.09764	0.09794
12	0.11347	0.11348	0.11350	0.11352	0.11356	0.11362	0.11368	0.11375	0.11384	0.11394	0.11405

TABLE VII

SYMMETRIC NONDIMENSIONAL FREQUENCIES ($\bar{\omega}$) OF AN OVAL CYLINDRICAL SHELL (m = 2)

m = 2				L_s = 75.4"			L_x = 24.0"		h = 0.032"		
ϵ / n	0.0	0.1	0.2	0.3	0.4	0.5	0.6	0.7	0.8	0.9	1.0
0	0.94922	0.95808	0.98202	1.01584	1.05525	1.09752	1.14101	1.18473	1.22803	1.27047	1.31174
1	0.84498	0.88673	0.93126	0.97725	1.02379	1.07020	1.11597	1.16069	1.20406	1.24581	1.28573
2	0.65220	0.64447	0.62423	0.59756	0.57024	0.54665	0.52943	0.51922	0.51510	0.51564	0.51957
3	0.48113	0.48014	0.47818	0.47645	0.47574	0.47644	0.47872	0.48254	0.48777	0.49423	0.50172
4	0.35437	0.35362	0.35111	0.34612	0.33760	0.32471	0.30794	0.29009	0.27513	0.26546	0.26081
5	0.26582	0.26535	0.26397	0.26173	0.25883	0.25562	0.25253	0.24999	0.24831	0.24764	0.24800
6	0.20515	0.20486	0.20397	0.20244	0.20008	0.19654	0.19118	0.18359	0.17552	0.17240	0.17300
7	0.16434	0.16421	0.16382	0.16320	0.16241	0.16162	0.16115	0.16124	0.16187	0.16285	0.16400
8	0.13833	0.13852	0.13930	0.14066	0.14209	0.14313	0.14342	0.14247	0.13968	0.13526	0.13098
9	0.12413	0.12631	0.12795	0.12851	0.12795	0.12632	0.12370	0.12026	0.11622	0.11193	0.10782
10	0.11970	0.11847	0.11531	0.11092	0.10561	0.09941	0.09213	0.08325	0.07139	0.05400	0.03081
11	0.12320	0.12019	0.11606	0.11125	0.10575	0.09950	0.09237	0.08422	0.07497	0.06472	0.05397
12	0.13278	0.13306	0.13315	0.13227	0.13045	0.12780	0.12419	0.11916	0.11183	0.10212	0.09307
13	0.14691	0.14703	0.14740	0.14800	0.14870	0.14921	0.14914	0.14831	0.14687	0.14518	0.14351
14	0.16446	0.16452	0.16468	0.16497	0.16537	0.16592	0.16657	0.16722	0.16719	0.16434	0.16139
15	0.18473	0.18476	0.18484	0.18499	0.18520	0.18548	0.18582	0.18623	0.18673	0.18730	0.18795

TABLE VIII

SYMMETRIC NONDIMENSIONAL FREQUENCIES ($\bar{\omega}$) OF AN OVAL CYLINDRICAL SHELL (m = 3)

	m = 3			L_s = 75.4"			L_x = 24.0"			h = 0.032"	
c / n	0.0	0.1	0.2	0.3	0.4	0.5	0.6	0.7	0.8	0.9	1.0
0	0.95208	0.97321	1.02020	1.07667	1.13685	1.19866	1.26112	1.32370	1.38606	1.44796	1.50920
1	0.90723	0.95689	1.01316	1.07292	1.13451	1.19699	1.25982	1.32260	1.38506	1.44700	1.50824
2	0.79762	0.78049	0.74669	0.71585	0.69655	0.68975	0.69222	0.70059	0.71268	0.72718	0.74333
3	0.66747	0.66552	0.66292	0.66263	0.66579	0.67244	0.68215	0.69436	0.70851	0.72416	0.74095
4	0.54567	0.54393	0.53764	0.52406	0.50163	0.47417	0.44963	0.43368	0.42616	0.42432	0.42602
5	0.44340	0.44236	0.43929	0.43453	0.42892	0.42358	0.41952	0.41737	0.41728	0.41909	0.42253
6	0.36207	0.36136	0.35920	0.35530	0.34887	0.33827	0.32199	0.30289	0.28869	0.28234	0.28144
7	0.29939	0.29892	0.29749	0.29506	0.29168	0.28756	0.28331	0.27973	0.27755	0.27704	0.27809
8	0.25240	0.25213	0.25131	0.24995	0.24797	0.24522	0.24145	0.23831	0.23805	0.23867	0.23937
9	0.21857	0.21856	0.21860	0.21896	0.22001	0.22159	0.22305	0.22399	0.22431	0.22415	0.22370
10	0.19608	0.19704	0.19991	0.20269	0.20437	0.20447	0.20255	0.19756	0.18803	0.17690	0.16828
11	0.18357	0.17826	0.17166	0.16397	0.15523	0.14534	0.13409	0.12117	0.10636	0.08981	0.07261
12	0.17983	0.17724	0.17137	0.16389	0.15521	0.14531	0.13392	0.12025	0.10221	0.07561	0.04204
13	0.18356	0.18715	0.18850	0.18748	0.18442	0.17969	0.17349	0.16596	0.15745	0.14863	0.14033
14	0.19340	0.19359	0.19217	0.18932	0.18527	0.17998	0.17319	0.16396	0.15026	0.13230	0.11674
15	0.20813	0.20842	0.20924	0.21011	0.20997	0.20832	0.20533	0.20135	0.19680	0.19216	0.18779

TABLE IX

SYMMETRIC NONDIMENSIONAL FREQUENCIES ($\bar{\omega}$) OF AN OVAL CYLINDRICAL SHELL (m = 4)

	m = 4			L_s = 75.4"			L_x = 24.0"			h = 0.032"	
ε / n	0.0	0.1	0.2	0.3	0.4	0.5	0.6	0.7	0.8	0.9	1.0
0	0.95331	0.98688	1.04785	1.11506	1.18462	1.25529	1.32649	1.39790	1.46931	1.54058	1.61159
1	0.92854	0.98301	1.04686	1.11469	1.18444	1.25518	1.32642	1.39785	1.46927	1.54054	1.61156
2	0.86201	0.83261	0.80241	0.78724	0.78987	0.80272	0.82111	0.84278	0.86657	0.89181	0.91806
3	0.77128	0.76856	0.76755	0.77266	0.78395	0.80011	0.81983	0.84209	0.86615	0.89152	0.91785
4	0.67354	0.67024	0.65678	0.62927	0.59626	0.57196	0.56083	0.55895	0.56236	0.56896	0.57764
5	0.58037	0.57852	0.57322	0.56588	0.55891	0.55442	0.55337	0.55567	0.56079	0.56810	0.57710
6	0.49767	0.49640	0.49240	0.48463	0.47022	0.44674	0.42089	0.40425	0.39769	0.39686	0.39910
7	0.42749	0.42660	0.42388	0.41928	0.41302	0.40604	0.39986	0.39583	0.39445	0.39546	0.39838
8	0.36986	0.36925	0.36740	0.36417	0.35914	0.35098	0.33733	0.32305	0.31987	0.32162	0.32409
9	0.32402	0.32366	0.32259	0.32081	0.31837	0.31555	0.31310	0.31175	0.31141	0.31155	0.31185
10	0.28900	0.28896	0.28891	0.28896	0.28893	0.28793	0.28447	0.27640	0.26597	0.25795	0.25190
11	0.26395	0.26458	0.26627	0.26709	0.26572	0.26219	0.25670	0.24958	0.24160	0.23363	0.22628
12	0.24813	0.24977	0.24878	0.24460	0.23823	0.22991	0.21929	0.20475	0.18300	0.15748	0.13728
13	0.24075	0.23583	0.22685	0.21616	0.20403	0.19035	0.17483	0.15701	0.13660	0.11392	0.09108
14	0.24096	0.23595	0.22690	0.21618	0.20404	0.19034	0.17466	0.15592	0.13108	0.09516	0.05491
15	0.24774	0.24946	0.24879	0.24474	0.23836	0.23006	0.21989	0.20790	0.19460	0.18107	0.16862
16	0.26008	0.26103	0.26370	0.26578	0.26548	0.26233	0.25593	0.24430	0.22705	0.21170	0.20024

studied. If the value of ϵ is less than zero (i.e., studying forms symmetric about axis 2-2 in Figure 1), most of this irregularity is erased. This effect is shown in Figure 23. For small n, the odd mode number frequencies are lower for $-\epsilon$ than for $+\epsilon$, but converge to the same value as n increases. Figure 22 also shows the same effect as described for Figures 17 and 18. These figures show that the frequencies converge to the same value for different values of m as n increases. Also, these figures show, about the lowest frequency, a cupping effect which is not obtained for the circular cylinder. This effect becomes more apparent as the eccentricity increases.

Because all the mode shapes vary a great deal with changes in eccentricity ϵ, only a few are shown in Figures 24 through 29. Figures 24 through 27 show how the shapes vary with eccentricity, and Figures 28 and 29 show the variation with eccentricity and m. These mode shapes are only for the radial displacement w and for $0 \leq \xi \leq 0.50$, because the mode shapes are symmetric with respect to the vertical axis 1-1 in Figure 1. The mode shape n is identified as the number of full circumferential waves, and m as the number of half longitudinal waves.

As the oval shell becomes flatter (i.e., ϵ increases), the shells tend to bend more in the flatter regions and less in the regions of higher curvature, therefore causing the irregular shapes.

Because there was no available information on the mode shapes of oval cylindrical shells in the literature, only a subjective analysis was made. But, from similar analysis of circular shells, these shapes appear to be quite reasonable.

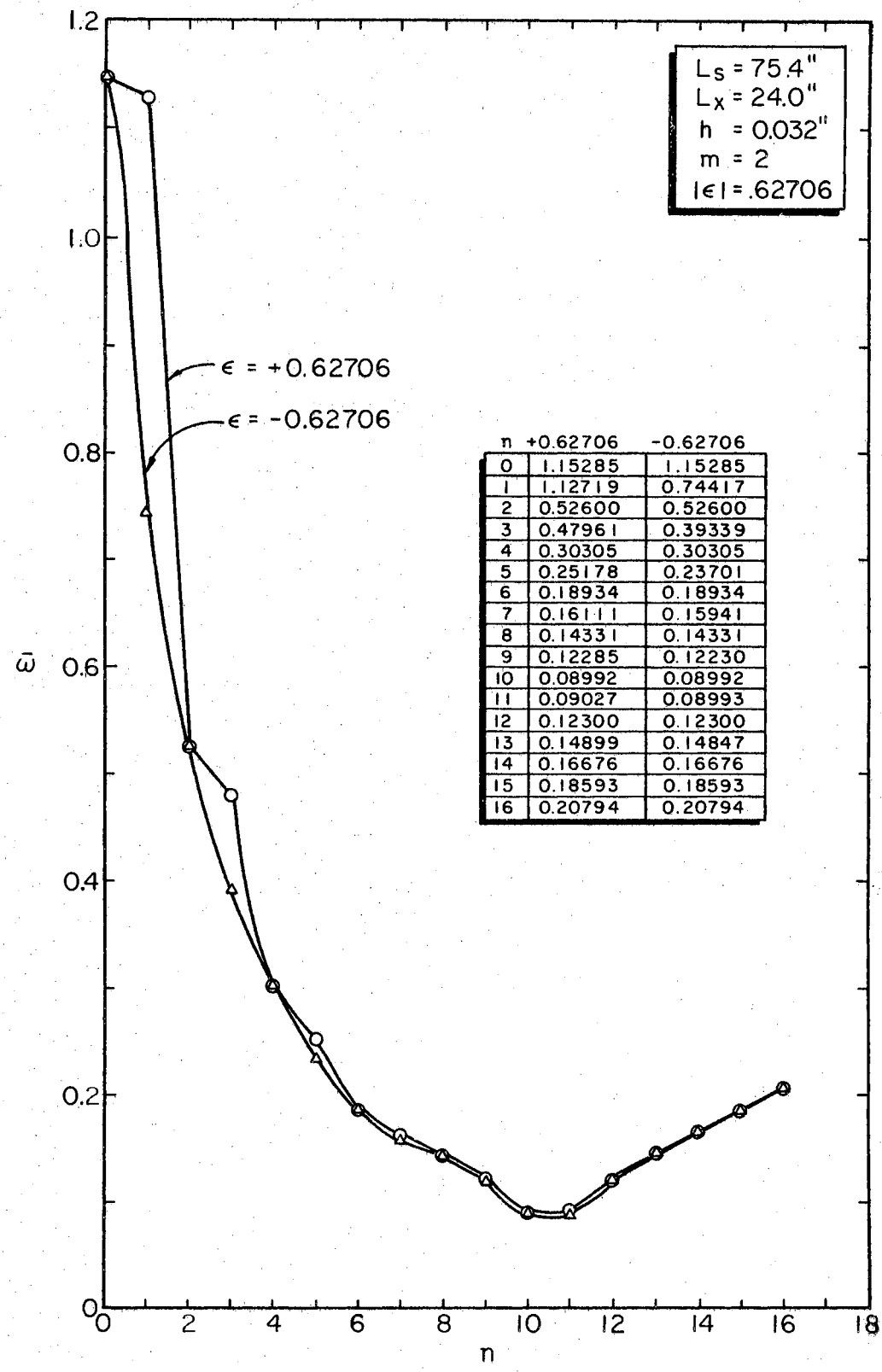

n	+0.62706	-0.62706
0	1.15285	1.15285
1	1.12719	0.74417
2	0.52600	0.52600
3	0.47961	0.39339
4	0.30305	0.30305
5	0.25178	0.23701
6	0.18934	0.18934
7	0.16111	0.15941
8	0.14331	0.14331
9	0.12285	0.12230
10	0.08992	0.08992
11	0.09027	0.08993
12	0.12300	0.12300
13	0.14899	0.14847
14	0.16676	0.16676
15	0.18593	0.18593
16	0.20794	0.20794

Figure 23. Comparison of Symmetric Nondimensional Frequencies ($\bar{\omega}$) Obtained with $\pm$ ϵ

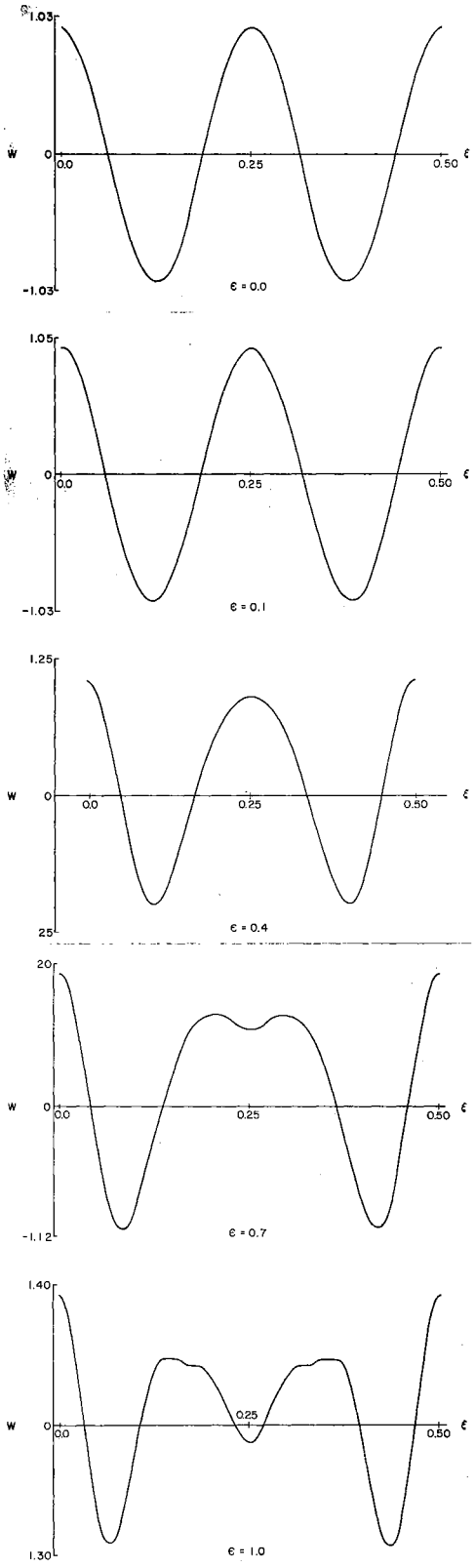

Figure 24. Mode Shapes (n = 4, m = 1)

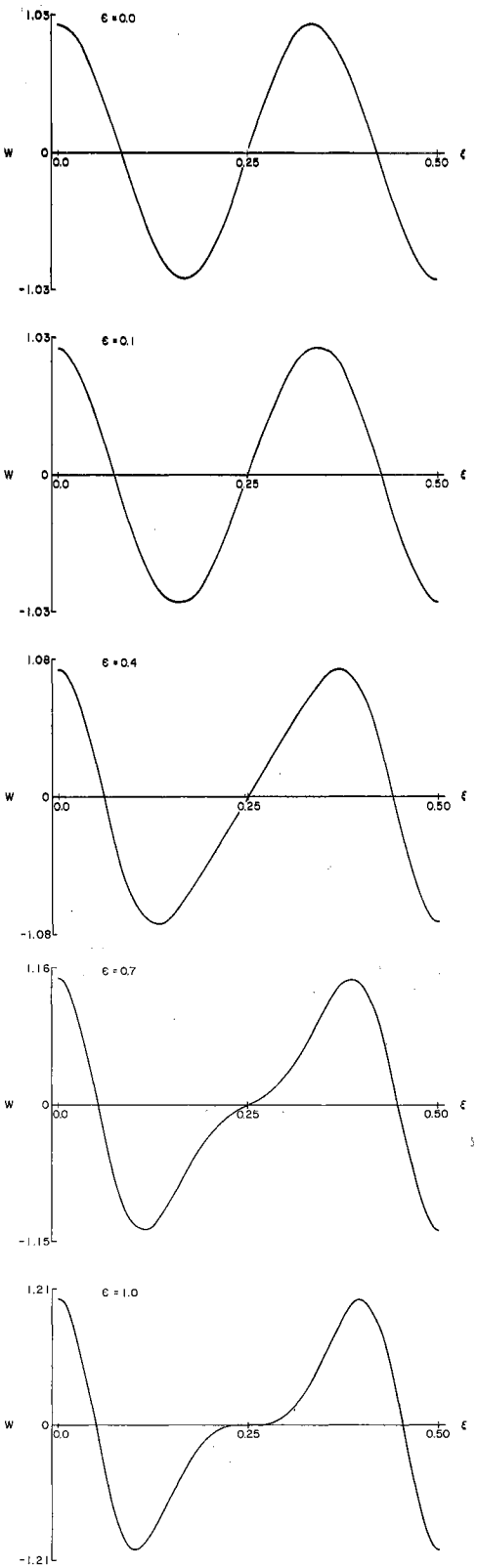

Figure 25. Mode Shapes (n = 3, m = 2)

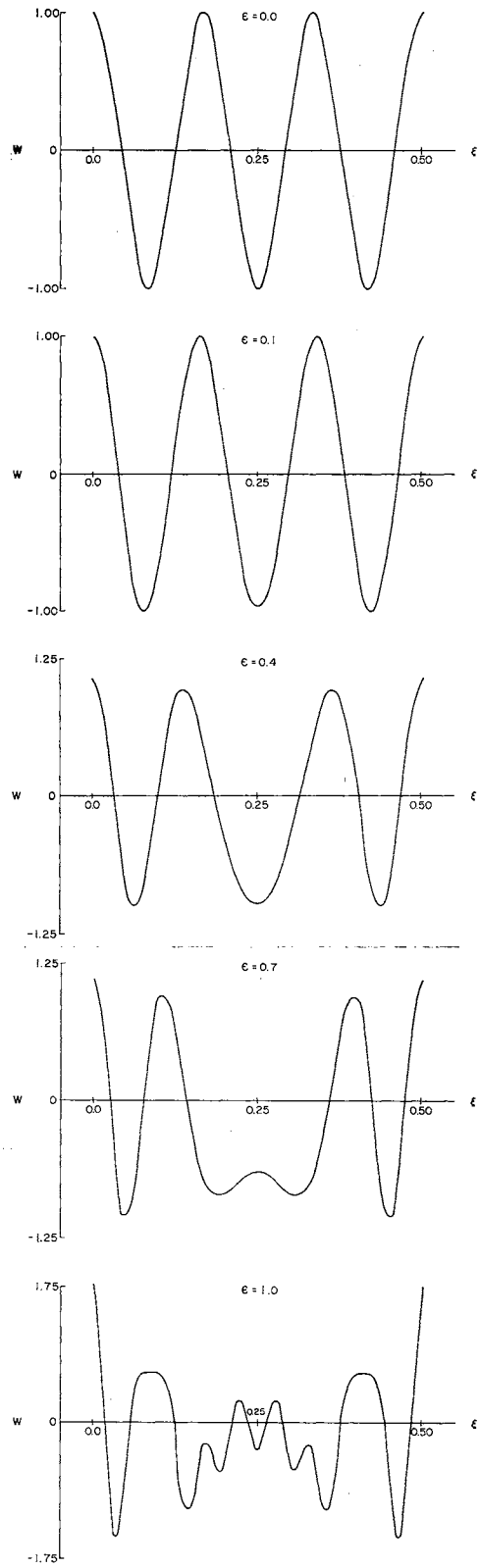

Figure 26. Mode Shapes (n = 6, m = 3)

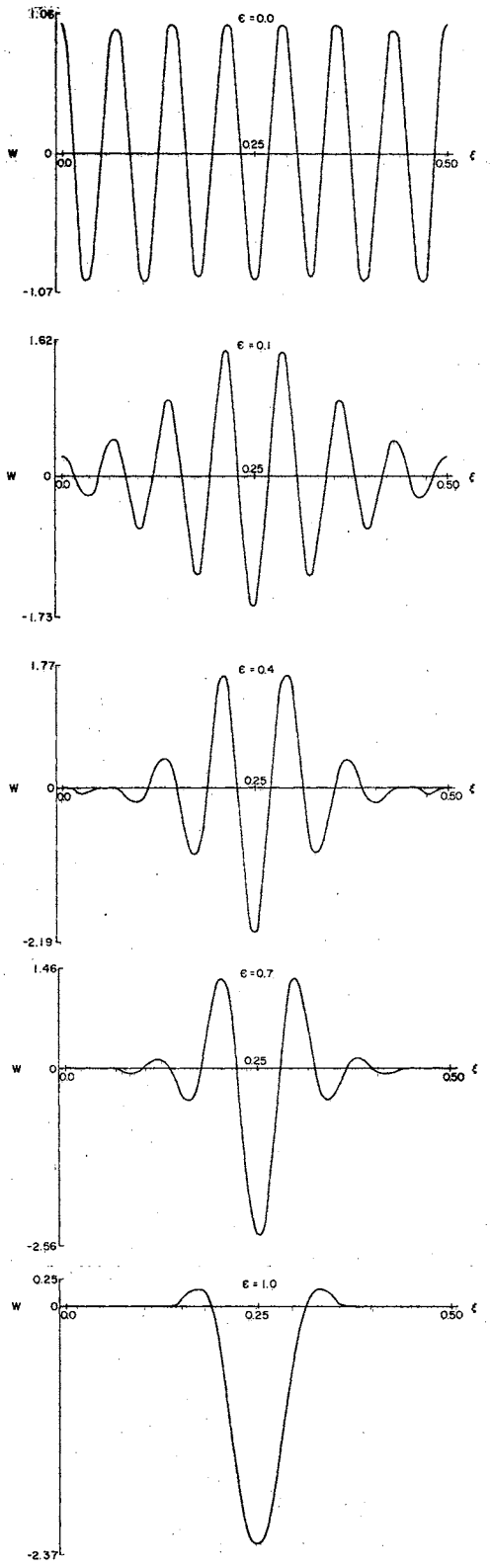

Figure 27. Mode Shapes (n = 14, m = 4)

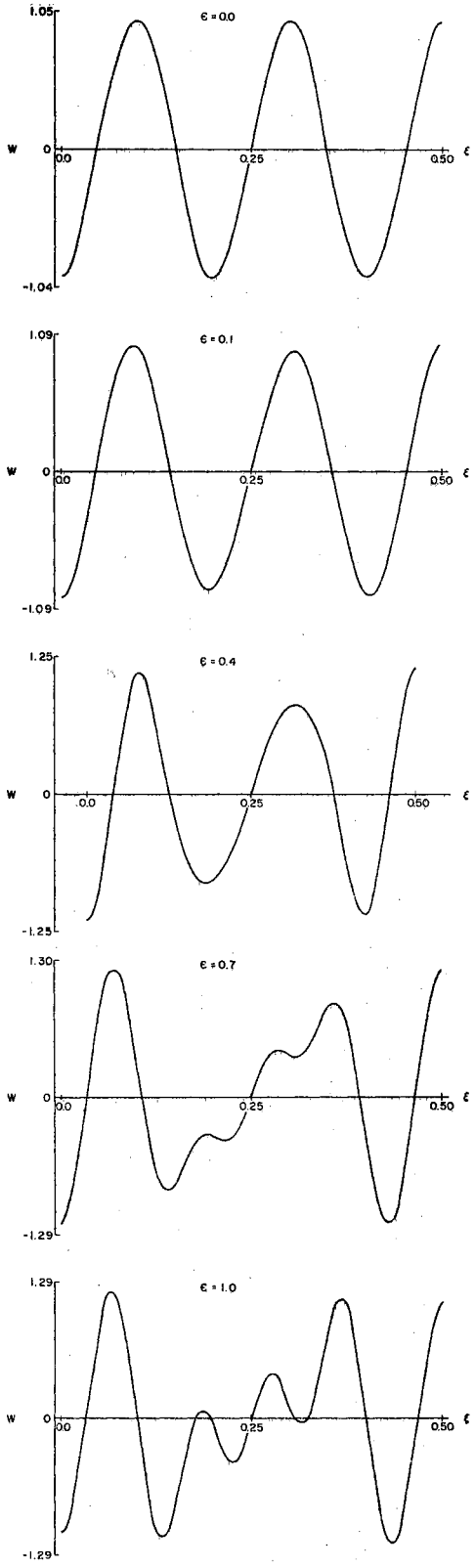

Figure 28. Mode Shapes (n = 5, m = 1)

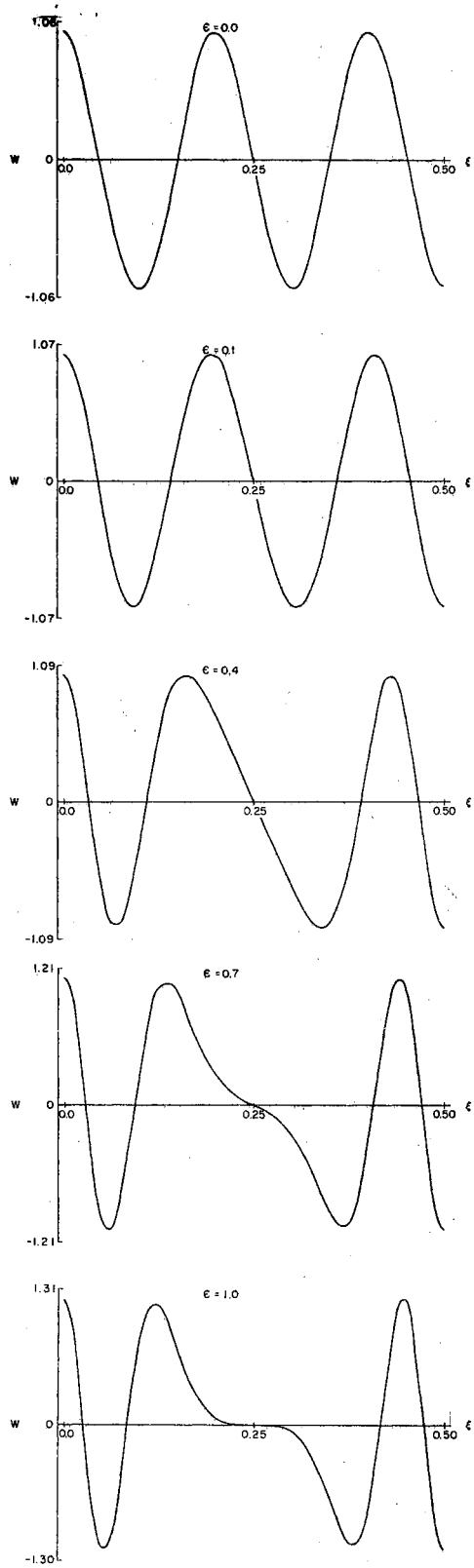

Figure 29. Mode Shapes (n = 5, m = 4)

4.5 Comparison of the Love and Donnell Equations

Love's equations were used for the previous study. In order to compare the results obtained by Donnell's equations to those obtained by Love's equations, frequencies were calculated for various lengths of shells. All variables were kept constant except the ratio L_s/L_x, because the Donnell equations usually give higher values for longer shells in the static case (28, pp. 224-227). Frequencies obtained by both sets of equations for a range from a relatively short shell ($\beta = 3.14$) to an extremely long shell ($\beta = 0.10$) are given in Tables X through XII. These are converged values for which $k = 25$.

These tables show that the Love and Donnell equations give almost identical results for this range of shell parameters. The Donnell equations give slightly higher frequencies for shorter shells and slightly lower frequencies for longer shells.

Because it is not the specific object of this study to investigate thoroughly the comparison of the Love and Donnell equations, the ratio L_s/L_x was the only parameter varied. These results show that the Donnell equations could be used with confidence in studying the free vibrations of freely supported oval cylindrical shells.

This study also indicated that the predominant displacement mode for the three frequencies obtained for each mode shape changed with the value of m and L_s/L_x. Armenakas obtained the result for circular shells (15, p. 99). A more thorough study should be made of this to see if his conclusions can be extended to noncircular shells.

TABLE X

COMPARISON OF THE NONDIMENSIONAL FREQUENCIES ($\bar{\omega}$) OBTAINED BY THE LOVE AND DONNELL EQUATIONS (m = 1)

m = 1	ϵ = 1.0		L_s = 75.4"		h = 0.032"	
β	3.14		1.0		.20	
n	Love	Donnell	Love	Donnell	Love	Donnell
0	0.92932	0.92932	0.29581	0.29580	0.05917	0.05916	0.02959	0.02958
1	0.71349	0.71349	0.15256	0.15256	0.00807	0.00804	0.00265	0.00201
2	0.24164	0.24164	0.03747	0.03743	0.00280	0.00264	0.00264	0.00246
3	0.19477	0.19477	0.02771	0.02766	0.00652	0.00627	0.00647	0.00641
4	0.09626	0.09627	0.00876	0.00875	0.01179	0.01167	0.01173	0.01161
5	0.08544	0.08545	0.01553	0.01551	0.01870	0.01864	0.01868	0.01862
6	0.06013	0.06013	0.02880	0.02876	0.02716	0.02712	0.02715	0.02711
7	0.03321	0.03322	0.03793	0.03791	0.03716	0.03713	0.03716	0.03712
8	0.01909	0.01909	0.04913	0.04911	0.04871	0.04868	0.04870	0.04868
9	0.06776	0.06777	0.06208	0.06207	0.06179	0.06177	0.06178	0.06176
10	0.08342	0.08343	0.07665	0.07664	0.07642	0.07640	0.07641	0.07639
11	0.09794	0.09795	0.09279	0.09278	0.09258	0.09257	0.09257	0.09256
12	0.11405	0.11405	0.11048	0.11047	0.11028	0.11027	0.11028	0.11027
13	0.13254	0.13254	0.12972	0.12971	0.12953	0.12952	0.12952	0.12951
14	0.15290	0.15291	0.15050	0.15049	0.15031	0.15030	0.15031	0.15030
15	0.17498	0.17498	0.17282	0.17282	0.17263	0.17263	0.17263	0.17262

TABLE XI

COMPARISON OF THE NONDIMENSIONAL FREQUENCIES ($\bar{\omega}$) OBTAINED BY THE LOVE AND DONNELL EQUATIONS (m = 2)

m = 2	ϵ = 1.0		L_s = 75.4"		h = 0.032"	
β	3.14		1.0		0.20		0.10	
n	Love	Donnell	Love	Donnell	Love	Donnell	Love	Donnell
0	1.31174	1.31175	0.59161	0.59161	0.11832	0.11832	0.05917	0.05916
1	1.28573	1.28573	0.41624	0.41623	0.03026	0.03023	0.00807	0.00804
2	0.51957	0.51959	0.12440	0.12440	0.00442	0.00436	0.00280	0.00264
3	0.50172	0.50174	0.09045	0.09044	0.00726	0.00714	0.00652	0.00627
4	0.26081	0.26085	0.04471	0.04470	0.01276	0.01264	0.01179	0.01167
5	0.24800	0.24804	0.02426	0.02425	0.01886	0.01879	0.01870	0.01864
6	0.17300	0.17307	0.01412	0.01412	0.02722	0.02718	0.02716	0.02712
7	0.16400	0.16407	0.04655	0.04654	0.03720	0.03717	0.03716	0.03713
8	0.13098	0.13101	0.05461	0.05460	0.04873	0.04871	0.04871	0.04868
9	0.10782	0.10784	0.06449	0.06448	0.06182	0.06180	0.06179	0.06177
10	0.03081	0.03081	0.07813	0.07812	0.07644	0.07642	0.07642	0.07640
11	0.05397	0.05398	0.09386	0.09385	0.09260	0.09259	0.09258	0.09257
12	0.09307	0.09308	0.11134	0.11134	0.11031	0.11030	0.11028	0.11027
13	0.14351	0.14354	0.13047	0.13046	0.12955	0.12954	0.12953	0.12952
14	0.16139	0.16143	0.15118	0.15118	0.15033	0.15033	0.15031	0.15030
15	0.18795	0.18800	0.17346	0.17346	0.17266	0.17265	0.17263	0.17263

TABLE XII

COMPARISON OF THE NONDIMENSIONAL FREQUENCIES ($\bar{\omega}$) OBTAINED BY THE LOVE AND DONNELL EQUATIONS (m = 3)

m = 3			ϵ = 1.0		L_s = 75.4"		h = 0.032"	
β	3.14		1.0		0.20		0.10	
n	Love	Donnell	Love	Donnell	Love	Donnell	Love	Donnell
0	1.50920	1.50921	0.88741	0.88741	0.17748	0.17748	0.08874	0.08874
1	1.50824	1.50824	0.67817	0.67817	0.06392	0.06390	0.01749	0.01741
2	0.74333	0.74336	0.22727	0.22727	0.00658	0.00656	0.00338	0.00326
3	0.74095	0.74098	0.18082	0.18083	0.00961	0.00954	0.00674	0.00660
4	0.42602	0.42607	0.09001	0.09002	0.01696	0.01686	0.01205	0.01193
5	0.42253	0.42259	0.08053	0.08054	0.01958	0.01951	0.01875	0.01871
6	0.28144	0.28154	0.01850	0.01850	0.02742	0.02738	0.02718	0.02714
7	0.27809	0.27820	0.03218	0.03219	0.03729	0.03726	0.03717	0.03714
8	0.23937	0.23946	0.05838	0.05838	0.04880	0.04877	0.04872	0.04869
9	0.22370	0.22378	0.06950	0.06951	0.06186	0.06185	0.06180	0.06178
10	0.16828	0.16830	0.08197	0.08197	0.07648	0.07647	0.07642	0.07641
11	0.07261	0.07262	0.09709	0.09710	0.09264	0.09263	0.09259	0.09258
12	0.04204	0.04204	0.11355	0.11356	0.11035	0.11034	0.11029	0.11028
13	0.14033	0.14034	0.13218	0.13218	0.12959	0.12958	0.12954	0.12953
14	0.11674	0.11674	0.15261	0.15262	0.15037	0.15036	0.15032	0.15031
15	0.18779	0.18782	0.17473	0.17474	0.17270	0.17269	0.17264	0.17264

CHAPTER V

SUMMARY AND CONCLUSIONS

5.1 Summary and Conclusions

An exact method has been presented in this study to determine the natural frequencies and mode shapes of freely supported oval cylindrical shells with the radius of curvature expressed as a cosine function of the circumferential coordinate s. Cases of circular shells, non-circular shells, and oval shells were investigated and the following observations were made.

1. Through comparison of the natural frequencies and mode shapes for circular cylinders, the Love and Donnell equations gave closely comparable results.
2. Comparison of the natural frequencies for oval cylinders showed that the exact method gave definitely different results than those obtained by the perturbation technique of Klosner for higher values of ϵ.
3. Because the frequencies did not compare favorably, the mode shapes obtained by Klosner and the author were not compared. Mode shapes were presented for the work done by the author during the comparison of Klosner's and the author's work.
4. Frequencies obtained for oval cylinders with low eccentricities compared with results obtained for the corresponding ellipses. As the eccentricity increased, the results were

less favorable. For a deviation of no more than 10%, the maximum allowable value of eccentricity is about 0.65.

5. As the longitudinal modes (m) were increased, the number of circumferential terms (k) had to be increased to obtain accurate frequencies and mode shapes. To obtain a minimum accuracy of three significant numbers for the normalized displacements, k was taken to be 25 for values of $m \leq 3$, and 27 for $m = 4$.

6. As the eccentricity and mode number n increased, it was found that the frequencies for increasing values of m decreased to a point, then increased.

7. As the eccentricity increased, curves of frequency versus n became highly irregular. This may have been due to the symmetric forms (axis 1-1 in Figure 1) studied. Frequencies obtained for symmetric forms about axis 2-2 in Figure 1 erased the greater percentage of this irregularity.

8. For positive and negative values of eccentricity, different values of the frequency were obtained for odd numbered values of n. As n increased, the two values converged.

9. As the eccentricity increased, the mode shapes varied a great deal from those of the circular cases. This was probably due to more bending in the flatter portions than in the highly curved portions.

10. The Love and Donnell equations gave almost identical results for noncircular cylinders for the range of shell parameters studied.

5.3 Suggestions for Further Work

During this study, many interesting topics were noted which could be studied. As noted in Section 4.3, the results obtained by Klosner were definitely different than those obtained by the author. An accurate method based on the perturbation technique could be developed to uncouple the partial differential equations of equilibrium and to solve for the natural frequencies and mode shapes.

As mentioned in Section 4.5, a study could be undertaken to determine if the remarks made by Armenakas (15, concerning predominant displacements) can be extended to noncircular shells.

Another extension of Section 4.5 would be to study other dynamic equilibrium equations for obtaining the natural frequencies, i.e., the Flügge-Lur'e-Byrne equations (29), the Morley equations (31), the Sanders' equations and others (29).

A study of forced vibrations would be an important extension of this study, because Klosner's (26) results for forced vibrations are based upon his free vibration study.

Results obtained by the author, which included the in-plane inertia terms, could be compared to results which neglect the in-plane inertia terms (32).

Studies of oval shells with different boundary conditions (13) could be undertaken and shells with a variable radius of curvature in the longitudinal direction, i.e., a tapered section, could be investigated.

Ring and stringer stiffened noncircular cylindrical shells could be studied.

Variational and approximate methods could be used to solve for the natural frequencies and mode shapes of an oval shell. Examples of these methods are: Rayleigh-Ritz, Galerkin, finite difference, and finite element. Sewall (21), presently, is using the Rayleigh-Ritz method to determine the natural frequencies and mode shapes of an elliptical cylinder.

In order to verify results obtained herein, an experimental study could be undertaken (21).

BIBLIOGRAPHY

1. Rayleigh, John William Strutt (Lord). The Theory of Sound. London: The Macmillian Co., Ltd., 1894.

2. Arnold, R. N., and G. B. Warburton. "Flexural Vibrations of the Walls of Thin Cylindrical Shells Having Freely Supported Ends." Proc. Roy. Soc. (London), Series A, Vol. 197 (1949), pp. 238-256.

3. Yamane, J. R. "Natural Frequency Curves of Simply Supported Cylindrical Shells." AIAA, Vol. 3, No. 1 (1965), pp. 180-181.

4. Yu, Yi-Yuan. "Free Vibrations of Thin Cylindrical Shells Having Finite Lengths with Freely Supported and Clamped Edges." Jour. of Appl. Mech., Trans. ASME, Vol. 99 (1955), pp. 547-552.

5. Weingarten, V. I. "Free Vibration of Thin Cylindrical Shells." AIAA, Vol. 2, No. 4 (1964), pp. 717-722.

6. Ivanyuta, E. I., and R. M. Finkel'shteyn. "Determination of Frequencies of Free Vibrations of Cylindrical Shells." Investigation of Elasticity and Plasticity, AD 630414 (January, 1966), pp. 255-259.

7. Smith, Bert L. "Natural Frequencies of Clamped Cylindrical Shells." AIAA, Vol. 6 (April, 1968), pp. 720-721.

8. Warburton, B. B. "Vibration of Thin Cylindrical Shells." Jour. of Mech. Engr. Science, Vol. 7 (December, 1965), pp. 399-407.

9. Kumar, Ram. "Axially Symmetric Vibrations of a Finite, Isotropic Cylinder." Jour. of the Acous. Soc. of Amer., Vol. 38 (November, 1965), pp. 851-854.

10. Brogan, William L. "Radial Vibrations of a Thin Cylindrical Shell." Jour. of the Acous. Soc. of Amer., Vol. 37 (December, 1961), pp. 1778-1781.

11. Lin, Chi-Wen, and Francis L. Bell. "On the Non-Symmetric Vibrations of Thin Cylindrical Shells with Clamped-Clamped Edges." Nuc. Engr. and Des., Vol. 7 (March, 1968), pp. 194-200.

12. Yu, Yi-Yuan. "Vibrations of Thin Cylindrical Shells Analyzed by Means of Donnell-Type Equations." Jour. of the Aero. Sciences (December, 1958), pp. 699-715.

13. Forsberg, Kevin. "Influence of Boundary Conditions on the Modal Characteristics of Thin Cylindrical Shells." AIAA, Vol. 2 (December, 1964), pp. 2150-2157.

14. Baron, M. L., and H. H. Bleich. "Tables for Frequencies and Modes of Free Vibration of Infinitely Long Thin Cylindrical Shells." Jour. of Appl. Mech, Vol. 21 (June, 1954), pp. 178-184.

15. Armenakas, Anthony E. "On the Accuracy of Some Dynamic Shell Theories." Jour. of the Engr. Mech. Div., ASCE, No. EM5 (October, 1967), pp. 95-109.

16. Flügge, W. Stresses in Shells. New York: Springer-Verlag Inc., 1966.

17. Donnell, L. H. "Stability of Thin-Walled Tubes Under Torsion." NACA, Rep. No. 479 (1934).

18. Marguerre, K. "Stabilitat der Zylinderschale veranderlicher Krummung." NACA, TM 1302 (July, 1951).

19. Malkina, R. L. "Vibrations of Noncircular Cylindrical Shells." NASA, N67-13085 (1967).

20. Herrmann, G., and I. Mirsky. "On the Vibrations of Cylindrical Shells of Elliptic Cross-Section, Contract No. AF 18(600)-1247, Technical Note No. 5, Columbia University, December, 1957.

21. Sewall, J. L. Private Communication (to be published).

22. Romano, Frank, and Joseph Kempner. "Stresses in Short Noncircular Cylindrical Shells Under Lateral Pressure." Jour. of Appl. Mech., Trans. ASME (December, 1962), pp. 669-674.

23. Romano, Frank, and Joseph Kempner. "Stress and Displacement Analysis of a Simply Supported, Noncircular Cylindrical Shell Under Lateral Pressure." Polytechnic Institute of Brooklyn, PIBAL Rep. No. 415 (July, 1958).

24. Klosner, Jerome M., and Frederick V. Pohle. "Natural Frequencies of an Infinitely Long Noncircular Cylindrical Shell." Polytechnic Institute of Brooklyn, PIBAL Rep. No. 476 (July, 1958).

25. Klosner, J. M. "Frequencies of an Infinitely Long Noncircular Cylindrical Shell, Part II." Polytechnic Institute of Brooklyn, PIBAL Rep. No. 552 (December, 1959).

26. Klosner, Jerome M. "Free and Forced Vibrations of a Long Noncircular Cylindrical Shell." Polytechnic Institute of Brooklyn, PIBAL Rep. No. 561 (September, 1960).

27. Kempner, Joseph. "Energy Expressions and Differential Equations for Stress and Displacement Analyses of Arbitrary Cylindrical Shells." Jour. of Ship Res. (June, 1958), pp. 8-19.

28. Reissner, E. "A New Derivation of the Equations for the Deformation of Elastic Shells." Am. J. Math., Vol. 63, No. 1 (January, 1941), pp. 174-184.

29. Kraus, H. Thin Elastic Shells. New York: John Wiley and Sons, 1967.

30. Grad, J., and M. A. Brebner. "Eigenvalues and Eigenvectors of a Real General Matrix." Communications of the ACM, Vol. 11, No. 12 (December, 1968), pp. 820-826.

31. Morley, L. S. D. "An Improvement on Donnell's Approximations for Thin-Walled Circular Cylinders." Quart. J. Mech. Appl. Math., Vol. XII (1959), p. 93.

32. Ivanyuta, E. I., and R. M. Finkel'shteyn. "Determination of the Free Oscillations of a Cylindrical Shell of Elliptical Cross Section." NASA TT F-12, 548 (August, 1969).

APPENDIX A

DERIVATION OF THE RECURRENCE FORMULAS

A.1 Assumptions

The following assumptions were made in this study:

1. The thickness of the shell is small compared with the radius of curvature of its middle surface.
2. The stress components normal to the middle surface are small compared with the other stress components and may be neglected in the stress-strain relations.
3. The Kirchhoff-Love assumptions of thin-walled shell theory are applied; i.e., the normals of the undeformed middle surface are deformed into the normals of the deformed middle surface, and remain straight and unextended.
4. The displacements are sufficiently small that the equilibrium conditions for deformed elements are the same as though the elements were not deformed.
5. The ratio of $1/(1 - z/r)$ is equal to unity (i.e., Love's assumption).

For the Donnell (17) equations, two more simplifying assumptions were made:

1. The transverse shearing force makes a negligible

contribution to the equilibrium of forces in the circumferential direction.[1]

2. The circumferential displacements result in negligible contributions to the changes in curvature and twist.

A.2 Strain Displacement Relations

For Love's equations, the following strain-displacement relationships were verified by Reissner (28):

$$\begin{aligned} e_x &= u_x + z\, w_{xx} \\ e_s &= v_s + \frac{w}{r} + z\left[w_{ss} - \left(\frac{v}{r}\right)_s\right] \\ e_{xs} &= u_s + v_x + z\left[2w_{xs} - \frac{v_x}{r}\right]. \end{aligned} \tag{A.1}$$

For Donnell's equations, Kempner (22, 27) verified the following strain-displacement relations:

$$\begin{aligned} e_x &= u_x + z\, w_{xx} \\ e_s &= v_s + \frac{w}{r} + z\, w_{ss} \\ e_{xs} &= u_s + v_x + 2z\, w_{xs}. \end{aligned} \tag{A.2}$$

With the preceding strain-displacement relationships, Equations (A.1 and A.2), and applying Hamilton's principle, Klosner (26) verified the differential equations of equilibrium, Equation (2.1), and Kempner (22, 27) verified the equations of equilibrium, Equation (2.2).

---

[1] This assumption improves in accuracy as the ratio of the radius to the thickness of the shell increases (29).

A.3 Recurrence Formulas (Symmetric Displacements)

Substituting the displacements, Equation (2.7), into each term of the equilibrium equations, Equation (2.4), yields the following:

$$\frac{u_{\eta\eta}}{L_x^2} = -\frac{\pi^2}{L_x^2}\sum_{m=1}^{\infty}\sum_{n=0,2}^{\infty} A_{mn}(m^2)\cos m\pi\eta\cos n\pi\xi\cos\lambda t$$

$$\frac{\gamma}{L_s^2}u_{\xi\xi} = -\frac{\gamma\pi^2}{L_s^2}\sum_{m=1}^{\infty}\sum_{n=0,2}^{\infty} A_{mn}(n)^2\cos m\pi\eta\cos n\pi\xi\cos\lambda t$$

$$\frac{\alpha v_{\eta\xi}}{L_s L_x} = \frac{\alpha\pi^2}{L_s L_x}\sum_{m=1}^{\infty}\sum_{n=0,2}^{\infty} B_{mn}(mn)\cos m\pi\eta\cos n\pi\xi\cos\lambda t$$

$$\frac{\mu}{rL_x}w_{\eta} = \frac{\mu\pi^2}{L_x L_s}\sum_{m=1}^{\infty}\sum_{n=0,2}^{\infty}(m)\left[(2+\epsilon\delta_2^n)C_{mn} + \epsilon(1+\delta_4^n)C_{mn-4} + \epsilon C_{mn+4}\right]$$
$$\cos m\pi\eta\cos n\pi\xi\cos\lambda t$$

$$-\frac{1-\mu^2}{E}\rho u_{tt} = \frac{\rho(1-\mu^2)}{E}\sum_{m=1}^{\infty}\sum_{n=0,2}^{\infty} A_{mn}(\lambda^2)\cos m\pi\eta\cos n\pi\xi\cos\lambda t$$

$$\frac{v_{\xi\xi}}{L_s^2} = -\frac{\pi^2}{L_s^2}\sum_{m=1}^{\infty}\sum_{n=0,2}^{\infty} B_{mn}(n)^2\sin m\pi\eta\sin n\pi\xi\cos\lambda t$$

$$\frac{\gamma}{Lx^2}v_{\eta\eta} = -\frac{\gamma\pi^2}{L_x^2}\sum_{m=1}^{\infty}\sum_{n=0,2}^{\infty} B_{mn}(m)^2\sin m\pi\eta\sin n\pi\xi\cos\lambda t$$

$$\frac{\alpha}{L_s L_x}u_{\eta\xi} = \frac{\alpha\pi^2}{L_s L_x}\sum_{m=1}^{\infty}\sum_{n=0,2}^{\infty} A_{mn}(mn)\sin m\pi\eta\sin n\pi\xi\cos\lambda t$$

$$\frac{1}{L_s}\left(\frac{w}{r}\right)_\xi = -\frac{\pi^2}{L_s^2}\sum_{m=1}^{\infty}\sum_{n=0,2}^{\infty}(n)\,[(2+\epsilon\delta_2^n)\,C_{mn} + \epsilon(1+\delta_4^n)\,C_{mn-4}$$

$$+ \epsilon C_{mn+4}]\sin m\pi\eta\sin n\pi\xi\cos\lambda t$$

$$\frac{h^2}{12}\frac{\gamma}{L_x^2}\frac{v_{\eta\eta}}{r^2} = -\frac{h^2\gamma\pi^4}{3L_x^2L_s^2}\sum_{m=1}^{\infty}\sum_{n=0,2}^{\infty}(m)^2\Big\langle B_{mn}\left[1+\frac{\epsilon^2}{2}-\epsilon\delta_2^n-\frac{\epsilon^2}{4}\delta_4^n\right]$$

$$+ B_{mn-4}\left[\epsilon(1-\delta_4^n)-\frac{\epsilon^2}{4}\delta_6^n\right] + B_{mn+4}\left[\epsilon-\frac{\epsilon^2}{4}\delta_2^n\right]$$

$$+ B_{mn-8}\left[\frac{\epsilon^2}{4}(1-\delta_8^n)\right] + B_{mn+8}\left[\frac{\epsilon^2}{4}\right]\Big\rangle\sin m\pi\eta\sin n\pi\xi\cos\lambda t$$

$$-\frac{h^2}{12}\frac{1}{L_x^2L_s}\frac{w_{\eta\eta\xi}}{r} = -\frac{h^2\pi^4}{6L_x^2L_s^2}\sum_{m=1}^{\infty}\sum_{n=0,2}^{\infty}(m^2)\left[C_{mn}\,n\left(1-\frac{\epsilon}{2}\delta_2^n\right)\right.$$

$$\left.+\frac{\epsilon}{2}(n+4)\,C_{mn+4} + \frac{\epsilon}{2}(n-4)\,C_{mn-4}\right]\sin m\pi\eta\sin n\pi\xi$$

$$\cos\lambda t$$

$$-\frac{h^2}{12L_s^3}\frac{w_{\xi\xi\xi}}{r} = -\frac{h^2\pi^4}{6\,L_s^4}\sum_{m=1}^{\infty}\sum_{n=0,2}^{\infty}\left[n^3\left(1-\frac{\epsilon}{2}\delta_2^n\right)C_{mn} + \frac{\epsilon}{2}(n+4)^3\,C_{mn+4}\right.$$

$$\left.+\frac{\epsilon}{2}(n-4)^3\,C_{mn-4}\right]\sin m\pi\eta\sin n\pi\xi\cos\lambda t$$

$$\frac{h^2}{12}\frac{1}{L_s^2}\frac{1}{r}\left(\frac{v}{r}\right)_{\xi\xi} = -\frac{h^2\pi^4}{3\,L_s^4}\sum_{m=1}^{\infty}\sum_{n=0,2}^{\infty}\Big\langle\left[n^2(1-\epsilon\delta_2^n) + \frac{\epsilon^2}{4}(n+4)^2(1-\delta_0^n)\right.$$

$$\left.+\frac{\epsilon^2}{4}(n+4)^2\right]B_{mn} + \left[\frac{\epsilon^2}{4}(n-4)^2(1-\delta_8^n)\right]B_{mn-8} +$$

$$+\left[n^2\frac{\varepsilon}{2}(1-\delta_4^n)+\frac{\varepsilon}{2}(n-4)^2\left(1-\frac{\varepsilon}{2}\delta_6^n\right)\right]B_{mn-4}$$

$$+\left[n^2\frac{\varepsilon}{2}+(n+4)^2\frac{\varepsilon}{2}-n^2\frac{\varepsilon^2}{4}\delta_2^n\right]B_{mn+4}$$

$$+\left[\frac{\varepsilon^2}{4}(n+4)^2\right]B_{mn+8}\Big\rangle \sin m\pi\eta \sin n\pi\xi \cos\lambda t$$

$$-\frac{(1-\mu^2)}{E}\rho v_{tt}=\frac{\rho(1-\mu^2)}{E}\sum_{m=1}^{\infty}\sum_{n=0,2}^{\infty}B_{mn}(\lambda)^2 \sin m\pi\eta \sin n\pi\xi \cos\lambda t$$

$$\frac{w}{r^2}=\frac{\pi^2}{L_s^2}\sum_{m=1}^{\infty}\sum_{n=0,2}^{\infty}\Big[(4+2\varepsilon^2+\varepsilon^2\delta_4^n+4\varepsilon\delta_2^n)C_{mn}$$

$$+\varepsilon(4+4\delta_4^n+\varepsilon\delta_6^n)C_{mn-4}+\varepsilon(4+\varepsilon\delta_2^n)C_{mn+4}+\varepsilon^2(1+\delta_8^n)C_{mn-8}$$

$$+\varepsilon^2 C_{mn+8}\Big]\sin m\pi\eta\cos n\pi\xi\cos\lambda t$$

$$\frac{1}{L_s}\frac{v_\xi}{r}=\frac{\pi^2}{L_s^2}\sum_{m=1}^{\infty}\sum_{n=0,2}^{\infty}\Big[(2+\varepsilon\delta_2^n)nB_{mn}+\varepsilon(1+\delta_4^n)(n-4)B_{mn-4}$$

$$+\varepsilon(n+4)B_{mn+4}\Big]\sin m\pi\eta\cos n\pi\xi\cos\lambda t$$

$$\frac{\mu}{L_x}\frac{u_\eta}{r}=-\frac{\mu\pi^2}{L_xL_s}\sum_{m=1}^{\infty}\sum_{n=0,2}^{\infty}m\Big[(2+\varepsilon\delta_2^n)A_{mn}+\varepsilon(1+\delta_4^n)A_{mn-4}+\varepsilon A_{mn+4}\Big]$$

$$\sin m\pi\eta\cos n\pi\xi\cos\lambda t$$

$$\frac{h^2}{12}\nabla^4 w=\frac{h^2\pi^4}{12L_s^4}\sum_{m=1}^{\infty}\sum_{n=0,2}^{\infty}C_{mn}\left[\beta^4m^4+2\beta^2m^2n^2+n^4\right]\sin m\pi\eta\cos n\pi\xi$$

$$\cos\lambda t$$

$$-\frac{h^2}{12 L_x^2 L_s}\left(\frac{v_{\eta\eta}}{r}\right)_{\xi} = \frac{h^2 \pi^4}{6 L_x^2 L_s^2} \sum_{m=1}^{\infty} \sum_{n=0,2}^{\infty} m^2 n\Big[(1-\frac{\epsilon}{2}\delta_2^n) B_{mn} + \frac{\epsilon}{2}(1-\delta_4^n) B_{mn-4} + \frac{\epsilon}{2} B_{mn+4}\Big] \sin m\pi\eta \cos n\pi\xi \cos\lambda t$$

$$\frac{h^2}{12 L_s^3}\left(\frac{v}{r}\right)_{\xi\xi\xi} = \frac{-h^2 \pi^4}{6 L_s^4} \sum_{m=1}^{\infty} \sum_{n=0,2}^{\infty} n^3\Big[(1-\frac{\epsilon}{2}\delta_2^n) B_{mn} + \frac{\epsilon}{2}(1-\delta_4^n) B_{mn-4} + \frac{\epsilon}{2} B_{mn+4}\Big] \sin m\pi\eta \cos n\pi\xi \cos\lambda t$$

$$\frac{(1-\mu^2)\rho}{E} w_{tt} = -\frac{\rho(1-\mu^2)}{E} \sum_{m=1}^{\infty} \sum_{n=0,2}^{\infty} C_{mn}(\lambda)^2 \sin m\pi\eta \cos n\pi\xi \cos\lambda t. \qquad (A.3)$$

The following identities are very useful for determining the preceding terms.

$$\cos n\pi\xi \cos 4\pi\xi = \tfrac{1}{2}[\cos(n+4)\pi\xi + \cos(n-4)\pi\xi]$$

$$\sin n\pi\xi \cos 4\pi\xi = \tfrac{1}{2}[\sin(n+4)\pi\xi + \sin(n-4)\pi\xi]$$

$$\cos n\pi\xi \cos^2 4\pi\xi = \tfrac{1}{4}[2\cos n\pi\xi + \cos(n+8)\pi\xi + \cos(n-8)\pi\xi] \qquad (A.4)$$

$$\sin n\pi\xi \cos^2 4\pi\xi = \tfrac{1}{4}[2\sin n\pi\xi + \sin(n+8)\pi\xi + \sin(n-8)\pi\xi].$$

Substituting Equation (A.3) into Equation (2.4a) and multiplying the entire equation by $-L_s^2/\pi^2$ yields the following:

$$\sum_{m=1}^{\infty} \sum_{n=0,2}^{\infty} \Big\{A_{mn}\Big[\beta^2 m^2 + \gamma_n^2 - \frac{(1-\mu^2)\rho L_s^2}{E\pi^2}\lambda^2\Big] + B_{mn}[-\beta\alpha m n] + C_{mn-4}\Big[-\beta\mu m\ \epsilon(1+\delta_4^n)\Big] +$$

$$+ C_{mn}\left[-\beta\mu m(2+\varepsilon\delta_2^n)\right] + C_{mn+4}\left[-\beta\mu m\varepsilon\right]\Big\} \cos m\pi\eta \cos n\pi\xi \cos\lambda t$$

$$= 0. \qquad (A.5)$$

Substituting Equation (A.3) into Equation (2.4b) and multiplying the entire equation by $-L_s^2/\pi^2$ yields the following:

$$\sum_{m=1}^{\infty}\sum_{n=0,2}^{\infty}\Big\{A_{mn}\left[-\beta\alpha m n\right] + B_{mn-8}\, L\left[\frac{h^2\pi^2}{3L_s^2}\frac{\varepsilon^2}{4}(1-\delta_8^n)\left\langle(n-4)^2+m^2\beta^2\gamma\right\rangle\right]$$

$$+ B_{mn-4}\, L\left[\frac{h^2\pi^2}{3L_s^2}\Big\langle m^2\beta^2\gamma\Big\{\varepsilon(1-\delta_4^n) - \frac{\varepsilon^2}{4}\delta_6^n\Big\} + n^2\frac{\varepsilon}{2}(1-\delta_4^n)\right.$$

$$\left. + \frac{\varepsilon}{2}(n-4)^2\left(1-\frac{\varepsilon}{2}\delta_6^n\right)\Big\rangle\right] + B_{mn}\Big[n^2+\gamma\beta^2m^2 + L\frac{h^2\pi^2}{3L_s^2}\Big\langle\gamma m^2\beta^2\cdot$$

$$\left(1+\frac{\varepsilon^2}{2}-\varepsilon\delta_2^n-\frac{\varepsilon^2}{4}\delta_4^n\right) + n^2(1-\varepsilon\delta_2^n) + \frac{\varepsilon^2}{4}(n+4)^2(1-\delta_0^n)$$

$$+ \frac{\varepsilon^2}{4}(n-4)^2\Big\rangle - \frac{(1-\mu^2)}{E\pi^2}\rho L_s^2\lambda^2\Big] + B_{mn+4}\, L\Big[\frac{h^2\pi^2}{3L_s^2}\Big\langle m^2\beta^2\gamma\cdot$$

$$\left(\varepsilon-\frac{\varepsilon^2}{4}\delta_2^n\right) + n^2\frac{\varepsilon}{2} + (n+4)^2\frac{\varepsilon}{2} - n^2\frac{\varepsilon^2}{4}\delta_2^n\Big\rangle\Big]$$

$$+ B_{mn+8}\, L\Big[\frac{h^2\pi^2}{3L_s^2}\frac{\varepsilon^2}{4}\Big\langle m^2\beta^2\gamma + (n+4)^2\Big\rangle\Big] + C_{mn-4}\Big[n\varepsilon(1+\delta_4^n)$$

$$+ L\frac{h^2\pi^2}{6L_s^2}\frac{\varepsilon}{2}(n-4)\left\langle\beta^2m^2 + (n-4)^2\right\rangle\Big] + C_{mn}\Big[n(2+\varepsilon\delta_2^n)$$

$$+ L\frac{h^2\pi^2}{6L_s^2}n\left(1-\frac{\varepsilon}{2}\delta_2^n\right)(\beta^2m^2+n^2)\Big] + C_{mn+4}\Big[n\varepsilon + L\frac{h^2\pi^2}{6L_s^2}\frac{\varepsilon}{2}(n+4)$$

$$\left\langle\beta^2m^2 + (n+4)^2\right\rangle\Big]\Big\}\sin m\pi\eta \sin n\pi\xi\cos\lambda t = 0. \qquad (A.6)$$

Substituting Equation (A.3) into Equation (2.4c) and multiplying the entire equation by $+L_s^2/\pi^2$ yields the following:

$$\sum_{m=1}^{\infty}\sum_{n=0,2}^{\infty}\Big\{A_{mn-4}\Big[-\mu m\beta\,\epsilon(1+\delta_4^n)\Big] + A_{mn}\Big[-\mu m\beta(2+\epsilon\delta_2^n)\Big] + A_{mn+4}\cdot$$
$$\cdot\Big[-\mu m\beta\epsilon\Big] + B_{mn-4}\Big[\epsilon(n-4)(1+\delta_4^n) + L\frac{h^2\pi^2}{6L_s^2}\frac{\epsilon}{2}(1-\delta_4^n)\,n$$
$$(\beta^2m^2-n^2)\Big] + B_{mn}\Big[n(2+\epsilon\delta_2^n) + L\frac{h^2\pi^2}{6L_s^2}\,n\,(1-\frac{\epsilon}{2}\delta_2^n)\cdot$$
$$(\beta^2m^2-n^2)\Big] + B_{mn+4}\Big[\epsilon(n+4) + L\frac{h^2\pi^2}{6L_s^2}\frac{\epsilon}{2}\,n\,(\beta^2m^2-n^2)\Big]$$
$$+ C_{mn-8}\Big[\epsilon^2(1+\delta_8^n)\Big] + C_{mn-4}\Big[\epsilon(4+4\delta_4^n+\epsilon\delta_6^n)\Big] + C_{mn}\Big[(4+2\epsilon^2$$
$$+\epsilon^2\delta_4^n+4\epsilon\delta_2^n) + \frac{h^2\pi^2}{12L_s^2}(\beta^2m^2+n^2)^2 - \frac{(1-\mu^2)\,\rho\,L_s^2}{E\qquad\pi^2}\lambda^2\Big]$$
$$+ C_{mn+4}\Big[\epsilon(4+\epsilon\delta_2^n\Big] + C_{mn+8}\Big[\epsilon^2\Big]\Big\}\sin m\pi\eta\cos n\pi\xi\cos\lambda t = 0. \tag{A.7}$$

These equations (Equations A.1, A.2, and A.3) must now be satisfied for each m and n and can therefore be rewritten without the summations.

In these equations, it was beneficial for the n's to be consecutive (i.e., n = 1, 2, 3, ...). Therefore, the following substitutions were made:

$$n = 2n-2$$
$$A_{mn-4} = A_{mn-2}$$
$$A_{mn+4} = A_{mn+2}$$
$$B_{mn-8} = B_{mn-4}$$
$$B_{mn+8} = B_{mn+4}$$

$$B_{mn-4} = B_{mn-2} \tag{A.8}$$

$$B_{mn+4} = B_{mn+2}$$

$$C_{mn-8} = C_{mn-4}$$

$$C_{mn+8} = C_{mn+4}$$

$$C_{mn-4} = C_{mn-2}$$

$$C_{mn+4} = C_{mn+2}$$

$$\delta_0^{2n-2} = \delta_1^n$$

$$\delta_2^{2n-2} = \delta_2^n$$

$$\delta_4^{2n-2} = \delta_3^n$$

$$\delta_6^{2n-2} = \delta_4^n$$

$$\delta_8^{2n-2} = \delta_5^n \quad .$$

Making these substitutions into Equations (A.5), (A.6), and (A.7), Equations (2.8), (2.9), and (2.10) were obtained.

A.4 Recurrence Formulas (Anti-Symmetric Displacements)

If the anti-symmetric displacements (Equations (2.7) with the sine and cosine functions in the ξ-direction interchanged) are substituted into Love's equations (Equation (2.4)), the recurrence formulas for the anti-symmetric case are obtained. Utilizing the simplifications used in the symmetric case, the recurrence formulas are as follows:

$$A_{mn}\left[\beta^2 m^2 + \gamma(2n-2)^2 - \omega^2\right] + B_{mn}\left[\alpha\beta m(2n-2)\right] + C_{mn-2}\left[-\beta\mu m\,\epsilon(1-\delta_3^n)\right]$$

$$+ C_{mn}\left[-\beta\mu m(2-\epsilon\delta_2^n)\right] + C_{mn+2}\left[-\beta\mu m\epsilon\right] = 0. \tag{A.9}$$

$$A_{mn}[\alpha\beta m(2n-2)] + B_{mn-4}\, L\left[\frac{h^2\pi^2}{12 L_s^2}\epsilon^2(1+\delta_5^n)\left\langle m^2\beta^2\gamma + (2n-6)^2\right\rangle\right]$$

$$+ B_{mn-2}\, L\left[\frac{h^2\pi^2}{3 L_s^2}\left\{(2n-2)^2\frac{\epsilon}{2}(1+\delta_3^n) + \frac{\epsilon}{2}(2n-6)^2\left(1+\frac{\epsilon}{2}\delta_4^n\right)\right.\right.$$

$$\left.\left. + m^2\beta^2\gamma\left\langle\epsilon(1+\delta_3^n) + \frac{\epsilon^2}{4}\delta_4^n\right\rangle\right\}\right] + B_{mn}\left[(2n-2)^2 + \gamma\beta^2 m^2 + L\frac{h^2\pi^2}{3 L_s^2}\right.$$

$$\left\langle(2n-2)^2(1+\epsilon\delta_2^n) + \frac{\epsilon^2}{4}(2n+2)^2(1+\delta_1^n-\delta_1^n) + \frac{\epsilon^2}{4}(2n-6)^2\right.$$

$$\left.\left. + \gamma m^2\beta^2\left(1+\frac{\epsilon^2}{2} + \epsilon\delta_2^n + \frac{\epsilon^2}{4}\delta_3^n\right)\right\rangle - \omega^2\right] + B_{mn+2}\, L\left[\frac{h^2\pi^2}{3 L_s^2}\left\langle(2n-2)^2\frac{\epsilon}{2}\right.\right.$$

$$\left.\left.(1+\frac{\epsilon}{2}\delta_2^n) + (2n+2)^2\frac{\epsilon}{2} + m^2\beta^2\gamma(\epsilon + \frac{\epsilon^2}{4}\delta_2^n)\right\rangle\right] + B_{mn+4}$$

$$L\left[\frac{h^2\pi^2}{12 L_s^2}\epsilon^2\left\langle\gamma m^2\beta^2 + (2n+2)^2\right\rangle\right] - C_{mn-2}\left[(2n-2)\epsilon(1-\delta^n{}_3)\right.$$

$$\left. + L\frac{h^2\pi^2}{12 L_s^2}\epsilon(2n-6)\left\langle\beta^2m^2 + (2n-6)^2\right\rangle\right] - C_{mn}\left[(2n-2)(2-\epsilon\delta_2^n)\right.$$

$$\left. + L\frac{h^2\pi^2}{6 L_s^2}(1+\frac{\epsilon}{2}\delta_2^n)(2n-2)\left\langle\beta^2m^2 + (2n-2)^2\right\rangle\right] - C_{mn+2}\left[(2n-2)\epsilon\right.$$

$$\left. + \frac{L\,h^2\pi^2}{12 L_s^2}\epsilon(2n+2)\left\langle\beta^2m^2 + (2n+2)^2\right\rangle\right] = 0. \qquad \text{(A.10)}$$

$$A_{mn-2}\left[-\mu m\beta\epsilon(1-\delta_3^n)\right] + A_{mn}\left[-\mu m\beta(2-\epsilon\delta_2^n)\right] + A_{mn+2}\left[-\mu m\beta\epsilon\right]$$

$$- B_{mn-2}\left[\epsilon(2n-6)(1-\delta_3^n) + L\frac{h^2\pi^2}{12 L_s^2}(1+\delta_3^n)\epsilon(2n-2)\left\langle\beta^2m^2 - \right.\right.$$

$$\left.\left. - (2n-2)^2\right\rangle\right] - B_{mn}\left[(2n-2)(2-\epsilon\delta_2^n) + L\frac{h^2\pi^2}{6 L_s^2}(2n-2)(1+\frac{\epsilon}{2}\delta_2^n)\right.$$

$$\langle m^2\beta^2 - (2n-2)^2\rangle\Big] - B_{mn+2}\Big[\epsilon(2n+2) + L\,\frac{h^2\,\pi^2}{12\,L_s^{\,2}}\,\epsilon(2n-2)$$

$$\langle m^2\beta^2 - (2n-2)^2\rangle\Big] + C_{mn-4}\Big[\epsilon^2(1-\delta_5^n)\Big] + C_{mn-2}\Big[\epsilon(4-4\delta_3^n - \epsilon\delta_4^n)\Big]$$

$$+ C_{mn}\Big[(4+2\epsilon^2 - \epsilon^2\delta_3^n - 4\epsilon\delta_2^n) + \frac{h^2\,\pi^2}{12\,L_s^{\,2}}\,\langle\beta^2 m^2 + (2n-2)^2\rangle^2 - \omega^2\Big]$$

$$+ C_{mn+2}\Big[\epsilon(4-\epsilon\delta_2^n)\Big] + C_{mn+4}\Big[\epsilon^2\Big] = 0. \qquad (A.11)$$

APPENDIX B

COMPUTER PROGRAM

```
CARD
0001  C     REFERENCE:
0002  C
0003  C     " FREE VIBRATIONS OF FREELY SUPPORTED OVAL CYLINDRICAL SHELLS "
0004  C
0005  C
0006  C     PURPOSE:
0007  C          TO COMPUTE THE NATURAL FREQUENCIES OF FREELY SUPPORTED OVAL
0008  C     CYLINDRICAL SHELLS AND THE U, V, AND W NORMALIZED DISPLACEMENTS AT
0009  C     THE POINT OF MAXIMUM DISPLACEMENT ALONG THE LONGITUDINAL AXIS.
0010  C
0011  C
0012  C     THIS PROGRAM IS DOUBLE PRECISION.
0013  C
0014  C
0015  C     PROGRAMMER:
0016  C
0017  C
0018  C     LARRY D. CULBERSON
0019  C     SCHOOL OF CIVIL ENGINEERING
0020  C     OKLAHOMA STATE UNIVERSITY
0021  C     STILLWATER, OKLAHOMA
0022  C
0023  C
0024  C     DESCRIPTION OF PARAMETERS:
0025  C
0026  C
0027  C     H       = THICKNESS OF THE SHELL
0028  C     LS      = CIRCUMFERENTIAL LENGTH
0029  C     LX      = LONGITUDINAL LENGTH
0030  C     NUM     = NUMBER OF PROBLEMS TO BE COMPUTED
0031  C     BET     = RATIO LS OVER LX
0032  C     PR      = POISSONS RATIO
0033  C     HOLS    = RATIO H OVER LS
0034  C     M       = NUMBER OF TERMS IN X-DIRECTION (M)
0035  C     K       = NUMBER OF TERMS IN S-DIRECTION (N)
0036  C     ECC     = ECCENTRICITY PARAMETER
0037  C     L       = +1 FOR LOVES EQUATIONS
0038  C             =  0 FOR DONNELLS EQUATIONS
0039  C     KP1     = -1 FOR FREELY SUPPORTED END CONDITIONS (CULBERSONS WORK)
0040  C             = +1 FOR KLOSNERS END CONDITIONS
0041  C     J       = +1 FOR SYMMETRIC MODE SHAPES
0042  C             = -1 FOR ANTI-SYMMETRIC MODE SHAPES
0043  C     A       = FREQUENCY MATRIX
0044  C     KK      = SIZE OF A :  3*K
0045  C     PI      = 3.141592653589793
0046  C     ALP     = ( 1 + PR ) / 2
0047  C     GAM     = ( 1 - PR ) / 2
0048  C     DEL1    = KRONECKER DELTA  ( N , 1 )
0049  C     DEL2    = KRONECKER DELTA  ( N , 2 )
0050  C     DEL3    = KRONECKER DELTA  ( N , 3 )
0051  C     DEL4    = KRONECKER DELTA  ( N , 4 )
0052  C     DEL5    = KRONECKER DELTA  ( N , 5 )
0053  C     XII     = DIVISIONS OF LS TO DETERMINE DISPLACEMENTS
0054  C             = ( K - 1 ) * 6
0055  C     II      = NUMBER OF POINTS AT WHICH DISPLACEMENTS ARE CALCULATED IN
```

```
CARD
0056  C              LS / 2
0057  C            = ( K - 1 ) * 3 + 1
0058  C     U      = LONGITUDINAL DISPLACEMENT
0059  C     V      = CIRCUMFERENTIAL DISPLACEMENT
0060  C     W      = RADIAL DISPLACEMENT
0061  C     Z      = DUMMY VARIABLE USED IN 'PLOT'
0062  C     XI     = CIRCUMFERENTIAL COORDINATE XI
0063  C     VECR   = MATRIX OF REAL EIGENVECTORS.  THE COEFFICIENTS OF U ARE
0064  C              STORED IN THE UPPER PART, THE COEFFICIENTS OF V ARE STORED
0065  C              IN THE MIDDLE PART; AND THE COEFFICIENTS OF W ARE STORED
0066  C              IN THE LOWER PART.
0067  C     VECI   = MATRIX OF IMAGINARY EIGENVECTORS
0068  C     EVR    = VECTOR OF REAL EIGENVALUES, NONDIMENSIONALIZED NATURAL
0069  C              FREQUENCIES FROM ' EIGENP ', THEN CHANGED TO THE SQUARE ROOT
0070  C              OF EVR/4. I.E., EVR = DSQRT(EVR/4.0)
0071  C     EVI    = VECTOR OF IMAGINARY EIGENVALUES
0072  C
0073  C
0074  C
0075  C     SUBROUTINES REQUIRED:
0076  C
0077  C
0078  C     1.  EIGENP
0079  C     2.  PLOT
0080  C
0081  C
0082  C     INPUT FORMAT SPECIFICATIONS:
0083  C
0084  C     1 ST CARD --------NUM:   FORMAT   I5          1- 5
0085  C     2 ND CARD --------BET:   FORMAT   F22.10      1-22
0086  C                       PR:    FORMAT   F5.2       23-27
0087  C                       HOLS:  FORMAT   F20.10     28-47
0088  C                       M:     FORMAT   I2          48-49
0089  C                       K:     FORMAT   I2          50-51
0090  C                       ECC:   FORMAT   F10.5       52-61
0091  C                       L:     FORMAT   I1          62
0092  C                       KP1:   FORMAT   I2          63-64
0093  C                       J:     FORMAT   I2          65-66
0094  C
0095  C
0096  C
0097  C
0098  C
0099        REAL*8 BET,PR,HOLS,ECC,PI,ALP,GAM,EVR,EVI,A,VECR,VECI,DELI,DEL2,
0100       1 DEL3,DEL4,DEL5,DSQRT,DFLOAT,DCOS,DSIN,XII
0101        DIMENSION A(81,81),VECR(81,81),VECI(81,81),EVR(81),EVI(81),
0102       1  INDIC(81), XI(79),U(79),V(79),W(79),Z(79)
0103        READ (5,107) NUM
0104        DO 18 JOB=1,NUM
0105        WRITE (6,105)
0106        READ(5,100) BET,PR,HOLS,M,K,ECC,L,KP1,J
0107        KK=3*K
0108        PI=3.14159265358979300
0109        ALP=(1.0D0+PR)/2.0D0
0110        GAM=(1.0D0-PR)/2.0D0
```

```
CARD
0111        DO 15 I=1,KK
0112        EVR(I)=0.0D0
0113     15 EVI(I)=0.0D0
0114        DO 16 I=1,KK
0115        DO 16 II=1,KK
0116        A(I,II)=0.0D0
0117        VECR(I,II)=0.0D0
0118     16 VECI(I,II)=0.0D0
0119   C
0120   C     RECURRENCE FORMULA 1
0121   C
0122        DO 2 N=1,K
0123        DEL2=0.0D0
0124        DEL3=0.0D0
0125        IF(N .EQ. 2) DEL2=1.0D0
0126        IF(N .EQ. 3) DEL3=1.0D0
0127        A(N,N)=DFLOAT(M*M)*BET*BET+GAM*DFLOAT((2*N-2)*(2*N-2))
0128        A(N,K+N)=DFLOAT(KP1)*DFLOAT(M*(2*N-2))*ALP*BET*DFLOAT(J)
0129        A(N,2*K+N)=DFLOAT(KP1)*PR*BET*DFLOAT(M)*(2.0D0+DFLOAT(J)*ECC*DEL2)
0130        IF(N .LT. 3) GO TO 3
0131        A(N,2*K+N-2)=DFLOAT(KP1)*PR*BET*DFLOAT(M)*ECC*(1.0D0+DFLOAT(J)*DEL
0132       13)
0133      3 IF(N .GT. K-2) GO TO 2
0134        A(N,2*K+N+2)=DFLOAT(KP1)*PR*BET*DFLOAT(M)*ECC
0135      2 CONTINUE
0136   C
0137   C     END OF RECURRENCE FORMULA 1
0138   C
0139   C
0140   C     RECURRENCE FORMULA 2
0141   C
0142        DO 4 N=1,K
0143        DEL1=0.0D0
0144        DEL2=0.0D0
0145        DEL3=0.0D0
0146        DEL4=0.0D0
0147        DEL5=0.0D0
0148        IF(N .EQ. 1) DEL1=1.0D0
0149        IF(N .EQ. 2) DEL2=1.0D0
0150        IF(N .EQ. 3) DEL3=1.0D0
0151        IF(N .EQ. 4) DEL4=1.0D0
0152        IF(N .EQ. 5) DEL5=1.0D0
0153        A(K+N,N)=DFLOAT(KP1)*DFLOAT(M*(2*N-2))*ALP*BET*DFLOAT(J)
0154        IF(N .LT. 5) GO TO 40
0155        A(K+N,K+N-4)=((1.0D0-DFLOAT(J)*DEL5)*(HOLS*HOLS*PI*PI*ECC*ECC/12.0
0156       1D0)*(DFLOAT(M*M)*BET*BET*GAM+DFLOAT((2*N-6)*(2*N-6))))*DFLOAT(L)
0157     40 IF(N .LT. 3) GO TO 41
0158        A(K+N,K+N-2)=((HOLS*HOLS*PI*PI/3.0D0)*((DFLOAT(M*M)*BET*BET*GAM*EC
0159       1C*((1.0D0-DFLOAT(J)*DEL3)-DFLOAT(J)*ECC/4.0D0*DEL4))+((ECC/2.0D0)*
0160       2(DFLOAT((2*N-2)*(2*N-2))*(1.0D0-DFLOAT(J)*DEL3)+(DFLOAT((2*N-6)*(2
0161       3*N-6))*(1.0D0-DFLOAT(J)*ECC/2.0D0*DEL4))))))*DFLOAT(L)
0162     41 A(K+N,K+N)=GAM*DFLOAT(M*M)*BET*BET+DFLOAT((2*N-2)*(2*N-2))*DFLOAT(
0163       1L)*(HOLS*HOLS*PI*PI/3.0D0)*(((DFLOAT(M*M)*BET*BET*GAM*(1.0D0+ECC*EC
0164       2C/2.0D0-DFLOAT(J)*ECC*DEL2-DFLOAT(J)*ECC*ECC/4.0D0*DEL3))+DFLOAT((
0165       32*N-2)*(2*N-2))*(1.0D0-DFLOAT(J)*ECC*DEL2)+(ECC*ECC/4.0D0)*(DFLOAT
```

```
CARD
0166       4((2*N+2)*(2*N+2))*(1.0D0-DFLOAT(J+1)*0.50D0*DEL1)+DFLOAT((2*N-6)*(
0167       52*N-6))))
0168        IF(N .GT. K-2) GO TO 42
0169        A(K+N,K+N+2)=((HOLS*HOLS*PI*PI/3.0D0)*((DFLOAT(M*M)*BET*BET*GAM*EC
0170       1C*(1.0D0-DFLOAT(J)*ECC/4.0D0*DEL2))+((ECC/2.0D0)*(DFLOAT((2*N-2)*(
0171       22*N-2))*(1.0D0-DFLOAT(J)*ECC/2.0D0*DEL2)+DFLOAT((2*N+2)*(2*N+2)))
0172       3))*DFLOAT(L)
0173      42 IF(N .GT. K-4) GO TO 43
0174         A(K+N,K+N+4)=((HOLS*HOLS*PI*PI*ECC*ECC/12.0D0)*(DFLOAT(M*M)*BET*BE
0175       1T*GAM+DFLOAT((2*N+2)*(2*N+2))))*DFLOAT(L)
0176      43 IF(N .LT. 3) GO TO 5
0177         A(K+N,2*K+N-2)=(DFLOAT(2*N-2)*ECC*(1.0D0+DFLOAT(J)*DEL3)+DFLOAT(L)
0178       1*(HOLS*HOLS*PI*PI*ECC*DFLOAT(2*N-6)/12.0D0)*(BET*BET*DFLOAT(M*M)+
0179       2DFLOAT((2*N-6)*(2*N-6))))*DFLOAT(J)
0180       5 A(K+N,2*K+N)=(DFLOAT(2*N-2)*(2.0D0+DFLOAT(J)*ECC*DEL2)+DFLOAT(L)*(
0181       1HOLS*HOLS*PI*PI*(1.0D0-DFLOAT(J)*ECC/2.0D0*DEL2)*DFLOAT(2*N-2)/6.0
0182       2D0)*(BET*BET*DFLOAT(M*M)+DFLOAT((2*N-2)*(2*N-2))))*DFLOAT(J)
0183        IF(N .GT. K-2) GO TO 4
0184        A(K+N,2*K+N+2)=(DFLOAT(2*N-2)*ECC*DFLOAT(L)*(HOLS*HOLS*PI*PI*ECC*D
0185       1FLOAT(2*N+2)/12.0D0)*(BET*BET*DFLOAT(M*M)+DFLOAT((2*N+2)*(2*N+2)))
0186       2)*DFLOAT(J)
0187       4 CONTINUE
0188  C
0189  C     END OF RECURRENCE FORMULA 2
0190  C
0191  C
0192  C     RECURRENCE FORMULA 3
0193  C
0194        DO 1 N=1,K
0195        DEL2=0.0D0
0196        DEL3=0.0D0
0197        DEL4=0.0D0
0198        DEL5=0.0D0
0199        IF(N .EQ. 2) DEL2=1.0D0
0200        IF(N .EQ. 3) DEL3=1.0D0
0201        IF(N .EQ. 4) DEL4=1.0D0
0202        IF(N .EQ. 5) DEL5=1.0D0
0203        IF(N .LT. 3) GO TO 7
0204        A(2*K+N,N-2)=DFLOAT(KP1)*PR*BET*ECC*DFLOAT(M)*(1.0D0+DFLOAT(J)*DEL
0205       13)
0206       7 A(2*K+N,N)=DFLOAT(KP1)*PR*BET*DFLOAT(M)*(2.0D0+DFLOAT(J)*ECC*DEL2)
0207        IF(N .GT. K-2) GO TO 8
0208        A(2*K+N,N+2)=DFLOAT(KP1)*PR*BET*ECC*DFLOAT(M)
0209       8 IF(N .LT. 3) GO TO 9
0210         A(2*K+N,K+N-2)=(ECC*DFLOAT(2*N-6)*(1.0D0+DFLOAT(J)*DEL3)+DFLOAT(L)
0211       1*(HOLS*HOLS*PI*PI*ECC*DFLOAT(2*N-2)*(1.0D0-DFLOAT(J)*DEL3)/12.0D0)
0212       2*(BET*BET*DFLOAT(M*M)-DFLOAT((2*N-2)*(2*N-2))))*DFLOAT(J)
0213       9 A(2*K+N,K+N)=(DFLOAT(2*N-2)*(2.0D0+DFLOAT(J)*ECC*DEL2)+DFLOAT(L)*(
0214       1HOLS*HOLS*PI*PI*DFLOAT(2*N-2)*(1.0D0-DFLOAT(J)*ECC/2.0D0*DEL2)/6.0
0215       2D0)*(BET*BET*DFLOAT(M*M)-DFLOAT((2*N-2)*(2*N-2))))*DFLOAT(J)
0216        IF(N .GT. K-2) GO TO 10
0217        A(2*K+N,K+N+2)=(ECC*DFLOAT(2*N+2)+DFLOAT(L)*(HOLS*HOLS*PI*PI*ECC*D
0218       1FLOAT(2*N-2)/12.0D0)*(BET*BET*DFLOAT(M*M)-DFLOAT((2*N-2)*(2*N-2)))
0219       2)*DFLOAT(J)
0220      10 IF(N .LT. 5) GO TO 11
```

```
CARD
0221          A(2*K+N,2*K+N-4)=ECC*ECC*(1.0D0+DFLOAT(J)*DEL5)
0222       11 IF(N .LT. 3) GO TO 12
0223          A(2*K+N,2*K+N-2)=ECC*(4.0D0+DFLOAT(J)*4.0D0*DEL3+DFLOAT(J)*ECC*DEL
0224         14)
0225       12 A(2*K+N,2*K+N)=4.0D0+DFLOAT(J)*4.0D0*ECC*DEL2+ECC*ECC*(2.0D0+DFLOA
0226         1T(J)*DEL3)+HOLS*HOLS*PI*PI/12.0D0*((BET*BET*DFLOAT(M*M)+DFLOAT((2*
0227         2N-2)*(2*N-2)))**2)
0228          IF(N .GT. K-2) GO TO 13
0229          A(2*K+N,2*K+N+2)=ECC*(4.0D0+DFLOAT(J)*ECC*DEL2)
0230       13 IF(N .GT. K-4) GO TO 1
0231          A(2*K+N,2*K+N+4)=ECC*ECC
0232        1 CONTINUE
0233  C
0234  C       END OF RECURRENCE FORMULA 3
0235  C
0236  C
0237  C       BEGIN CALCULATIONS FOR FREQUENCIES AND NONDIMENSIONALIZED VECTORS
0238          CALL EIGENP (KK,81,A,56.0D0,EVR,EVI,VECR,VECI,INDIC)
0239  C       END   CALCULATIONS FOR FREQUENCIES AND NONDIMENSIONALIZED VECTORS
0240  C
0241          WRITE(6,103) BET,PR,HOLS,M,K,ECC
0242          IF(L .EQ. 1  .AND.  KP1 .EQ. -1) GO TO 44
0243          IF(L .EQ. 1  .AND.  KP1 .EQ.  1) GO TO 46
0244          IF(L .EQ. 0  .AND.  KP1 .EQ.  1) GO TO 47
0245          WRITE(6,108)
0246          GO TO 45
0247       47 WRITE(6,111)
0248          GO TO 45
0249       46 WRITE(6,110)
0250          GO TO 45
0251       44 WRITE(6,109)
0252       45 IF(J .EQ. -1) GO TO 48
0253          WRITE(6,112)
0254          GO TO 49
0255       48 WRITE(6,113)
0256       49 WRITE(6,102)
0257          DO  6 I=1,KK
0258       14 EVR(I)=DSQRT(EVR(I)/4.0D0)
0259        6 WRITE (6,101) EVR(I),EVI(I),INDIC(I)
0260  C
0261  C       BEGIN CALCULATION OF THE MODE SHAPES
0262  C
0263          XII=DFLOAT((K-1)*6)
0264          II=(K-1)*3+1
0265          JBL=1
0266          DO 32 JJB=JBL,KK
0267          JB=KK+JBL-JJB
0268       53 DO 31 III=1,II
0269          XI(III)=DFLOAT(III-1)/XII
0270          U(III)=0.0D0
0271          V(III)=0.0D0
0272          W(III)=0.0D0
0273          IF(J .EQ. -1) GO TO 50
0274  C
0275  C       SYMMETRIC MODE SHAPES
```

```
CARD
0276  C
0277        DO 30 JJ=1,K
0278        U(III)=U(III)+VECR(JJ,JB)*DCOS(DFLOAT(2*JJ-2)*PI*XI(III))
0279        V(III)=V(III)+VECR(K+JJ,JB)*DSIN(DFLOAT(2*JJ-2)*PI*XI(III))
0280     30 W(III)=W(III)+VECR(2*K+JJ,JB)*DCOS(DFLOAT(2*JJ-2)*PI*XI(III))
0281        GO TO 31
0282  C
0283  C     ANTI-SYMMETRIC MODE SHAPES
0284  C
0285     50 DO 52 JJ=1,K
0286        U(III)=U(III)+VECR(JJ,JB)*DSIN(DFLOAT(2*JJ-2)*PI*XI(III))
0287        V(III)=V(III)+VECR(K+JJ,JB)*DCOS(DFLOAT(2*JJ-2)*PI*XI(III))
0288     52 W(III)=W(III)+VECR(2*K+JJ,JB)*DSIN(DFLOAT(2*JJ-2)*PI*XI(III))
0289  C
0290     31 CONTINUE
0291        WRITE(6,105)
0292        WRITE(6,114) EVR(JB)
0293        DO 60 I=1,II
0294     60 WRITE(6,104) XI(I),U(I),V(I),W(I)
0295        CALL PLOT (XI,0,U,0,Z,0,II,1,1,0,2,0,1)
0296        DO 70 III=1,II
0297     70 XI(III)=DFLOAT(III-1)/XII
0298        CALL PLOT (XI,0,V,0,Z,0,II,1,1,0,2,0,1)
0299        DO 71 III=1,II
0300     71 XI(III)=DFLOAT(III-1)/XII
0301        CALL PLOT (XI,0,W,0,Z,0,II,1,1,0,2,0,1)
0302     32 CONTINUE
0303    100 FORMAT(F22.10,F5.2,F20.10,I2,I2,F10.5,I1,I2,I2)
0304    101 FORMAT(10X,D20.10,10X,D20.10,10X,I5)
0305    102 FORMAT(//,14X,'FREQUENCIES',17X,'IMAGINARY VALUES',12X,'INDIC',//)
0306    103 FORMAT (//,2X,'RATIO LS OVER LX = ',D15.8,//,2X,'POISSONS RATIO =
0307       1',09.2,//,2X,'H OVER LS = ',D15.8,//,2X,'M = ',I2,//,2X,'N = ',I2,
0308       2//,2X,'ECCENTRICITY RATIO = ',D12.5,//)
0309    104 FORMAT(6(1X,D18.10))
0310    105 FORMAT(1H1)
0311    106 FORMAT(//)
0312    107 FORMAT(I5)
0313    108 FORMAT(2X,'DONNELLS EQUATIONS ARE BEING USED WITH CULBERSONS WORK'
0314       1 ,//)
0315    109 FORMAT(2X,'LOVES EQUATIONS ARE BEING USED WITH CULBERSONS WORK',//
0316       1 )
0317    110 FORMAT(2X,'LOVES EQUATIONS ARE BEING USED WITH KLOSNERS WORK',//)
0318    111 FORMAT(2X,'DONNELLS EQUATIONS ARE BEING USED WITH KLOSNERS WORK',
0319       1 //)
0320    112 FORMAT(2X,'SYMMETRIC MODES AND FREQUENCIES',//)
0321    113 FORMAT(2X,'ANTI-SYMMETRIC MODES ANO FREQUENCIES',//)
0322    114 FORMAT(///,10X,'XI',18X,'U',18X,'V',18X,'W',20X,'FREQUENCY = ',D18
0323       1 .10,/)
0324     18 CONTINUE
0325        STOP
0326        END
```

VITA

Larry Dale Culberson

Candidate for the Degree of

Doctor of Philosophy

Thesis: FREE VIBRATIONS OF FREELY SUPPORTED OVAL CYLINDRICAL SHELLS

Major Field: Engineering

Biographical:

Personal Data: Born March 10, 1944, in Pana, Illinois, the son of Mr. and Mrs. Robert N. Culberson.

Education: Graduated from Pana Senior High School, Pana, Illinois, in May, 1962. Attended John Brown University from September, 1962, to May, 1963. Attended M. I. T. from June, 1965, to July, 1965. Received the Degree of Bachelor of Science in Civil Engineering (Magna Cum Laude) from Bradley University in June, 1966, and the Degree of Master of Science (Civil Engineering) from Oklahoma State University in May, 1968. Completed requirements for the Degree of Doctor of Philosophy from Oklahoma State University in July, 1970.

Professional Experience: Laborer and carpenter with the Culberson Construction Company, Summers of 1961-64, 1967-68. Engineering Technician IV with the Illinois Division of Highways, Summer of 1965. Civil Engineer I with the Illinois Division of Highways, Summer of 1966. Graduate Teaching Assistant, Oklahoma State University, 1968-70.

Professional Organizations: Associate Member of the American Society of Civil Engineers, Sigma Tau, Tau Beta Pi, and Phi Kappa Phi.